Penelec / GPU

JCP&L / GPU

Met-Ed / GPU

Service

Nuclear

GENERAL PUBLIC UTILITIES

STEADY STATE REACTOR PHYSICS METHODOLOGY

FOR TMI-1

TOPICAL REPORT 091

(REV. 0)

BA NO.: 135400

AUTHOR:

HUI-HSING FU
ENGINEER, TMI FUEL PROJECTS

January 23, 1995

APPROVALS:

J. D. LUOMA
MANAGER, TMI FUEL PROJECTS

G. R. BOND
DIRECTOR, NUCLEAR ANALYSIS & FUEL

ABSTRACT

This report describes the CASMO-3/SIMULATE-3 code package for calculating TMI-1 nuclear physics data by GPUN. The methodology has been verified against critical experiments and TMI-1 operating data. The results from these analyses demonstrate that the CASMO-3/SIMULATE-3 methodology is accurate and GPUN is capable of performing inhouse physics calculations. Nuclear reliability factors based on this methodology are determined. GPUN intends to use this methodology for performing nuclear design calculations for TMI-1.

LIST OF TABLES

LIST OF FIGURES

1.0 INTRODUCTION

This report describes the steady state physics method in use at GPUN for TMI-1. The method utilizes the incore fuel management computer codes CASMO-3, TABLES-3 and SIMULATE-3 (Refs. 1-3) developed by Studsvik. CASMO-3 is a multi-group two-dimensional transport theory code for the burnup calculation. TABLES-3 is a linkage code which reformats the two group cross sections from CASMO-3 output files according to the SIMULATE-3 format. SIMULATE-3 is a three-dimensional two group steady state reactor analysis code which predicts assembly power, control rod worth, reactivity, boron concentrations, kinetics input, pin power, etc.

The CASMO-3/SIMULATE-3 methodology has been thoroughly benchmarked by Studsvik, the developer of the codes. CASMO-3 has been benchmarked against critical experiments such as KRITZ experiments, B&W criticals, BAPL and ESADA (Refs. 4-12). SIMULATE-3 has been benchmarked against B&W criticals, KWU reactors, and IAEA PWR problems (Refs. 13-15). These verify that CASMO-3/SIMULATE-3 can accurately simulate the reactor core during steady state operations. The methodology is now widely used by utilities for core analysis because it is accurate, easy to use and not CPU intensive. Since the computer codes have been extensively benchmarked by the vendor and other utilities (Refs. 16-18), it is unnecessary to duplicate all of the benchmark work. Therefore, the GPUN benchmark efforts are concentrated on how the CASMO-3/SIMULATE-3 methodology can be accurately applied to TMI-1. The purpose is to demonstrate GPUN's understanding of the methodology and the capability of using the codes. TMI-1 Cycles 1 to 10 (Refs. 19-28) operations are modeled and the results are compared with the plant measurements. In addition, pin cell criticals, B&W criticals and comparisons with PDQ (Ref. 29) results are also performed. The results of all the benchmarking establishes a basis of confidence for GPUN core analysis.

Section 2 of this report provides a brief overview of the computer codes. Section 3 gives the CASMO-3 verifications and Section 4 gives the SIMULATE-3 verifications. The accuracy of SIMULATE-3 pin power reconstruction is shown in Section 5. The determinations of the associated nuclear reliability factors are shown in Section 6. Section 7 summarizes the methodology and its basis of confidence.

2.0 METHODOLOGY OVERVIEW

The steady state physics calculation uses CASMO-3 for fuel lattice cross section generation and SIMULATE-3 for three-dimensional reactor simulation. TABLES-3 is used to generate the SIMULATE-3 cross section library from CASMO-3 cross section files. Brief descriptions of these three computer codes are given in this chapter.

2.1 CASMO-3 Description

CASMO-3 is a multi-group two-dimensional transport theory code for burnup calculations on BWR and PWR assemblies or simple pin cells. It models cylindrical fuel rods in a square pitch array with allowance for fuel rods loaded with gadolinium, burnable absorber rods, cluster control rods, instrument tube, water gaps, boron steel curtains, and cruciform control rods in the regions separating fuel assemblies. It can also be used to model fuel storage racks, asymmetric PWR fuel bundles, four BWR bundles, PWR colorset, and reflector data.

At GPUN CASMO-3 is used to generate group cross sections, discontinuity factors, fission products data, detector reaction rates, pin power data, and reflector cross sections required by SIMULATE-3. It is also used for automatic generation of effective cross sections for PDQ since it has a two-dimensional diffusion theory routine. CASMO-3 has a 40 group and a 70 group nuclear data library. Both libraries are based on ENDF/B-IV with some data taken from ENDF/B-V. The library contains absorption, fission, nufission, transport and P_0 scattering cross sections. Data is tabulated as functions of temperature if needed. The library also contains yield values for fission products and decay constants. The 40 group library is condensed from the 70 group library using typical light water reactor spectra for the various nuclides. The 40 group library is used at GPUN for all production runs and the

benchmark work performed at GPUN as recommended in Ref. 4. For fuel lattices containing gadolinia pins, the computer code MICBURN-3 (Ref. 30), is used to generate effective Gd cross sections as a function of burnup.

A simplified flow diagram for CASMO-3 is shown in Figure 2.1. Effective resonance cross sections are calculated individually for each fuel pin. The cross sections are then used in a series of micro group calculations to obtain detailed neutron energy spectra to be used for energy condensation and spatial homogenization of the pin cells. For PWR, the microgroup spectra are directly used to obtain broad group cross sections for smeared pin cells for the succeeding two-dimensional transmission probability calculations. The eigenvalue and the flux distribution are obtained in the transport calculation and a fundamental buckling mode is used to include effects of leakage. The isotopic depletion as a function of irradiation is calculated for each fuel pin and for each region containing a burnable absorber. A predictor-corrector approach is used for the burnup calculation. Cross sections for PDQ (Ref. 29) are generated by comparing automatically within CASMO-3 a diffusion theory solution (DIXY) with the CASMO-3 transport theory solution.

2.2 TABLES-3 Description

TABLES-3 is a linkage code which reads the CASMO-3 output and generates a binary library to SIMULATE-3. The cross section library consists of 2-dimensional and/or 3-dimensional tables which may be interpolated to provide data at intermediate conditions. The allowed variables are exposure, void, history averaged void, fuel temperature, history averaged fuel temperature, moderator temperature, history averaged moderator temperature, boron concentration, history averaged boron concentrations, control rod,

history averaged control rod, and burnable absorber exposure.

The base cross section values are generated at nominal reactor conditions as a function of assembly exposure. Changes in cross sections from their base values are determined by altering one variable from its base value at various exposures for modeling instantaneous change of operating conditions. For cumulative effects, the history data of cross sections are obtained by comparing branch cases from the base depletion to depletions performed at the branch conditions. SIMULATE-3 will interpolate or extrapolate the tabulated delta cross sections based on the reactor conditions being modelled and add them to the base cross sections to obtain the appropriate total cross sections.

TABLES-3 also collects and functionalizes the CASMO-3 data required for pin power reconstruction and kinetics calculation in SIMULATE-3. This data consists of pin-by-pin power distributions, corner-point flux ratios, detector flux peaking factors, detector microscopic cross sections, two-group neutron velocities, effective delayed neutron precursor yields, and precursor decay constants. The principal variations of these data are represented by a one dimensional table set in exposure. The additional dependencies of the data are represented by one-dimensional tables of the derivatives of the data as a function of exposure. SIMULATE-3 then reconstructs the pin power from these tables for the reactor conditions modeled.

2.3 SIMULATE-3 Description

SIMULATE-3 is a three-dimensional two group steady state reactor analysis code for performing incore fuel management studies, core design calculations, and calculations of safety parameters. It is an advanced nodal code which explicitly models the baffle and

reflector regions, thus eliminating the need for user adjustable parameters, or the need for data normalization with higher order codes.

A two group diffusion model, QPANDA, is used to determine the three dimensional distributions of neutron fluxes. The nodal equations are solved iteratively on nodal coupling coefficients and node-averaged fluxes. QPANDA is different from other advance nodal codes in that the intra-nodal flux shape in either the fast or thermal group is intimately coupled to the flux shape in the other group. It also constructs two-node problems for each nodal interface to obtain coupling relationships which involves only node-averaged fluxes and transverse leakages.

Conventional nodal codes have difficulty modeling the fluxes at assembly interfaces using the homogenized fluxes. SIMULATE-3 overcomes this difficulty by coupling the homogenized fluxes with the assembly discontinuity factors from CASMO-3. When used in the QPANDA model, the assembly discontinuity factors change the neutron currents between assemblies and effectively eliminate the homogenization errors. The flux and leakage distributions at the fuel/baffle interface as well as reaction rates in the baffle and reactor are generated using the CASMO-3 reflector option. The discontinuity factor concept is also used to treat the baffle/reflector homogenization in QPANDA. This provides accurate representation of the radial and axial reflector nodes, thus eliminating the use of albedos.

All cross section data are generated from CASMO-3 assembly calculations and are tabulated as multi-dimensional tables by the TABLES-3 code. Instead of a direct calculation of nuclide concentrations, SIMULATE-3 uses macroscopic cross section data functionalized

versus exposure and history variables. A weighting variable is determined internally for each fuel type and used in the history effects calculation. This is to account for the fact that cross sections are more sensitive to recent history values of state parameters and less sensitive to those of earlier history. Another characteristic of SIMULATE-3 depletion model is the spatial representation used to model the radial cross section variation within an assembly. Therefore, the subdivision of each assembly is not required in order to model the influence of large exposure gradients within fuel assemblies.

The SIMULATE-3 pin power reconstruction method is based on the assumption of separability of the global flux (homogeneous intranodal flux) and local flux shapes (heterogeneous "form functions"). The intranodal flux distributions are computed using biquadrate flux expansions and the form functions are computed from single assembly spectrum depletion calculations. Corner point fluxes are determined to preserve fluxes at nodal points assuming a biquadrate distribution. The spectral interactions between neighboring assemblies are explicitly modeled in the intranodal cross sections which allows evaluation of pin-by-pin distribution of fission cross sections.

Figure 2.1 Flow Diagram of CASMO-3

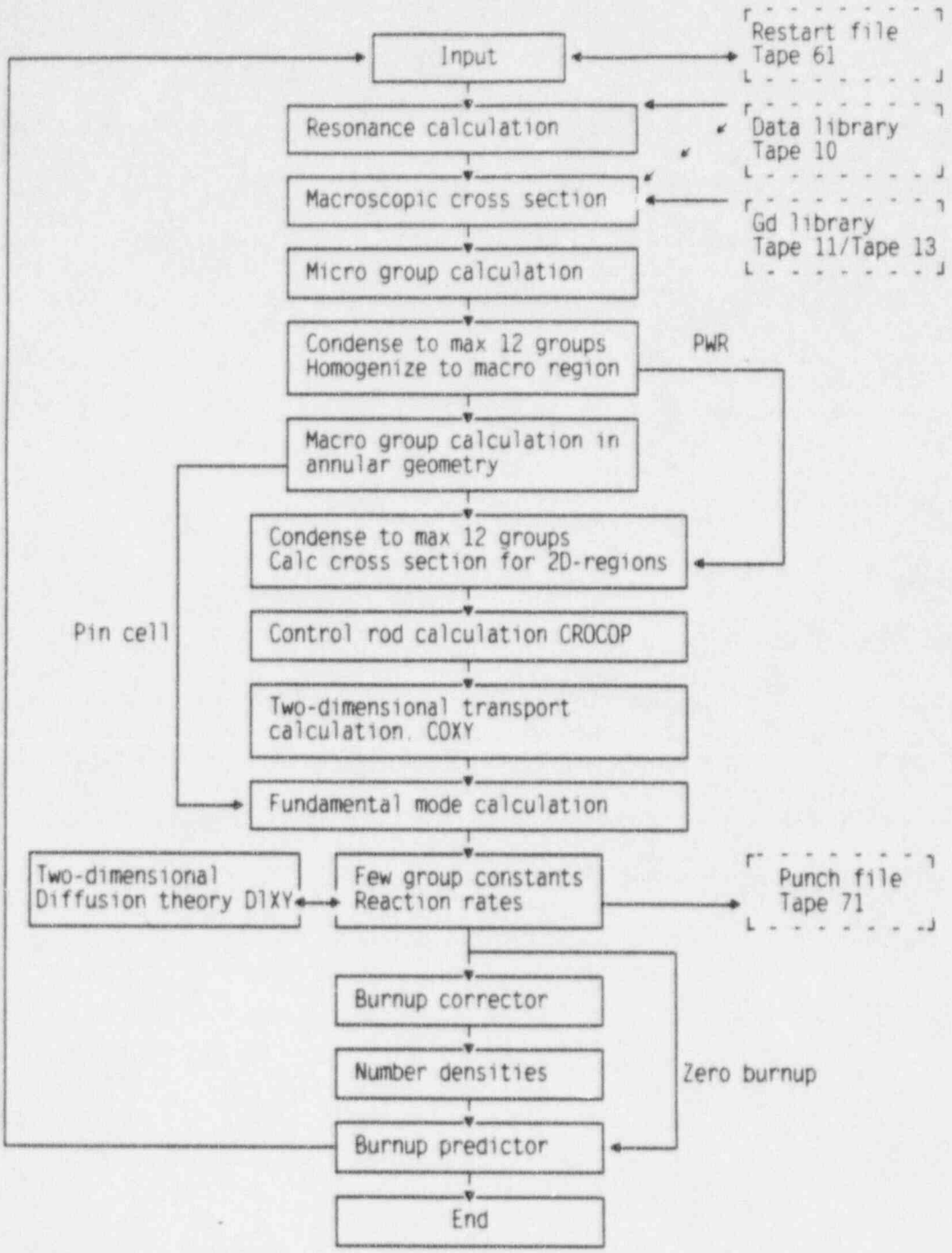

3.0 CASMO-3 VERIFICATION

CASMO-3 has been benchmarked by GPU Nuclear against selected pin cell critical experiments to verify the accuracy of the nuclear data library, neutron transport treatment and pin cell calculations. The GPUN benchmark used the options recommended by Studsvik and the results are described in Section 3.1. Other benchmarks are summarized in Section 3.2. Since the SIMULATE-3 cross section library is generated by CASMO-3 using the same vendor recommended options, the good agreement between the reactor operation data and CASMO-3/ SIMULATE-3 results shown in Chapter 4 indirectly validate the CASMO-3 modeling accuracy.

3.1 Comparison with Uniform Pin Cell Criticals

The purpose of the pin cell critical comparisons is to provide an integral verification of the nuclear data library and the treatment of neutron transport and spectrum in pin cells. The NS&E criticals (Ref. 5) and the KRITZ criticals (Ref. 6) are modeled using CASMO-3. The pin cells are modeled as infinite uniform lattices. The measured buckling values are used for leakage corrections. The 40 group library is used in the criticality calculation.

The NS&E criticals are room temperature critical experiments with variations in fuel lattice pitch, fuel enrichment, and the soluble boron concentration. The critical experiments of interest are the ones with uranium oxide fuel and a light water moderator with key parameters given in Table 3-1. The CASMO-3 calculated K-effectives are also listed in Table 3-1. The mean K-effective for the cases modeled is 0.99227 with a 0.00822 standard deviation.

The KRITZ pin cell criticals are a series of critical experiments performed at various moderator temperatures and boron concentrations. Uranium oxide fuel rods of 1.35 w/o are used in the experiments and the lattice pitch is 1.8 cm. The moderator temperature, boron concentration, the measured buckling values and the calculated K-effectives are listed in Table 3.2 together with the CASMO-3 calculated K-effectives. The mean K-effective for the 24 KRITZ criticals modeled is 0.99574 with a 0.00201 standard deviation.

The calculated multiplication factors of both sets are all close to unity and show no specific trend. The statistics of these pin cell comparisons are shown in Table 3.3. The average multiplication factors for the 63 cases studied is 0.99359 with a standard deviation of 0.00677. The calculated K-effectives are plotted against fuel enrichment, moderating ratio, pellet diameter and buckling in Figures 3.1 to 3.6 which show no obvious trend in any parameter. Considering the experimental uncertainty in the measured buckling and a lack of an asymptotic spectrum in small cores, the agreement is very good. The pin cell criticals benchmark the accuracy of CASMO-3 nuclear data library, treatment of neutron transport and spectrum in pin cells.

3.2 Validation by Studsvik

CASMO-3 has been benchmarked extensively by Studsvik Energitenik, the developer of CASMO-3 (Ref. 4). The benchmarking covers pin cell lattices, BWR lattices with and without gadolinium and cruciform control rod, PWR lattices with small and large water holes, Ag-In-Cd control rods and large B_4C burnable poison rods, and fuel storage rack configurations. The cases are:

- **Pin Cell Criticals**

  The BAPL, ESADA and TRX (Refs. 7, 8, 9) critical experiments are analyzed using the CASMO-3 fundamental mode to determine K-effective. The BAPL fuel is uranium oxide and the TRX fuel is uranium metal. The ESADA cases consist of 0.7 w/o U-235 with 1.8 w/o enriched Pu-239. The experimental data and the calculated K-effective are shown in Table 3.4.

- **KRITZ Critical Experiments**

  The KRITZ experiments (Ref. 10) consist of several core types: KRITZ-1 and KRITZ-2 are regular pin cell cores, KRITZ-3 contains PWR assemblies and KRITZ-4 contains BWR assemblies. The description of these critical cores are listed in Tables 3.5 and 3.6. The CASMO-3 calculated K-effectives are given in Table 3.7.

- **B&W Critical**

  Five B&W critical cores (Ref. 11); one regular pin cell lattice and four 3x3 PWR type assemblies (14x14) are modeled. All five cores have a U-235 enrichment of 2.46 percent. The calculated K-effectives are summarized in Table 3.8.

- **Other Pin Cell Cores**

  Four other pin cell cores, BAPL-UO_2 T6, B&W B20, ESADA A-1 and C-18, and B&W 20 (Refs. 7, 8, 12, respectively) are also analyzed. All the experiments are performed at room temperature.

  The BAPL-UO_2 T6 core has a 19 cm radius and 1.45 w/o enrichment. The B&W B20 core has a 31 cm radius and 2.46 w/o enrichment. The ESADA A-1 core has a 22 cm radius and the C18 core has two annular regions of 15 cm and 22 cm radii. The ESADA cores have natural UO_2 fuel containing 2% PuO_2. The fraction of Pu239 in total Pu for the A-1 fuel and the outer region C-18 fuel is 92% while it is 72% in the inner region of C-18 fuel. The Pu240 fractions are 8% and 24%, respectively. Other experimental data and calculated K-effectives are listed in Table 3.9.

  The calculated K-effective values are close to 1.000 as summarized in Table 3.10. There is no observed trend in K-effective versus any parameter. These provide a verification of the CASMO-3 nuclear data library, the two-dimensional transport theory calculation, and the absorber calculation.

Table 3.1 NS&E UO_2 Critical Experiments

Case Number	Enrichment at %	Volume Ratio $V_{H_2O}:V_u$	Fuel Density (g/cc)	Pellet Diameter (cm)	Lattice Pitch (cm)	Boron Conc. (ppm)	Measured Buckling (M^{-2})	K_{eff} (CASMO-3)
1	1.328	3.02	7.53	1.5265	2.205	0	28.37	0.99370
2	1.328	3.95	7.53	1.5265	2.359	0	30.17	0.99638
3	1.328	4.95	7.53	1.5265	2.512	0	29.06	0.99702
4	1.328	3.93	7.52	0.9855	1.558	0	25.28	0.99455
5	1.328	4.89	7.52	0.9855	1.652	0	25.21	0.99453
6	1.328	2.88	10.53	0.9728	1.558	0	32.59	0.99783
7	1.328	3.58	10.53	0.9728	1.652	0	35.47	0.99653
8	1.328	4.83	10.53	0.9728	1.806	0	34.22	0.99710
9	2.734	2.18	10.18	0.7620	1.0287	0	40.75	1.00120
10	2.734	2.93	10.18	0.7620	1.1049	0	53.23	0.99905
11	2.734	3.86	10.18	0.7620	1.1938	0	63.26	0.99500
12	2.734	7.02	10.18	0.7620	1.4554	0	65.64	1.00161
13	2.734	8.49	10.18	0.7620	1.5621	0	60.07	1.00627
14	2.734	10.38	10.18	0.7620	1.6891	0	52.92	1.00554
15	2.734	2.50	10.18	0.7620	1.0617	0	47.5	0.99744
16	2.734	4.51	10.18	0.7620	1.2522	0	68.8	0.98847
17	3.745	2.50	10.37	0.7544	1.0617	0	68.3	0.99609
18	3.745	4.51	10.37	0.7544	1.2522	0	95.1	0.98869
19	3.745	4.51	10.37	0.7544	1.2522	0	95.68	0.98702
20	3.745	4.51	10.37	0.7544	1.2522	462	74.64	0.98773
21	3.745	4.51	10.37	0.7544	1.2522	718	63.66	0.98848
22	3.745	4.51	10.37	0.7544	1.2522	1277	40.99	0.99170
23	3.745	4.51	10.37	0.7544	1.2522	1349	38.39	0.99171
24	3.745	4.51	10.37	0.7544	1.2522	1493	33.38	0.99120
25	4.069	2.55	9.46	1.1278	1.5113	0	88	0.98042
26	4.069	2.55	9.46	1.1278	1.5113	3431	17.2	0.99937
34	4.069	2.14	9.46	1.1278	1.45	0	79	0.97844
37	2.49	2.84	10.24	1.0297	1.5113	0	70.1	1.00609
42	3.037	2.64	9.28	1.1268	1.555	0	50.75	0.98582
43	3.037	8.16	9.28	1.1268	2.198	0	68.81	0.97672
44	4.069	2.59	9.45	1.1268	1.555	0	69.25	0.99003
45	4.069	3.53	9.45	1.1268	1.684	0	85.52	0.98158
46	4.069	8.02	9.45	1.1268	2.198	0	92.84	0.99594
47	4.069	9.90	9.45	1.1268	2.381	0	91.79	0.98509
50	2.49	2.84	10.24	1.0297	1.5113	1694	20.2	1.00298
52	2.096	3.09	10.38	1.5240	2.4052	0	80.6	0.99489
53	2.096	4.12	10.38	1.5240	2.6162	0	85.7	0.98056
54	2.096	6.14	10.38	1.5240	2.9891	0	77	0.97805
55	2.096	8.20	10.38	1.5240	3.3255	0	61.6	0.97755

Table 3.2 KRITZ Pin Cell Critical Experiments

Case Number	Core Type	Boron Conc. (ppm)	Temperature (°C)	Measured Buckling (M^{-2})	K_{eff} (CASMO-3)
1	39(0)36	0.8	20	40	0.99615
2		0.8	40	39	0.99602
3		0.8	90	37	0.99495
4		0.8	120	35	0.99426
5		0.8	140	34	0.99381
6		0.8	180	32	0.99314
7		0.8	195	30	0.99299
8		0.8	205	30	0.99293
9		0.8	215	29	0.99295
10		0.8	225	28	0.99299
11	46(0)36	47	90	35	0.99587
12		47	205	27	0.99464
13		47	225	26	0.99441
14		47	245	24	0.99454
15	46(0)36	175	20	30	0.99855
16		175	35	30	0.99832
17		175	50	29	0.99808
18		175	65	29	0.99788
19		175	80	28	0.99770
20		175	90	28	0.99754
21		175	160	25	0.99733
22		175	170	24	0.99740
23		175	185	23	0.99754
24		175	205	22	0.99766

Table 3.3 Pin Cell Critical Statistics

		CASMO-3	
Criticals	**Number of Experiments**	**K-effective Average**	**Standard Deviation**
NS&E	39	0.99227	0.00822
KRITZ	24	0.99574	0.00201
ALL	63	0.99359	0.00677

Table 3.4 K_{eff} for Pin Cell Criticals*

Pin Cell	Pin Radii (cm)	Pitch (cm)	Enr (w/o)		Boron Conc (ppm)	B^2 (M^{-2})	K_{eff} (CASMO-3)
BAPL-UO_2 T1	0.76	2.1	1.3		0	28	0.99424
BAPL-UO_2 T2	0.76	2.2	1.3		0	30	0.99608
BAPL-UO_2 T3	0.76	2.3	1.3		0	29	0.99528
BAPL-UO_2 T4	0.49	1.4	1.3		0	25	0.99591
BAPL-UO_2 T5	0.49	1.5	1.3		0	25	0.99565
BAPL-UO_2 T6	0.49	1.4	1.3		0	33	0.99888
BAPL-UO_2 T7	0.49	1.5	1.3		0	35	0.99736
BAPL-UO_2 T8	0.49	1.7	1.3		0	34	0.99705
TRX 1	0.49	1.7	1.3		0	57	0.99228
TRX 2	0.49	2.0	1.3		0	55	0.99137
			U^{235}	Pu^{239}			
ESADA A-1	0.64	1.8	0.7	1.8	0	69	0.98827
ESADA A-3	0.64	1.9	0.7	1.8	0	90	0.98295
ESADA A-4	0.64	2.5	0.7	1.8	0	105	0.99873
ESADA A-6	0.64	2.7	0.7	1.8	0	98	1.00044
ESADA A-7	0.64	3.5	0.7	1.8	0	50	0.99707
ESADA A-8	0.64	1.8	0.7	1.8	260	63	0.99651
ESADA A-9	0.64	2.5	0.7	1.8	260	84	0.99490
ESADA A-10	0.64	1.8	0.7	1.8	530	58	0.99517
ESADA A-11	0.64	2.5	0.7	1.8	530	63	0.99571
ESADA A-12	0.64	2.5	0.7	1.4	0	80	0.99737
ESADA A-13	0.64	2.7	0.7	1.4	0	73	0.99763

* Benchmark results by Studsvik Energitenik AB (Ref. 4).

Table 3.5 Data for the KRITZ Series of Critical Cores

Series	Enrichment (w/o)	Pitch (cm)	Pin Radii (cm)
K1	1.35	1.80	0.62
K2	1.86	1.48 & 1.63*	0.53
K3	3	1.4	0.5
K4	2.6	1.6	0.5

* For K2 2:1 and 2:13 respectively.

Table 3.6 Description of KRITZ Critical Cores

K3 U-WH1	16 1x1 water holes, including guide tubes in the central assembly.
K3 U-CR1	Same as U-WH1 but with Ag-In-Cd control rods inserted in the guide tubes.
K3 U-WH2	5 2x2 water holes in the central assembly and 3 in the peripheral ones.
K3 U-CR2	Same as U-WH2 but with boron-carbide control rods inserted in the central water holes.
K4 2:1	All assemblies unpoisoned.
K4 2:2	Same as 2:1 but with a control rod cross in the central water gap.
K4 2:5	Same as 2:1 but with 7 Gd rods in each of the 4 central assemblies.
K4 3:1	All assemblies unpoisoned.
K4 3:2	Same as 3:1 but with 5 Gd rods in each of the 4 central assemblies.
K4 3:5	Same as 3:1 but with 3 Gd rods in each of the 4 central assemblies.
K4 4:1	Same as 3:1 but with 5 Gd rods in every second of the assemblies, in a checker board configuration.
K4 4:2	Same as 3:1 but with 3 Gd rods in every second of the assemblies, in a checker board configuration.
K4 5:1	Same as 3:1 but with 3 Gd rods in each assembly.

Table 3.7 Calculated K_{eff} for KRITZ Cores*

Core	Temp (K)	Boron Conc (ppm)	K_{eff} (CASMO-3)
K1	290	180	0.99869
	480	180	0.99878
K2 2:1	290	220	1.00000
	520	30	1.00072
K2 2:13	290	450	0.99887
	520	280	0.99895
K3 U-WH1	300	1100	0.99880
	500	1000	0.99926
K3 U-CR1	300	700	1.00027
	500	500	0.99876
K3 U-WH2	300	1100	1.00031
	500	1000	1.00024
K3 U-CR2	300	700	0.99970
	500	500	0.99953
K4 2:1	300	300	1.00064
K4 2:2	300	100	1.00018
K4 2:5	300	50	1.00014
K4 3:1	300	300	1.00104
	500	350	1.00155
K4 3:2	300	100	1.00164
	500	50	1.00147
K4 3:5	300	200	1.00180
	500	200	1.00152
K4 4:1	300	100	1.00067
	500	50	1.00036
K4 4:2	300	200	1.00127
K4 5:1	300	50	1.00034
	500	0	0.99932

* Benchmark results by Studsvik Energitenik AB (Ref. 4).

Table 3.8 Summary of B&W Cores*

Core	Gap (Pitch)	Boron Conc. (ppm)	K_{eff} (CASMO-3)
I	---	0	1.00026
II	0	1040	1.00145
III	1	760	1.00291
IX	4	0	1.00037+
X	3	140	1.00240

* Benchmark results by Studsvik Energitenik AB (Ref. 4).

+ K_{eff} reduced by 0.00300 for comparison since the experimental K_{eff} was determined to be 1.00300.

Table 3.9 Summary of Data of the T6, B20 and ESADA Cores*

Core	Pin Radii (cm)	Pitch (cm)	Boron Conc (ppm)	K_{eff} (CASMO-3)
BAPL-UO_2 T6	0.49	1.45	0	1.00132
B&W B20	0.52	1.51	1670	1.00082
ESADA A-1	0.64	1.75	0	0.99937
ESADA C-18	0.64	1.75	0	1.00080

* Benchmark results by Studsvik Energitenik AB (Ref. 4).

Table 3.10 K_{eff} Statistics for CASMO-3*

		K_{eff} (CASMO-3)
Cold pin cells	(9 cases)	1.00018 ± .00102
Hot pin cells	(3 cases)	0.99948 ± .00107
All pin cells	(12 cases)	1.00001 ± .00103
Cold PWR cores	(4 cases)	0.99977 ± .00070
Hot PWR cores	(4 cases)	0.99945 ± .00062
All PWR cores	(8 cases)	0.99961 ± .00064
Cold BWR cores	(9 cases)	1.00086 ± .00062
Hot BWR cores	(5 cases)	1.00084 ± .00099
All BWR cores	(14 cases)	1.00085 ± .00073
Cold B&W cores	(5 cases)	1.00148 ± .00118
All cold cores	(25 cases)	1.00056 ± .00105
Cold cores which were also measured hot	(12 cases)	1.00018 ± .00104
All hot cores	(12 cases)	1.00004 ± .00108
All cores	(37 cases)	1.00039 ± .00107

* Benchmark results by Studsvik Energitenik AB (Ref. 4).

Figure 3.1
CASMO-3 PIN CELL CRITICALS
K-EFFECTIVE VS. ENRICHMENT

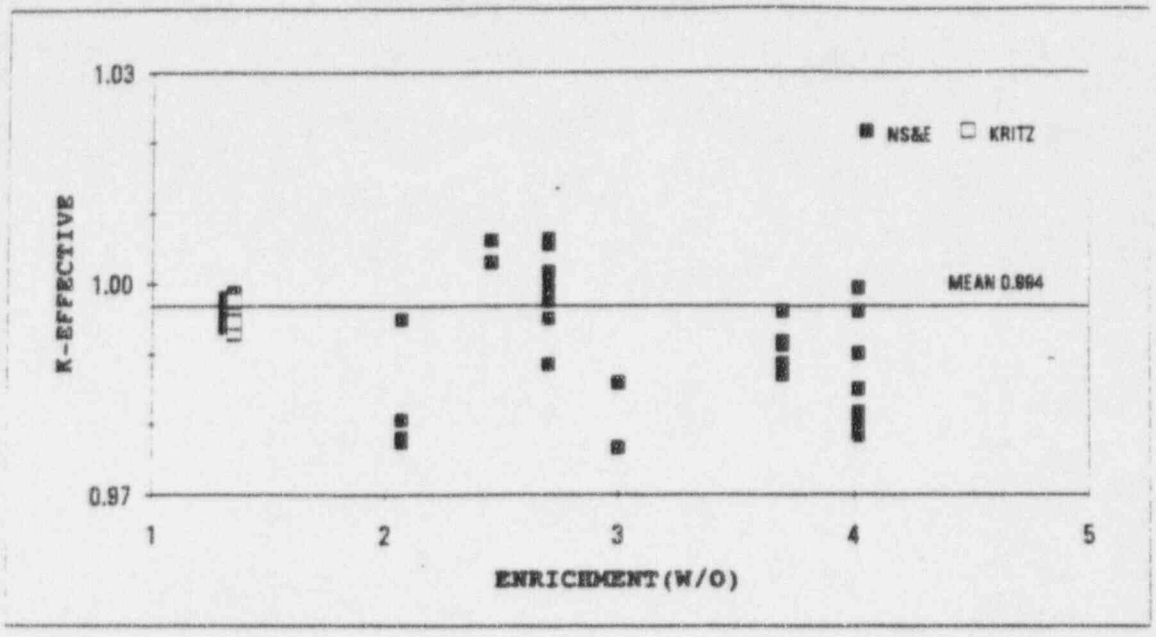

Figure 3.2
CASMO-3 PIN CELL CRITICALS
K-EFFECTIVE VS. LATTICE PITCH

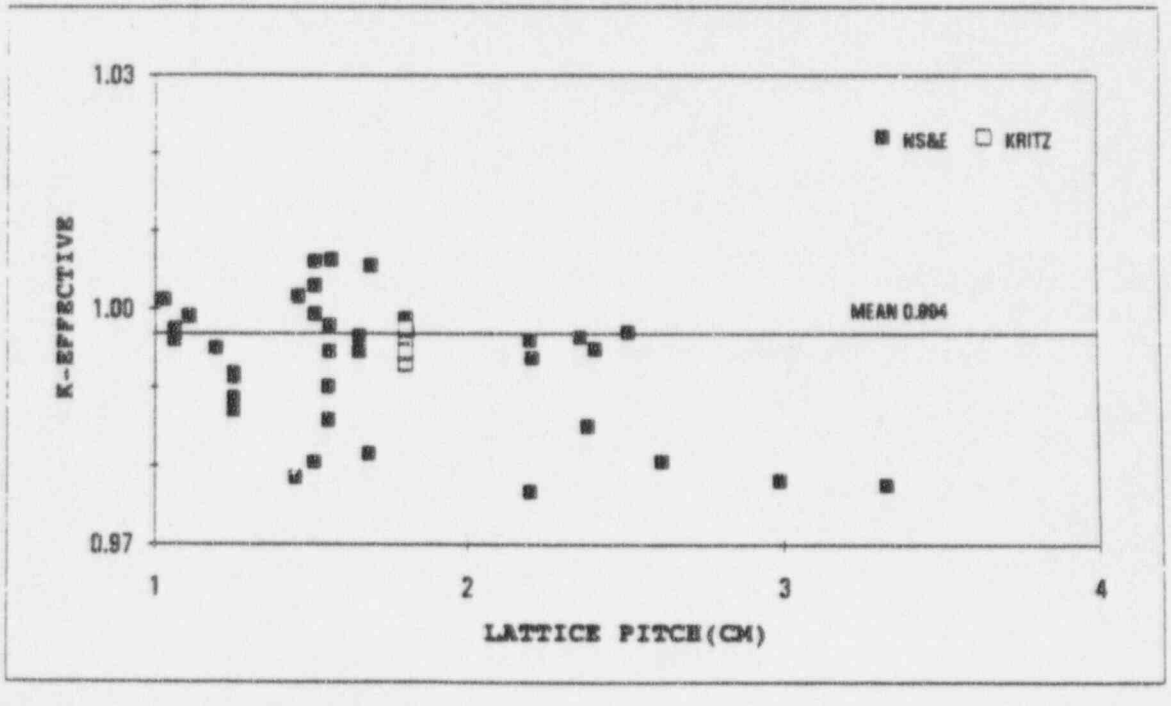

Figure 3.3

CASMO-3 PIN CELL CRITICALS

K-EFFECTIVE VS. H20/U VOLUME RATIO

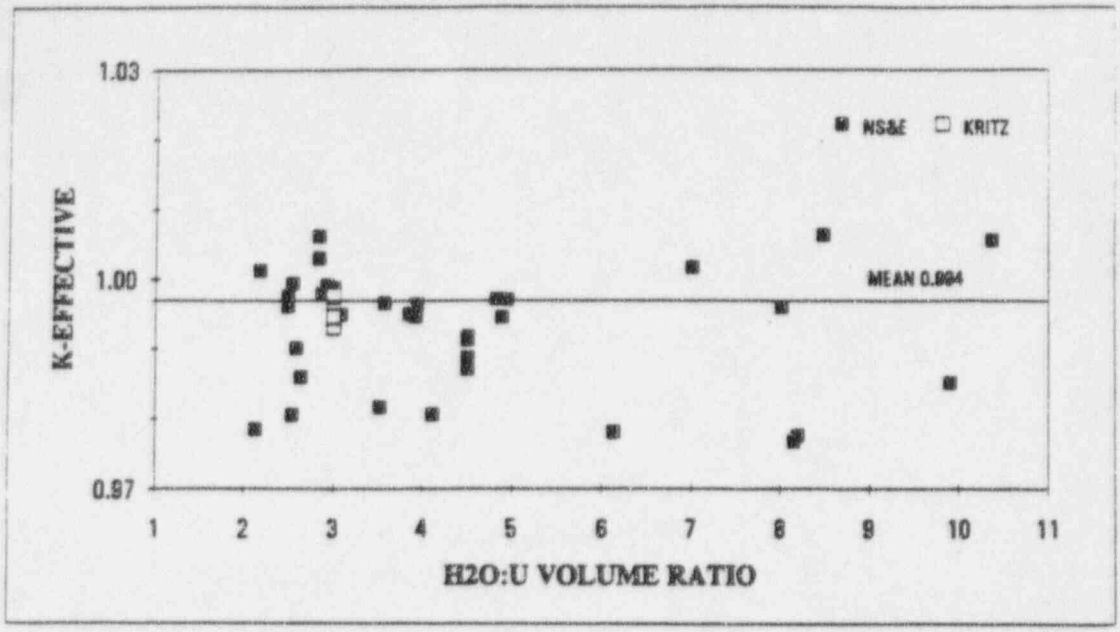

Figure 3.4

CASMO-3 PIN CELL CRITICALS

K-EFFECTIVE VS. BORON CONCENTRATION

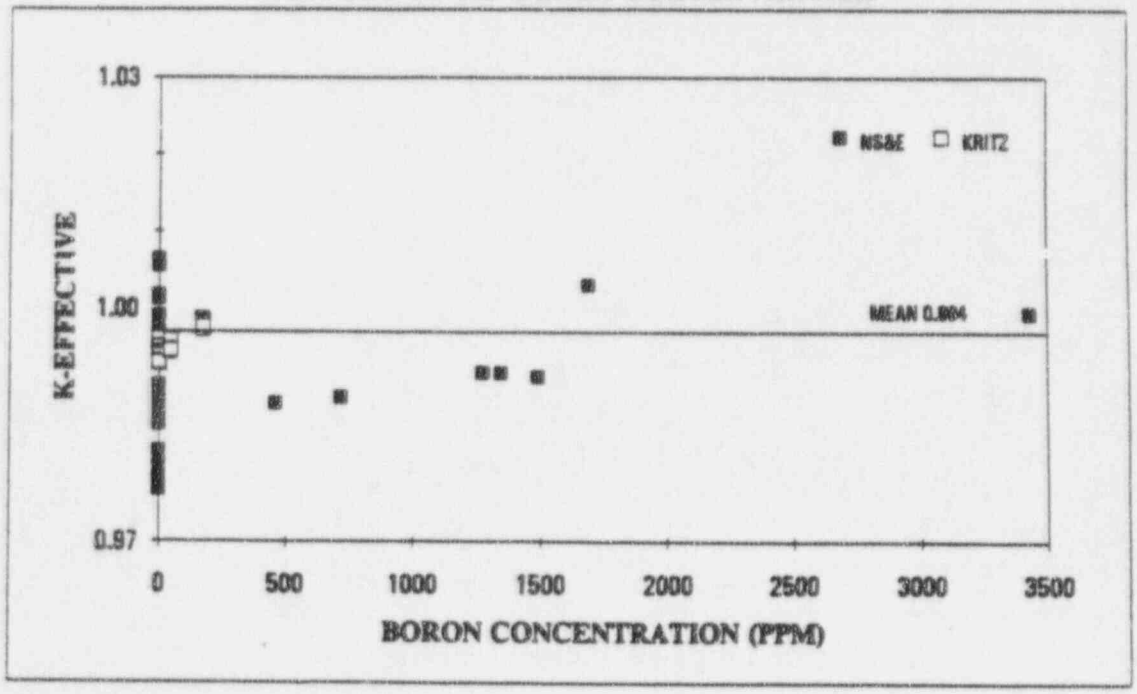

Figure 3.5

CASMO-3 PIN CELL CRITICALS

K-EFFECTIVE VS. MODERATOR TEMPERATURE

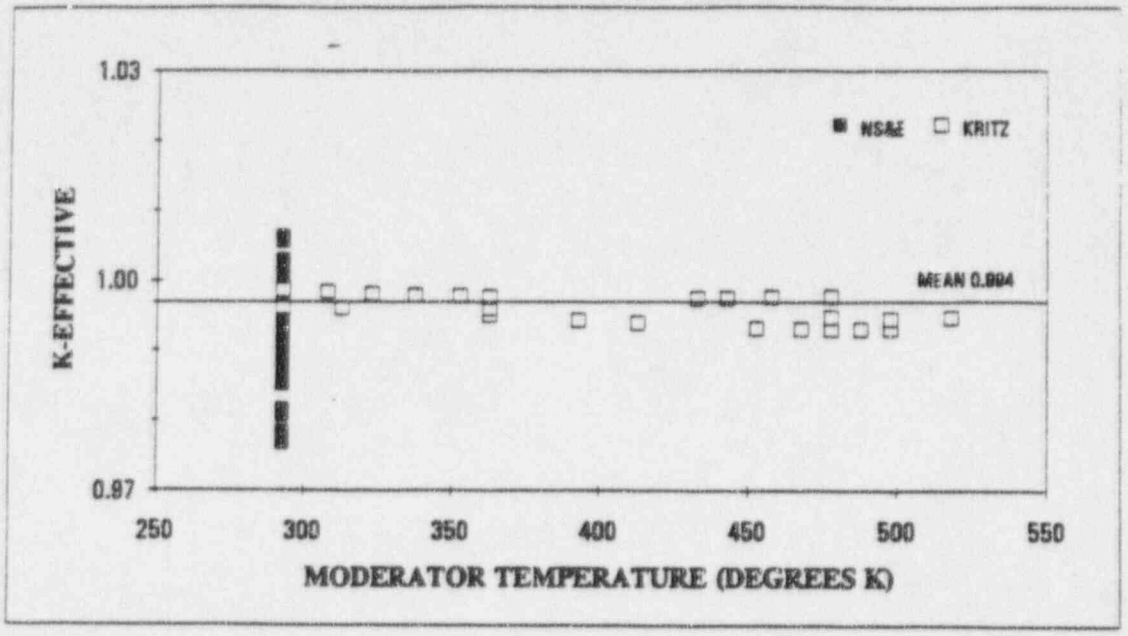

Figure 3.6

CASMO-3 PIN CELL CRITICALS

K-EFFECTIVE VS. MEASURED BUCKLING

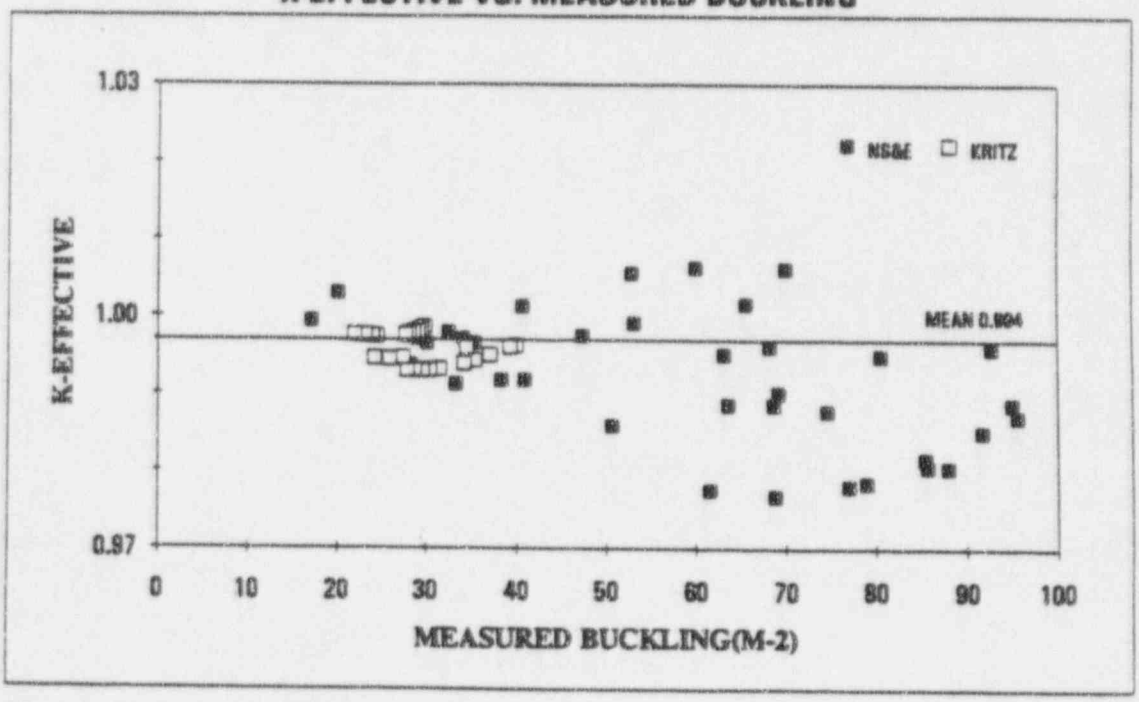

4.0 SIMULATE-3 VERIFICATION

The SIMULATE-3 model is a three-dimensional model with a 2x2 radial node mesh per assembly and twenty-four axial nodes. The top, bottom and radial reflector regions are also explicitly modeled. Thermal hydraulic feedback and Doppler feedback are used. Fuel temperature is expressed as a function of power and exposure. The boron history and moderator temperature history effect are included in the model. Close agreement between the modeling results and TMI-1 operating data (Refs. 19-28) validates the applicability of SIMULATE-3 to the TMI-1 core.

4.1 Boron Letdown Results

Critical boron concentration is measured regularly during operation. Hot full power depletions are performed to calculate the critical boron concentration for TMI-1 cycles. The SIMULATE-3 calculated values are compared to the measured data at steady state operation statepoints and the results are plotted in Figures 4.1 - 4.9. The difference in the letdown boron comparison is usually small at the beginning and at the end of the cycle, with the maximum difference occurring at the middle of the cycle. This phenomena is especially noticeable for Cycles 6, 7, 8, and 9 with longer cycle lengths as shown in Figure 4.10. The large dip in the middle of the cycle can be accounted for by the depletion of B-10 in the soluble boron.

Starting in Cycle 8, reactor coolant samples were taken regularly to measure the B-10 atomic %. The B-10 atomic % is close to 19.8% at the beginning of the cycle and it depletes to about 17% at the end of cycle assuming no replenishment of the coolant with fresh (natural) boron. Since the cross sections are generated based on constant B-10 atomic % of 19.8, adjustments are made to the plant measured boron values to compensate for the B-10 depletion effect. These are also plotted in Figures 4.8 and 4.9. With the B-10 depletion correction, the letdown boron comparison improves significantly as shown in Figure 4.10. Since future TMI-1 cycles will be two-year cycles with periodic

sampling of the B-10 atomic % as done in Cycles 8 and 9, the average difference of -9 ppm with a 9 ppm standard deviation is the model uncertainty for future cycles (see Table 4.1).

4.2 Hot Full Power Comparisons

The TMI-1 incore detector system consists of 52 detector strings with seven fixed rhodium detectors in each string. The detector strings are radially arranged to provide complete neutron flux information for one-quarter of a symmetric core. Symmetry can be applied to obtain full core neutron flux information. The detector signals are corrected for background, leakage, detector sensitivity and rhodium depletion.

The corrected signals from the rhodium detectors are connected to the assembly power by the plant process computer software (Ref. 31). The inferred measured assembly power distribution is compared to SIMULATE-3 predicted assembly powers at selected steady state points in the cycle. Results from Cycles 1-5 are not included here because of the change of process computer software (Ref. 32) and the breakdown of detector insulation which resulted in a large uncertainty in the plant measured power.

The calculated radial power distribution compares well with the measured power distribution. The average % difference is 1.76% with a 0.71% standard deviation based on a total of 106 state points comparisons. Table 4.2 summarizes the radial power comparison results for Cycles 6-9. Figures 4.11 - 4.22 give the radial power distribution comparisons at the beginning, middle, and end of Cycles 6-9.

The axial offset which is defined as:

$$A\text{-}O = \frac{P_T - P_B}{P_T + P_B} X\ 100$$

where

P_T = power in the top half of the core

P_B = power in the bottom half of the core

are also compared in Table 4.3. The average difference between the calculated and measured axial offset is 1.15% with a 1.22% standard deviation. The agreement is very good considering that the measured axial offset varies by 2% during a day due to boron dilution and control rod movement. Figures 4.23 - 4.34 provide the axial power distribution comparisons for Cycles 6-9. The overall agreement of the predictions with measurements for all four cycles is excellent.

4.3 Hot Zero Power Comparisons

The hot zero power (HZP) physics test is conducted at the beginning of the cycle to determine if the operating characteristics of the core are consistent with the design predictions and to assure that the core can be operated as designed. The test condition is 532°F and 2155 psig. This section compares the test results with the SIMULATE-3 predicted values.

4.3.1 All Rods Out Critical Boron Concentration

The all rods out critical boron concentration is determined by borating the core to an all rods out critical steady-state condition. Calculated and measured data are compared in Table 4.4. The average difference is -13 ppm with a 14 ppm standard deviation.

4.3.2 Control Rod Worth

There are 61 full length control rods and 8 partial length control rods at TMI. The control rods

are grouped into eight groups with Group 8 consisting of eight partial length control rods. Groups 1 through 4 are the safety rods while Groups 5 through 7 are the regulating control rods.

The control rod worth of Groups 5, 6, and 7 are measured during the HZP physics test using the boron swap technique. This technique establishes a deboration rate of the reactor coolant system with compensation for the reactivity change through insertion of the control rod group(s) of interest in incremented steps. The reactivity change is determined by a reactimeter. The control rod group worth is the sum of the reactivity changes for that group. Table 4.5 shows the comparison between the calculated and measured control rod group worths. The mean of % differences is -2.78 with a standard deviation of 4.21 for an individual regulating control rod group's worth. The mean of % difference is -2.93 with a standard deviation of 3.15 for the worth of all regulating control rod groups (See Table 4.6).

4.3.3 Isothermal Temperature Coefficient

The isothermal temperature coefficient at HZP is measured by first increasing the reactor coolant's inlet temperature by 5°F, then decreasing it by 10°F and finally increasing it by 5°F. The isothermal temperature coefficient is the change of reactivity divided by the corresponding temperature change. Table 4.7 compares the calculated and measured coefficient. The mean difference is 0.88 pcm/°F with a standard deviation of 0.34 pcm/°F.

4.4 TMI-1 Power Transient

On November 20, 1992, TMI-1 intentionally reduced power to 50% from 100% in order to clean Asiatic clams from the main condenser water boxes. After operating at 50% power for 3 days, the plant

returned to 100% power on November 23, 1992. The 100-50-100 power transient was successfully simulated with SIMULATE-3. Figure 4.35 provides graphs of the core power, Group 7 control rod position, and axial imbalance versus time for the SIMULATE-3 model. The calculated imbalance swing agrees very well with the measured imbalance with slightly higher peaks. During the power reduction, SIMULATE-3 estimated that the Group 7 control rod critical position was 27% withdrawn at 50% power which compares very well with the actual critical position of 34% withdrawn. In addition, SIMULATE-3 model predicted that 627 gallons of the Boric Acid Mix Tank (BAMT) borated water was needed in order to keep the reactor at 50% power while withdrawing Group 7 to 90%. This compares very well to the actual addition of 636 gallons. SIMULATE-3 estimates 5000 gallons of demineralized water would be required to deborate the core for the return to 100% power. This is also close to the actual 4750 gallons of water added.

SIMULATE-3 successfully calculated the axial imbalance, critical control rod position, and critical boron concentrations during the power transient. These comparisons demonstrate that SIMULATE-3 can model the xenon effects during a power transient.

Table 4.1 HFP Letdown Boron Comparisons*

Cycle	Number of State Points	Average Difference (PPM)	Standard Deviation (PPM)
8	27	-13	9
9	25	-4	7
8 & 9 combined	52	-9	9

* Difference = SIMULATE-3 - Measurement

Table 4.2 HFP Radial Power Distribution Comparisons*

Cycle	Number of State Points	Average Difference (%)	Standard Deviation (%)
6	30	1.00	0.20
7	24	1.35	0.15
8	27	2.61	0.13
9	25	2.15	0.51
6-9 combined	106	1.76	0.71

* % Difference = (SIMULATE-3 - Measurement) * 100 / Measurement

Table 4.3 HFP Axial Offset Comparisons*

Cycle	Number of State Points	Average Difference (%)	Standard Deviation (%)
6	30	1.46	1.14
7	24	0.73	1.05
8	27	1.51	1.49
9	23	0.77	1.03
6-9 combined	104	1.15	1.22

* % Difference = (SIMULATE-3 - Measurement) * 100 / Measurement

Table 4.4 BOC HZP ARO Critical Boron

Cycle	Measured (PPM)	SIMULATE-3 (PPM)	Difference (PPM)
1	1617	1608	-9
2	1384	1379	-5
3	1249	1235	-14
4	1231	1213	-18
5	1182	1151	-31
6	1449	1444	-5
7	1691	1663	-28
8	1846	1817	-29
9	2157	2172	15
10	2421	2418	-3
		Average	-13
		Standard Deviation	14

Table 4.5 BOC HZP Control Rod Worth–Individual Groups

Cycle	CR Group	Measured (PCM)	SIMULATE-3 (PCM)	Difference (%)
1	5	1030	1132	9.90
1	6	1250	1188	-4.96
1	7	1100	1102	0.18
2	5	675	665	-1.48
2	6	1056	1038	-1.70
2	7	772	779	0.91
3	5	1127	1058	-6.12
3	6	1013	990	-2.27
3	7	789	742	-5.96
4	5	1420	1384	-2.54
4	6	1070	971	-9.25
4	7	1480	1381	-6.69
5	5	946	951	0.53
5	6	863	813	-5.79
5	7	1400	1311	-6.36
6	5	1531	1534	0.20
6	6	759	781	2.90
6	7	964	967	0.31
7	5	1220	1240	1.64
7	6	934	936	0.21
7	7	926	939	1.40
8	5	1214	1147	-5.52
8	6	927	852	-8.09
8	7	974	911	-6.47
9	5	1134	1051	-7.32
9	6	817	807	-1.22
9	7	889	833	-6.30
10	5	1400	1318	-5.86
10	6	713	708	-0.70
10	7	981	913	-6.93
			Average	-2.78
			Standard Deviation	4.21

Table 4.6 BOC HZP Control Rod Worth–Regulating Groups

Cycle	Regulating CR Group	Measured (PCM)	SIMULATE-3 (PCM)	Difference (%)
1	5-7	3380	3422	1.24
2	5-7	2503	2482	-0.84
3	5-7	2929	2790	-4.75
4	5-7	3970	3736	-5.89
5	5-7	3209	3075	-4.18
6	5-7	3254	3282	0.86
7	5-7	3080	3115	1.14
8	5-7	3115	2910	-6.58
9	5-7	2840	2691	-5.25
10	5-7	3094	2939	-5.01
			Average	-2.93
			Standard Deviation	3.15

Table 4.7 BOC HZP Isothermal Temperature Coefficients

Cycle	Boron (ppm)	Measured (PCM/°F)	SIMULATE-3 (PCM/°F)	Difference (PCM/°F)
1	1601	4.49	5.43	0.94
1	1461	3.04	3.89	0.85
1	1269	-5.27	-3.98	1.29
1	1245	-6.04	-4.43	1.61
2	1366	0.94	1.70	0.76
2	1149	-5.31	-4.60	0.71
3	1248	-0.30	0.41	0.71
3	992	-6.80	-6.07	0.73
4	1234	0.26	1.01	0.75
4	880	-10.80	-9.26	1.54
5	1178	-2.25	-1.34	0.91
5	801	-12.96	-12.14	0.82
6	1445	0.57	1.04	0.47
7	1682	2.41	3.49	1.08
8	1840	1.50	2.00	0.50
9	2149	3.11	3.51	0.40
10	2417	2.13	3.00	0.87
			Average	0.88
			Standard Deviation	0.34

Figure 4.1
CYCLE 1 BORON COMPARISON

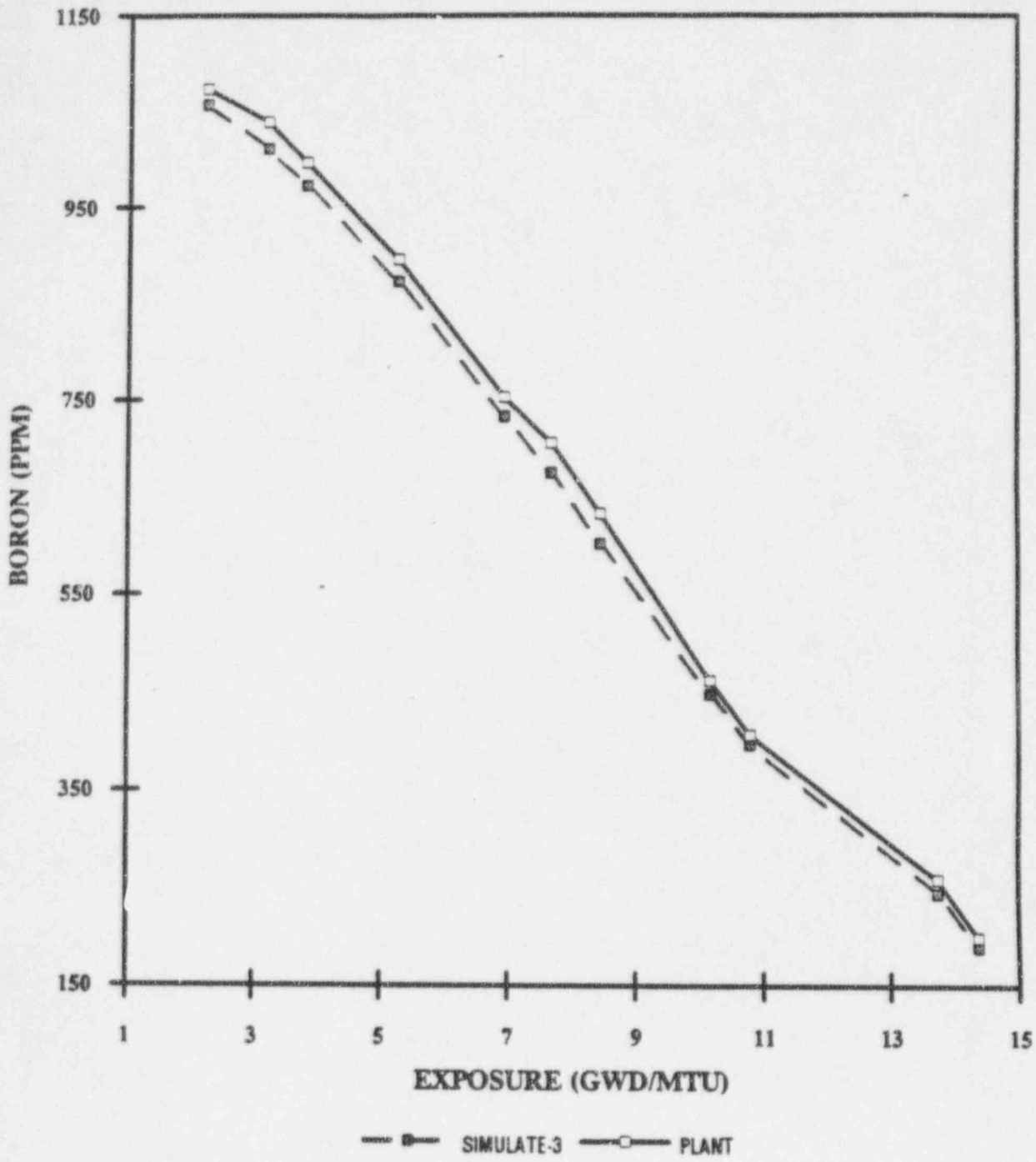

Figure 4.2
CYCLE 2 BORON COMPARISON

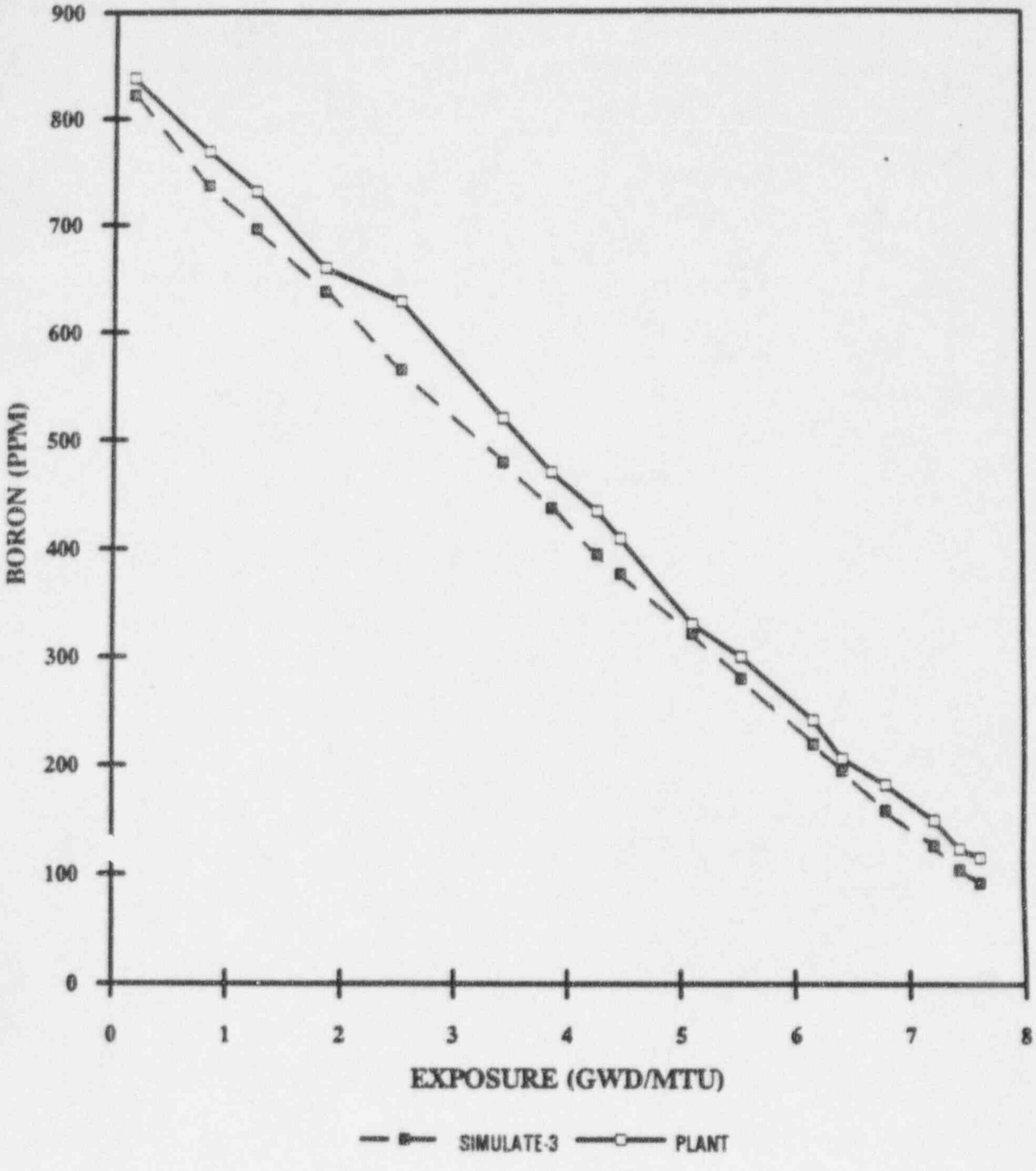

Figure 4.3

CYCLE 3 BORON COMPARISON

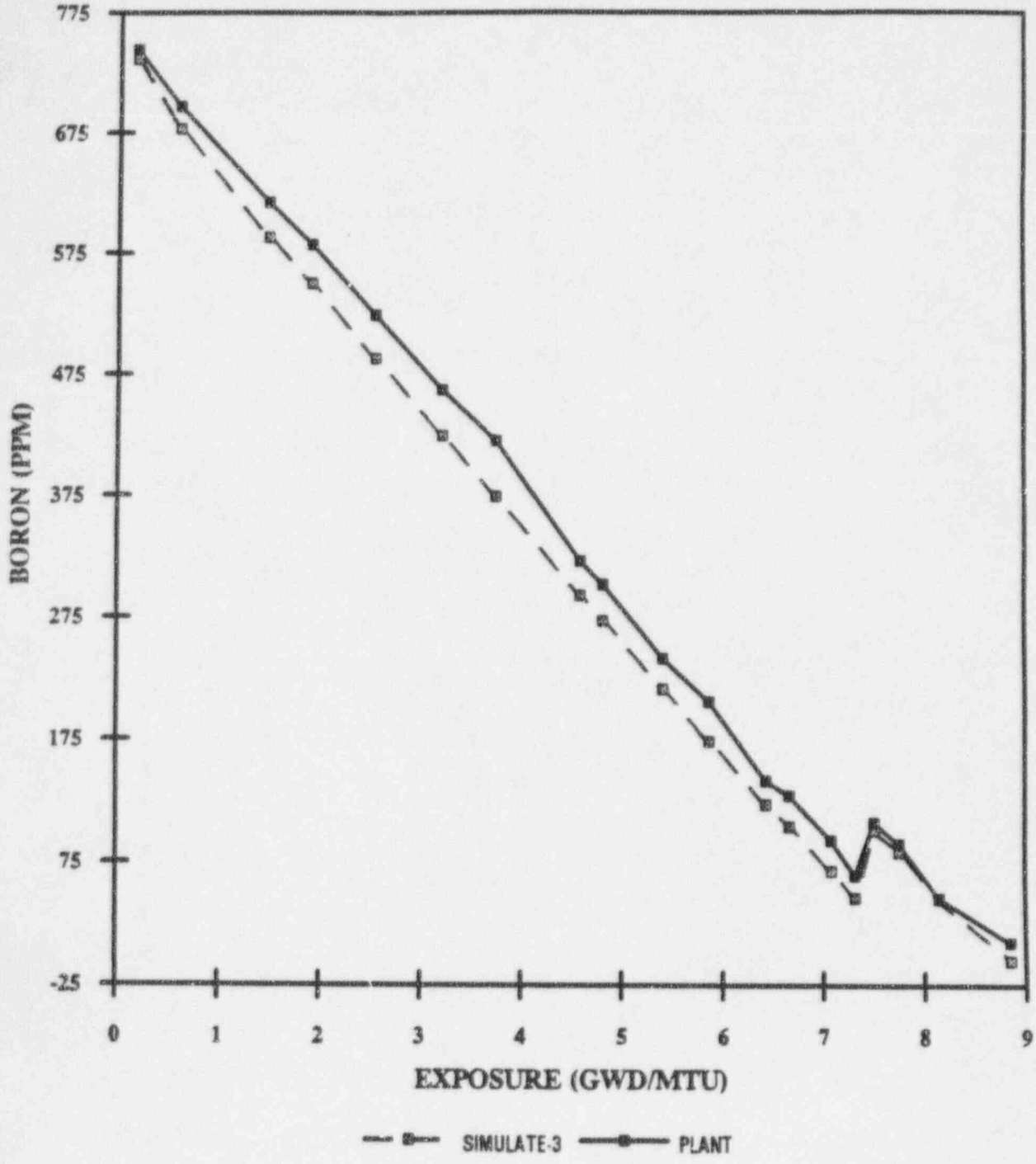

Figure 4.4

CYCLE 4 BORON COMPARISON

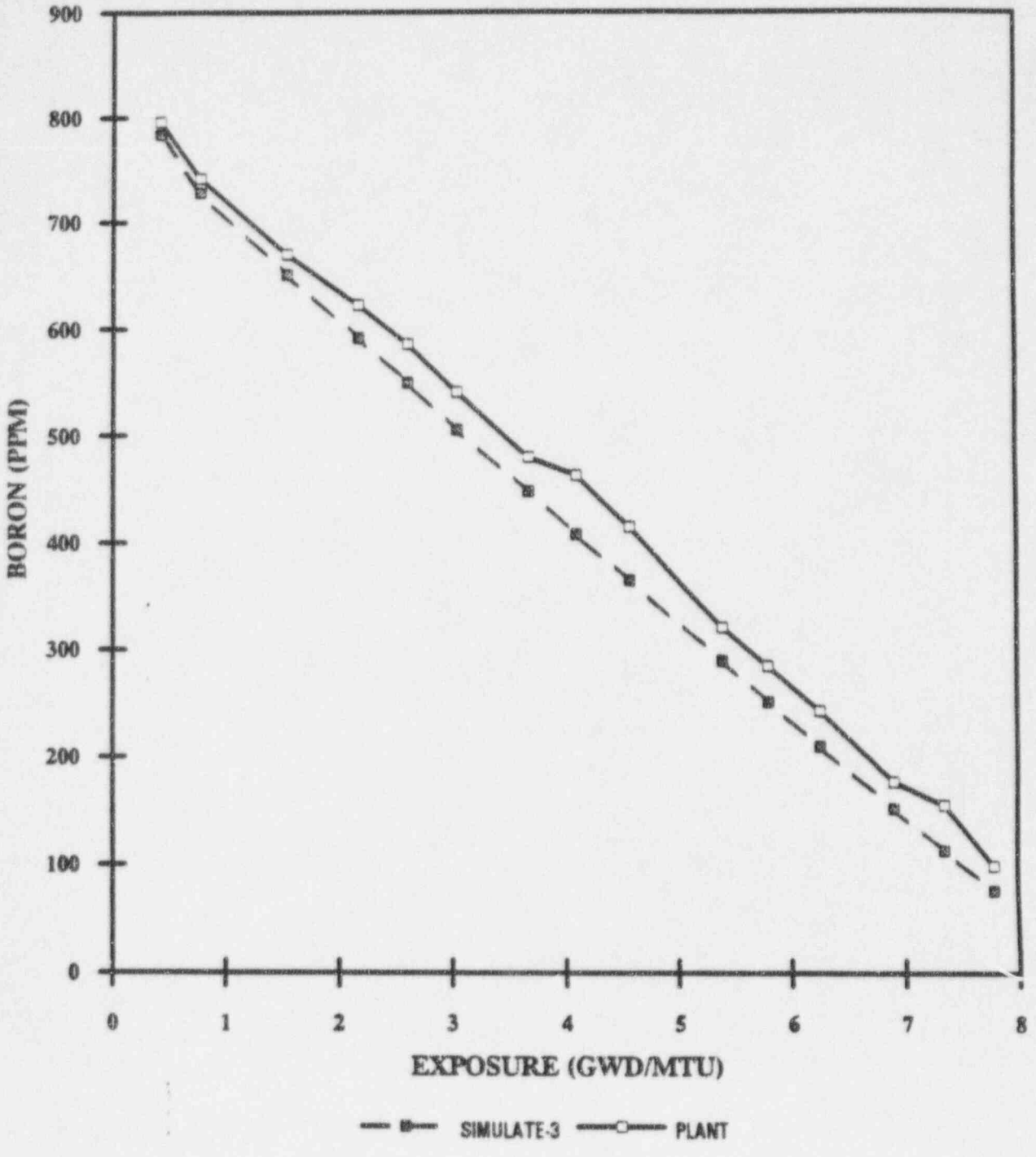

Figure 4.5
CYCLE 5 BORON COMPARISON

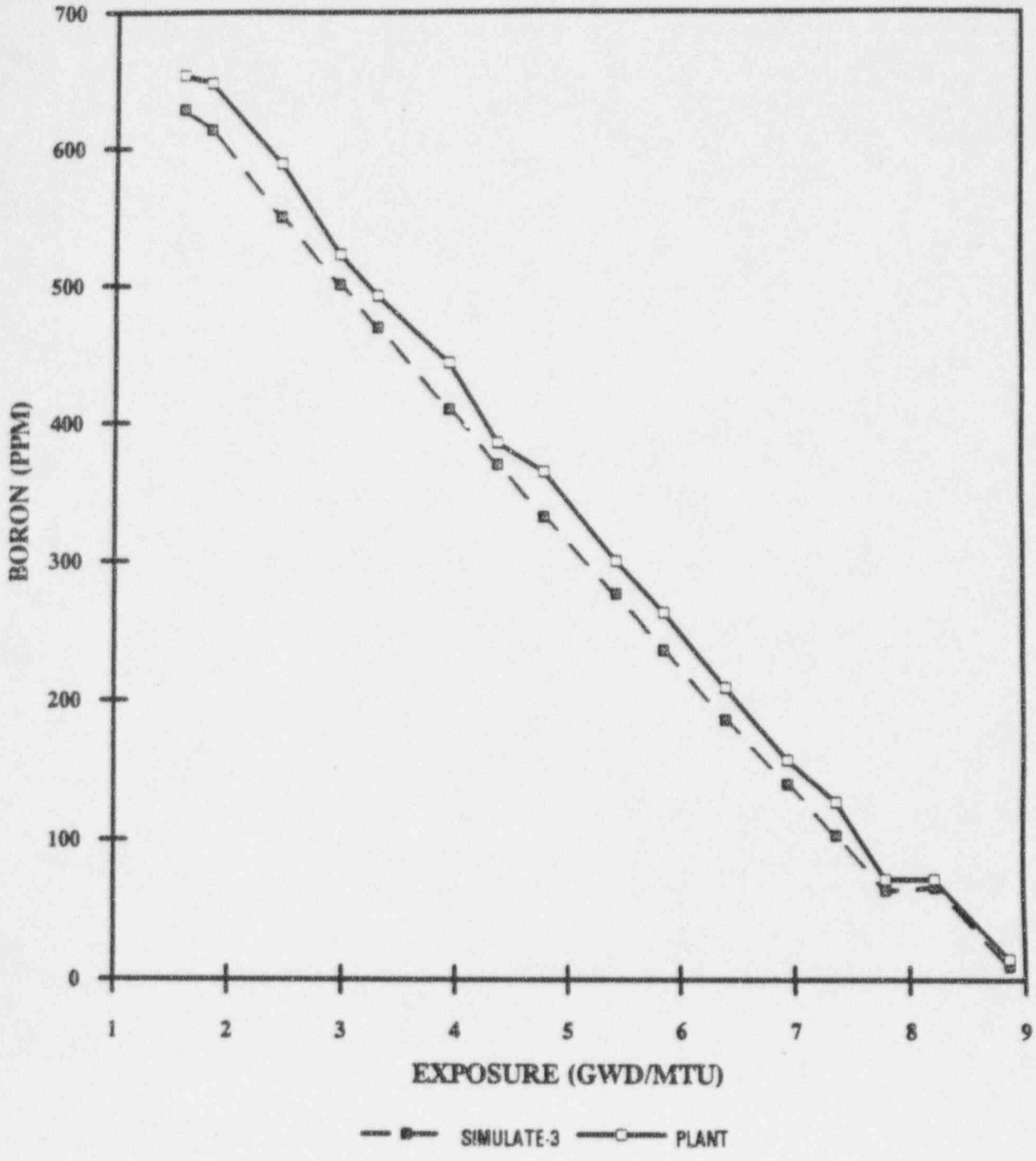

Figure 4.6

CYCLE 6 BORON COMPARISON

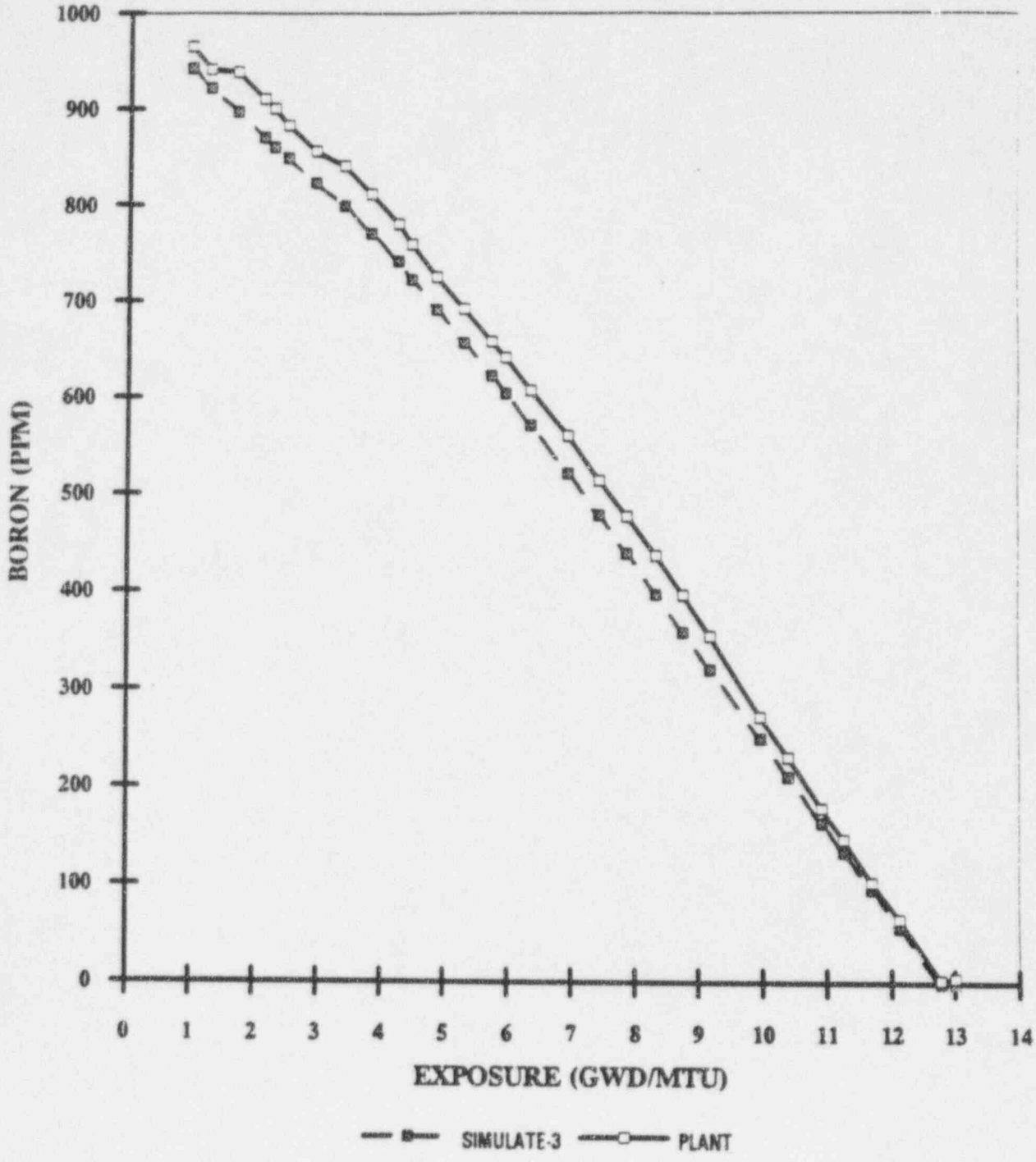

Figure 4.7
CYCLE 7 BORON COMPARISON

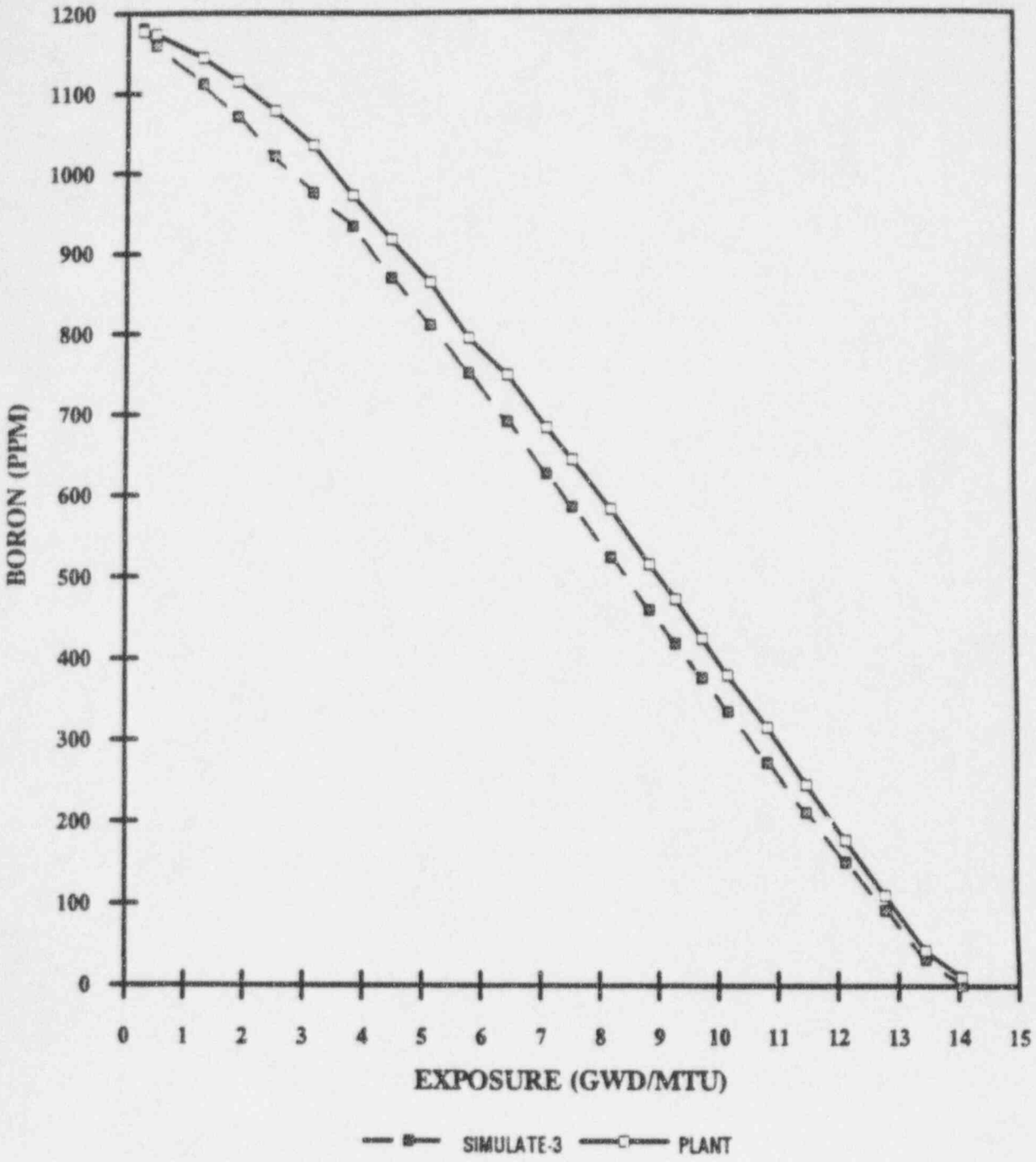

Figure 4.8

CYCLE 8 BORON COMPARISON

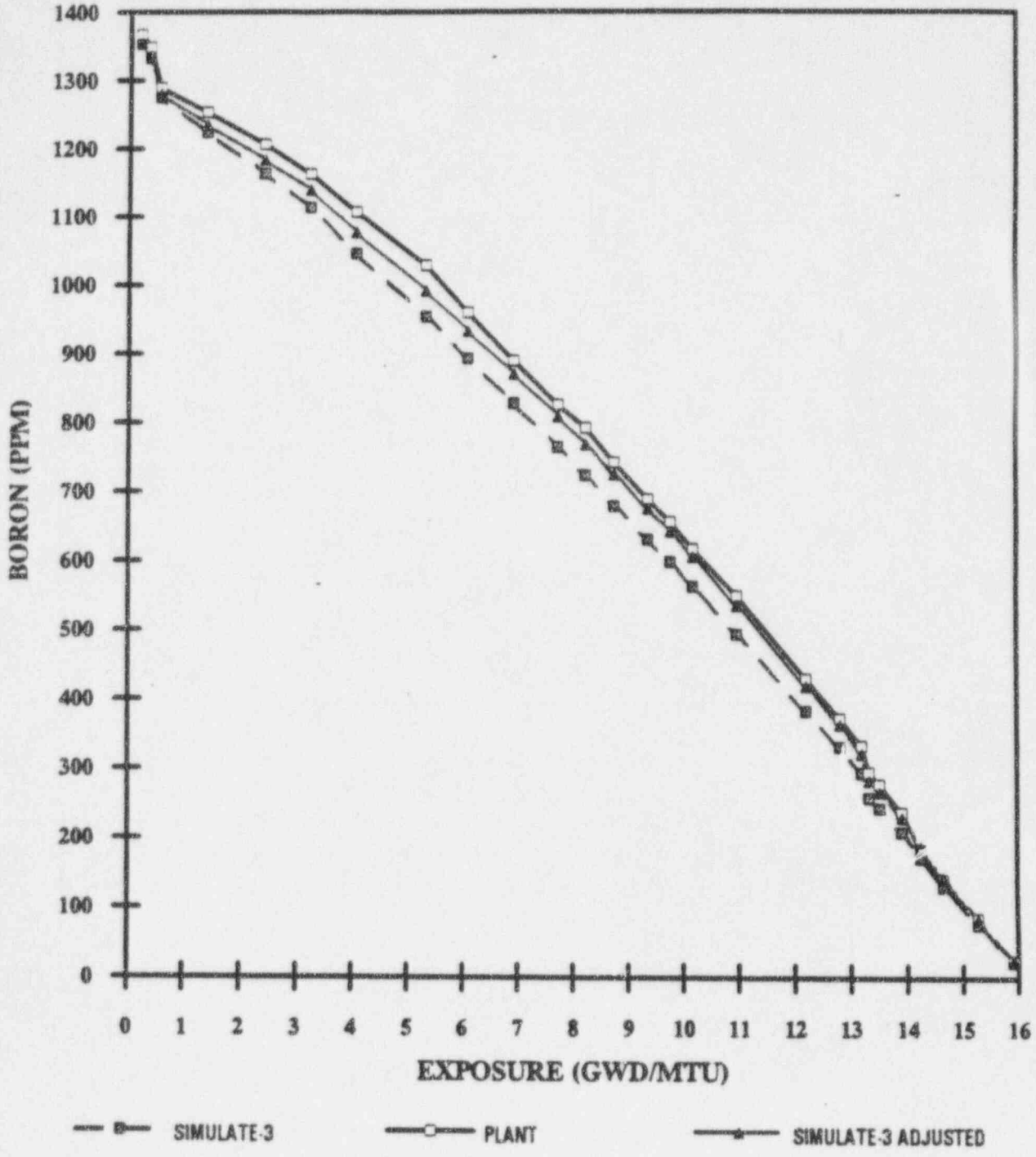

Figure 4.9

CYCLE 9 BORON COMPARISON

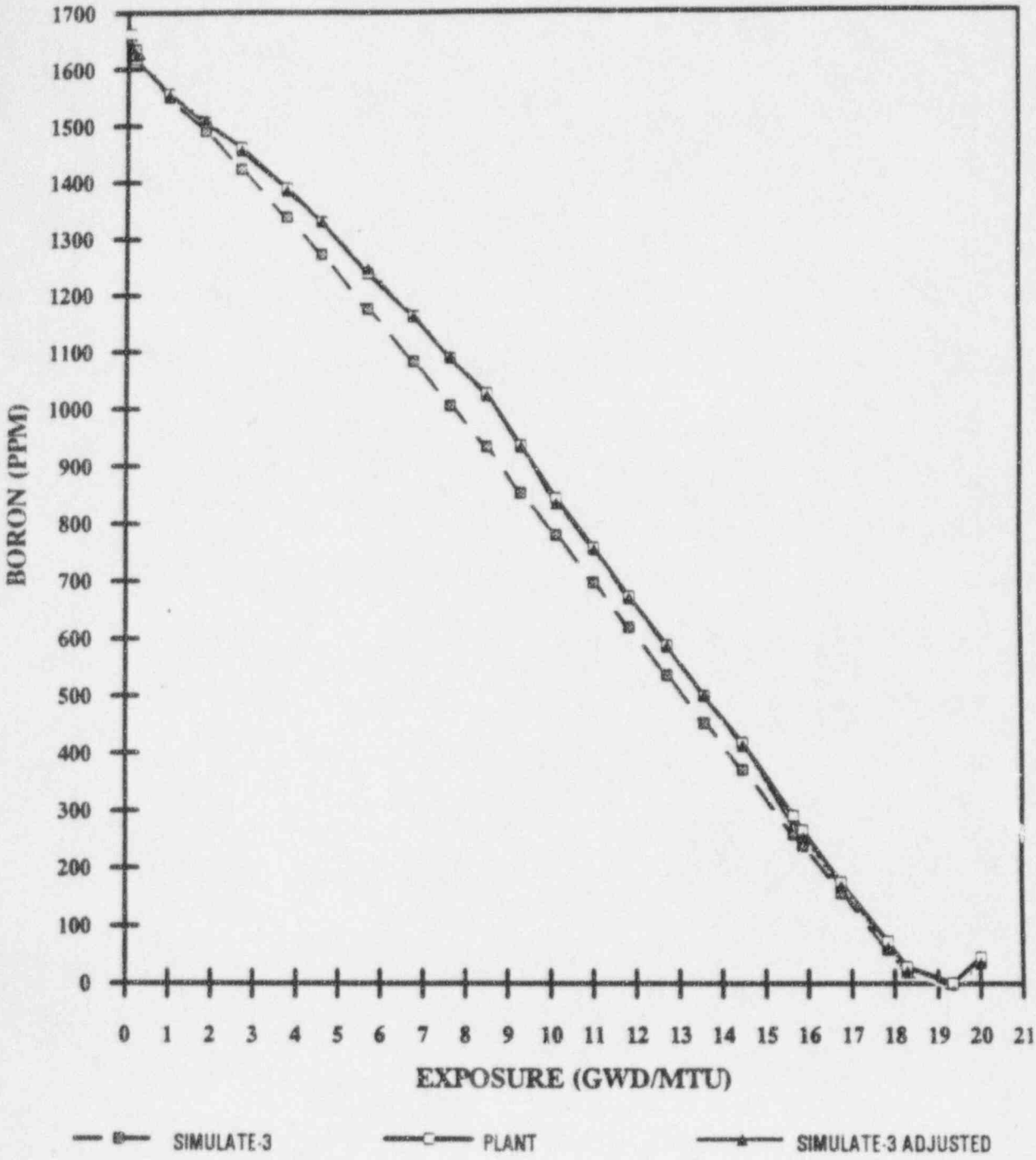

Figure 4.10

LETDOWN BORON DIFFERENCES

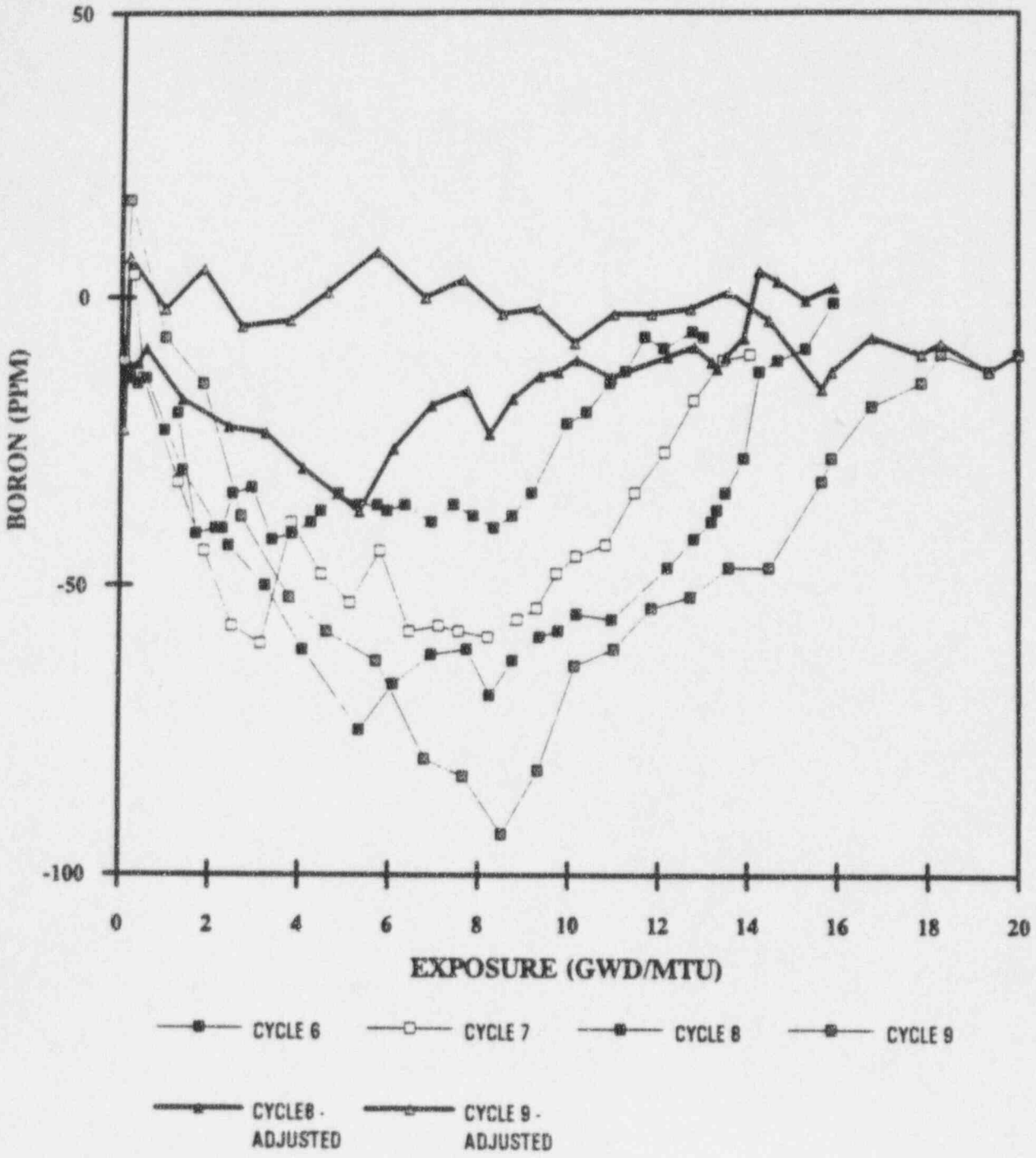

Figure 4.11

BOC 6 Radial Power Distribution

	8	9	10	11	12	13	14	15
H	0.992 0.989 0.324	1.142 1.140 0.175	1.026 0.993 3.335	1.179 1.190 −0.903	1.103 1.094 0.764	1.219 1.226 −0.596	0.836 0.838 −0.170	0.416 0.420 −1.022
K		1.011 0.992 1.875	1.152 1.150 0.201	1.118 1.101 1.546	1.233 1.225 0.653	1.240 1.228 0.981	1.051 1.066 −1.342	0.497 0.504 −1.463
L			1.053 1.058 −0.434	1.224 1.219 0.376	1.079 1.056 2.152	1.247 1.271 −1.849	0.984 0.998 −1.348	0.415 0.426 −2.589
M				1.095 1.059 3.481	1.239 1.253 −1.091	1.220 1.221 −0.009	0.887 0.905 −1.992	
N					1.033 1.014 1.864	1.020 1.033 −1.312	0.540 0.542 −0.298	
O						0.582 0.581 0.215		

AVERAGE % DIFFERENCE:	0.053
STANDARD DEVIATION	1.495

PREDICTED
MEASURED
% DIFFERENCE

Figure 4.12

MOC 6 Radial Power Distribution

	8	9	10	11	12	13	14	15
H	1.099 1.114 −1.288	1.308 1.321 −0.917	1.106 1.093 1.250	1.286 1.287 −0.140	1.103 1.095 0.726	1.221 1.224 −0.245	0.813 0.820 −0.797	0.427 0.426 0.176
K		1.106 1.108 −0.212	1.289 1.289 −0.051	1.148 1.142 0.583	1.281 1.283 −0.201	1.170 1.168 0.203	1.008 1.015 −0.664	0.498 0.497 0.119
L			1.108 1.120 −1.081	1.299 1.205 0.303	1.063 1.051 1.061	1.216 1.229 −1.048	0.916 0.927 −1.199	0.414 0.419 −1.253
M				1.090 1.073 1.565	1.231 1.227 0.285	1.113 1.112 0.104	0.822 0.817 0.639	
N					0.971 0.953 1.869	0.954 0.956 −0.214	0.514 0.519 −0.981	
O						0.558 0.561 −0.560		

AVERAGE % DIFFERENCE:	−0.068
STANDARD DEVIATION :	0.838

PREDICTED
MEASURED
% DIFFERENCE

Figure 4.13

EOC 6 Radial Power Distribution

	8	9	10	11	12	13	14	15
H	1.034 1.051 −1.579	1.224 1.220 0.310	1.048 1.053 −0.439	1.225 1.215 0.845	1.078 1.087 −0.866	1.194 1.173 1.797	0.852 0.870 −2.034	0.499 0.501 −0.411
K		1.044 1.051 −0.603	1.218 1.210 0.649	1.099 1.096 0.240	1.246 1.239 0.573	1.140 1.143 −0.197	1.028 1.038 −0.953	0.569 0.564 0.905
L			1.064 1.076 −1.188	1.261 1.251 0.756	1.109 1.104 0.384	1.204 1.213 −0.737	0.943 0.952 −1.023	0.480 0.482 −0.424
M				1.077 1.074 0.292	1.219 1.221 −0.120	1.105 1.109 −0.366	0.861 0.843 2.059	
N					0.994 0.999 −0.575	0.980 0.981 −0.020	0.570 0.576 −0.984	
O						0.617 0.622 −0.839		

AVERAGE % DIFFERENCE:	−0.157
STANDARD DEVIATION :	0.917

PREDICTED
MEASURED
% DIFFERENCE

Figure 4.14

BOC 7 Radial Power Distribution

	8	9	10	11	12	13	14	15
H	1.122 1.104 1.576	1.259 1.267 −0.568	1.239 1.219 1.680	1.249 1.234 1.234	1.128 1.124 0.292	1.238 1.230 0.696	0.830 0.832 −0.287	0.385 0.388 −0.872
K		1.186 1.192 −0.510	1.287 1.271 1.260	1.266 1.248 1.457	1.252 1.250 0.176	1.052 1.046 0.526	1.057 1.053 0.379	0.399 0.408 −2.104
L			1.225 1.230 −0.412	1.284 1.295 −0.810	1.104 1.130 −2.269	1.222 1.233 −0.939	0.806 0.833 −3.201	0.309 0.315 −1.878
M				1.242 1.247 −0.384	1.286 1.274 0.957	1.029 1.032 −0.254	0.867 0.874 −0.762	
N					1.079 1.016 6.240	1.050 1.049 0.128	0.421 0.438 −3.723	
O						0.484 0.502 −3.599		

AVERAGE % DIFFERENCE:	−0.206
STANDARD DEVIATION :	1.896

PREDICTED
MEASURED
% DIFFERENCE

Figure 4.15

MOC 7 Radial Power Distribution

	8	9	10	11	12	13	14	15
H	1.136 1.126 0.889	1.328 1.338 −0.692	1.204 1.216 −0.938	1.298 1.304 −0.395	1.109 1.107 0.184	1.311 1.301 0.793	0.880 0.879 0.198	0.451 0.459 −1.786
K		1.170 1.170 −0.046	1.316 1.311 0.386	1.210 1.198 0.988	1.264 1.256 0.616	1.060 1.056 0.423	1.097 1.094 0.303	0.460 0.461 −0.167
L			1.172 1.178 −0.526	1.284 1.281 0.229	1.062 1.073 −1.037	1.263 1.277 −1.156	0.835 0.854 −2.274	0.358 0.364 −1.487
M				1.141 1.135 0.527	1.198 1.197 0.116	0.984 0.983 0.135	0.865 0.847 2.221	
N					0.984 0.973 1.126	1.000 1.004 −0.416	0.437 0.448 −2.421	
O						0.489 0.503 −2.720		

AVERAGE % DIFFERENCE:	−0.239
STANDARD DEVIATION :	1.121

PREDICTED
MEASURED
% DIFFERENCE

Figure 4.16

EOC 7 Radial Power Distribution

	8	9	10	11	12	13	14	15
H	1.029 1.016 1.216	1.189 1.170 1.652	1.090 1.098 −0.694	1.200 1.174 2.179	1.073 1.086 −1.146	1.307 1.300 0.506	0.932 0.954 −2.321	0.533 0.542 −1.532
K		1.058 1.058 −0.012	1.189 1.161 2.435	1.126 1.115 1.024	1.216 1.206 0.872	1.072 1.083 −1.001	1.136 1.141 −0.418	0.540 0.541 −0.129
L			1.085 1.085 −0.005	1.214 1.208 0.531	1.110 1.103 0.659	1.293 1.313 −1.499	0.896 0.921 −2.696	0.432 0.434 −0.355
M				1.107 1.105 0.175	1.186 1.184 0.192	1.020 1.031 −1.113	0.934 0.916 1.956	
N					1.006 1.003 0.341	1.043 1.056 −1.315	0.502 0.501 0.128	
O						0.555 0.554 0.090		

AVERAGE % DIFFERENCE:	−0.010
STANDARD DEVIATION :	1.246

PREDICTED
MEASURED
% DIFFERENCE

Figure 4.17

BOC 8 Radial Power Distribution

	8	9	10	11	12	13	14	15
H	1.052 1.187 −11.359	1.265 1.263 0.162	1.060 1.052 0.796	1.146 1.142 0.306	1.031 0.985 4.708	1.251 1.211 3.307	1.002 1.002 0.089	0.377 0.388 −2.892
K		1.220 1.211 0.772	1.285 1.296 −0.872	1.025 1.014 1.132	1.223 1.211 0.946	1.195 1.169 2.180	1.117 1.130 −1.182	0.378 0.393 −3.630
L			1.035 1.033 0.218	1.197 1.205 −0.629	0.973 0.958 1.542	1.256 1.271 −1.165	1.052 1.087 −3.198	0.330 0.340 −2.790
M				1.018 0.982 3.724	1.248 1.245 0.166	1.157 1.180 −1.930	0.941 0.945 −0.422	
N					1.206 1.196 0.820	1.067 1.096 −2.668	0.405 0.412 −1.814	
O						0.596 0.588 1.276		

AVERAGE % DIFFERENCE:	−0.428
STANDARD DEVIATION :	2.886

PREDICTED
MEASURED
% DIFFERENCE

Figure 4.18

MOC 8 Radial Power Distribution

	8	9	10	11	12	13	14	15
H	0.940 0.999 −5.913	1.131 1.098 3.026	1.019 0.980 3.990	1.186 1.173 1.083	1.042 1.000 4.158	1.296 1.273 1.784	0.988 0.975 1.376	0.405 0.422 −4.146
K		1.119 1.079 3.717	1.300 1.303 −0.271	1.041 1.022 1.884	1.294 1.307 −1.013	1.165 1.131 2.971	1.108 1.120 −1.129	0.404 0.416 −3.018
L			1.048 1.037 1.033	1.285 1.318 −2.519	0.999 0.978 2.143	1.278 1.314 −2.800	1.002 1.032 −2.844	0.347 0.362 −4.099
M				1.046 1.008 3.803	1.292 1.310 −1.339	1.100 1.119 −1.736	0.891 0.888 0.284	
N					1.142 1.132 0.955	1.041 1.079 −3.506	0.412 0.419 −1.747	
O						0.593 0.585 1.463		

AVERAGE % DIFFERENCE:	−0.083
STANDARD DEVIATION :	2.759

PREDICTED
MEASURED
% DIFFERENCE

Figure 4.19

EOC 8 Radial Power Distribution

	8	9	10	11	12	13	14	15
H	0.934 0.979 −4.533	1.092 1.055 3.553	0.999 0.962 3.833	1.145 1.111 2.994	1.029 0.997 3.191	1.278 1.256 1.748	1.001 0.999 0.153	0.473 0.491 −3.674
K		1.078 1.045 3.134	1.259 1.245 1.076	1.031 1.014 1.705	1.282 1.284 −0.228	1.132 1.113 1.728	1.103 1.117 −1.325	0.469 0.485 −3.365
L			1.040 1.028 1.093	1.285 1.306 −1.663	1.003 0.988 1.497	1.263 1.292 −2.247	0.997 1.029 −3.158	0.403 0.420 −4.046
M				1.049 1.022 2.617	1.282 1.294 −0.938	1.082 1.101 −1.725	0.910 0.913 −0.394	
N					1.110 1.097 1.189	1.040 1.080 −3.691	0.461 0.475 −3.070	
O						0.639 0.624 2.317		

AVERAGE % DIFFERENCE:	−0.077
STANDARD DEVIATION	2.571

PREDICTED
MEASURED
% DIFFERENCE

Figure 4.20

BOC 9 Radial Power Distribution

	8	9	10	11	12	13	14	15
H	1.095 1.097 −0.16%	1.350 1.346 0.30%	1.281 1.248 2.65%	1.224 1.208 1.30%	1.130 1.113 1.52%	1.235 1.238 −0.23%	0.777 0.788 −1.38%	0.261 0.274 −4.65%
K		1.335 1.318 1.24%	1.349 1.354 −0.38%	1.186 1.164 1.90%	1.299 1.287 1.00%	1.080 1.076 0.41%	0.973 0.980 −0.76%	0.282 0.294 −3.90%
L			1.222 1.202 1.61%	1.322 1.279 3.39%	1.092 1.085 0.63%	1.212 1.222 −0.80%	1.048 1.083 −3.26%	0.274 0.303 −9.67%
M				1.155 1.143 1.09%	1.245 1.237 0.62%	1.042 1.043 −0.12%	0.886 0.905 −2.16%	
N					1.083 1.091 −0.68%	1.045 1.042 0.28%	0.385 0.401 −4.07%	
O						0.486 0.498 −2.48%		

AVERAGE % DIFFERENCE:	−0.578
STANDARD DEVIATION :	2.600

PREDICTED
MEASURED
% DIFFERENCE

Figure 4.21

MOC 9 Radial Power Distribution

	8	9	10	11	12	13	14	15
H	1.058 1.059 −0.06%	1.337 1.334 0.20%	1.179 1.131 4.21%	1.135 1.108 2.46%	1.087 1.064 2.17%	1.279 1.266 1.02%	0.841 0.842 −0.19%	0.328 0.340 −3.33%
K		1.234 1.204 2.43%	1.331 1.334 −0.26%	1.126 1.107 1.72%	1.324 1.324 −0.05%	1.082 1.071 1.02%	1.048 1.036 1.14%	0.343 0.349 −1.71%
L			1.165 1.159 0.57%	1.353 1.350 0.19%	1.085 1.082 0.25%	1.263 1.287 −1.88%	1.038 1.054 −1.45%	0.318 0.342 −6.89%
M				1.136 1.139 −0.24%	1.286 1.308 −1.69%	1.013 1.008 0.58%	0.874 0.881 −0.84%	
N					1.032 1.031 0.13%	0.985 0.990 −0.44%	0.403 0.414 −2.62%	
O						0.490 0.496 −1.17%		

AVERAGE % DIFFERENCE:	−0.163
STANDARD DEVIATION :	2.035

PREDICTED
MEASURED
% DIFFERENCE

Figure 4.22

EOC 9 Radial Power Distribution

	8	9	10	11	12	13	14	15
H	0.995 1.003 −0.73%	1.229 1.204 2.04%	1.096 1.071 2.26%	1.081 1.062 1.77%	1.051 1.044 0.66%	1.256 1.240 1.33%	0.899 0.907 −0.90%	0.409 0.419 −2.30%
K		1.133 1.115 1.62%	1.234 1.233 0.09%	1.074 1.070 0.34%	1.277 1.275 0.14%	1.079 1.083 −0.43%	1.096 1.080 1.50%	0.419 0.425 −1.25%
L			1.100 1.103 −0.28%	1.298 1.286 0.89%	1.065 1.068 −0.25%	1.274 1.291 −1.33%	1.073 1.081 −0.77%	0.387 0.403 −4.17%
M				1.109 1.128 −1.69%	1.283 1.304 −1.59%	1.037 1.042 −0.48%	0.933 0.918 1.55%	
N					1.043 1.051 −0.80%	1.023 1.018 0.51%	0.470 0.474 −0.82%	
O						0.557 0.552 1.07%		

AVERAGE % DIFFERENCE:	−0.070
STANDARD DEVIATION :	1.429

PREDICTED
MEASURED
% DIFFERENCE

Figure 4.23

BOC 6 Total Power Distribution

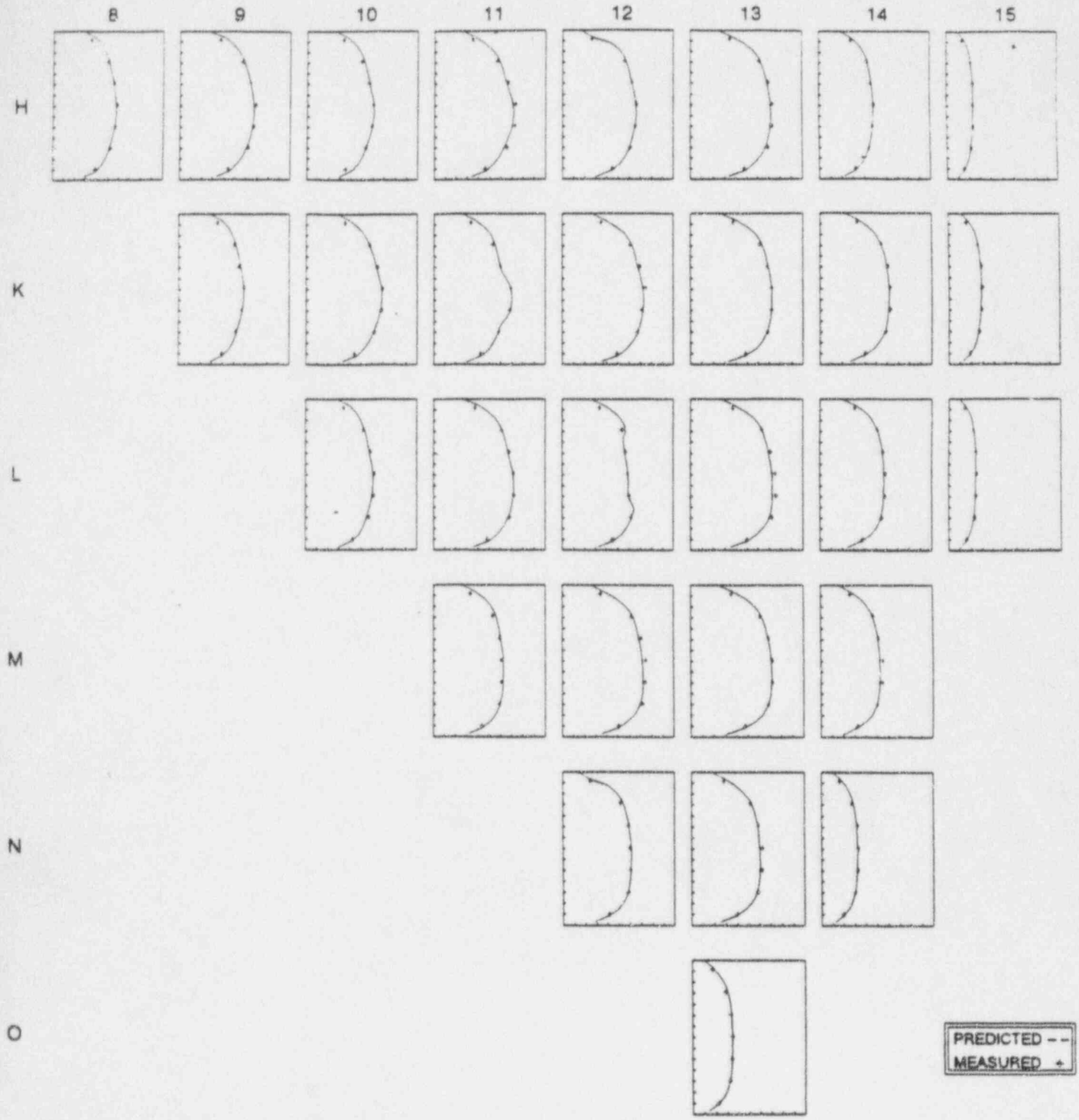

Figure 4.24

MOC 6 Total Power Distribution

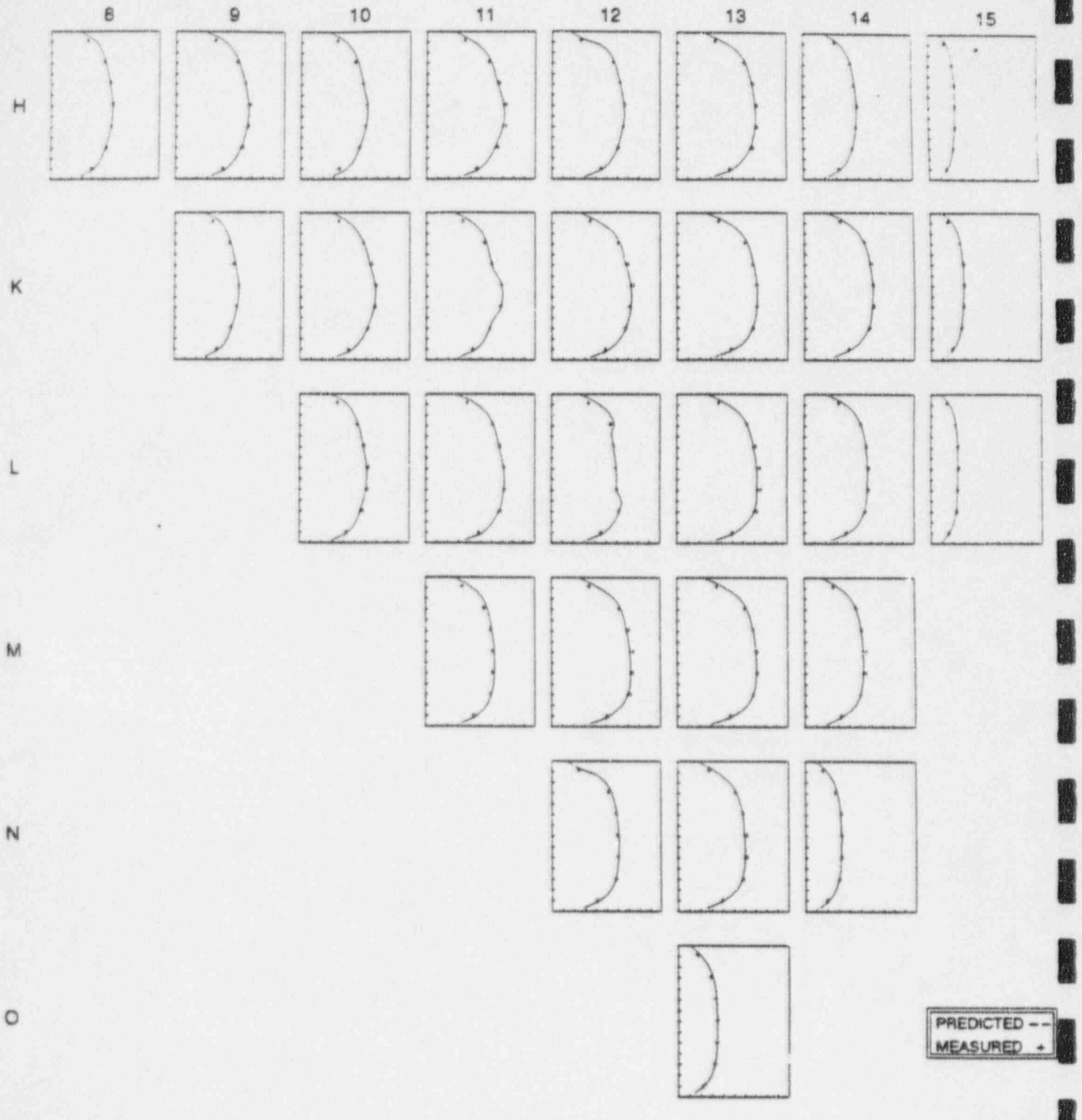

Figure 4.25

EOC 6 Total Power Distribution

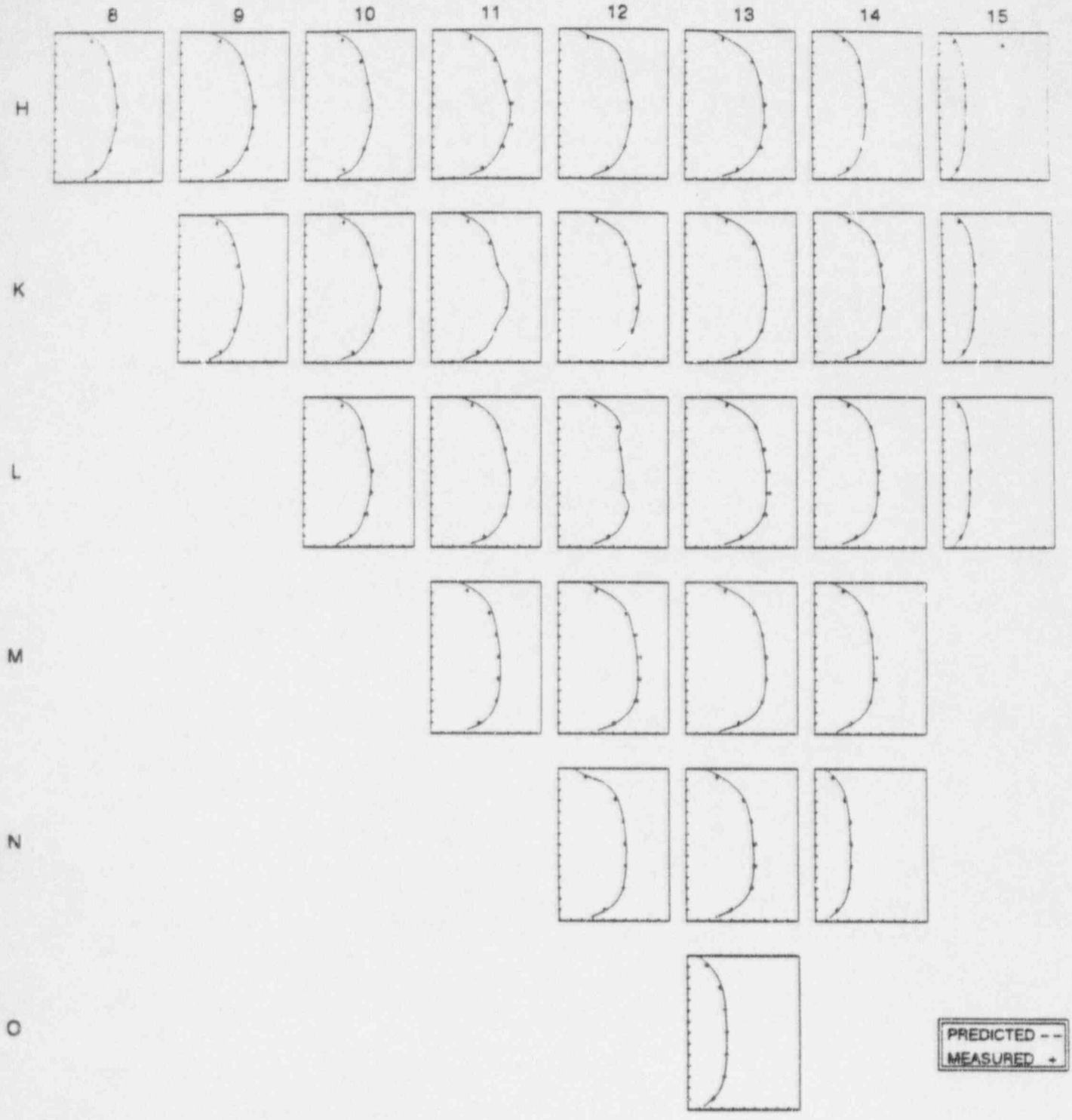

Figure 4.26

BOC 7 Total Power Distribution

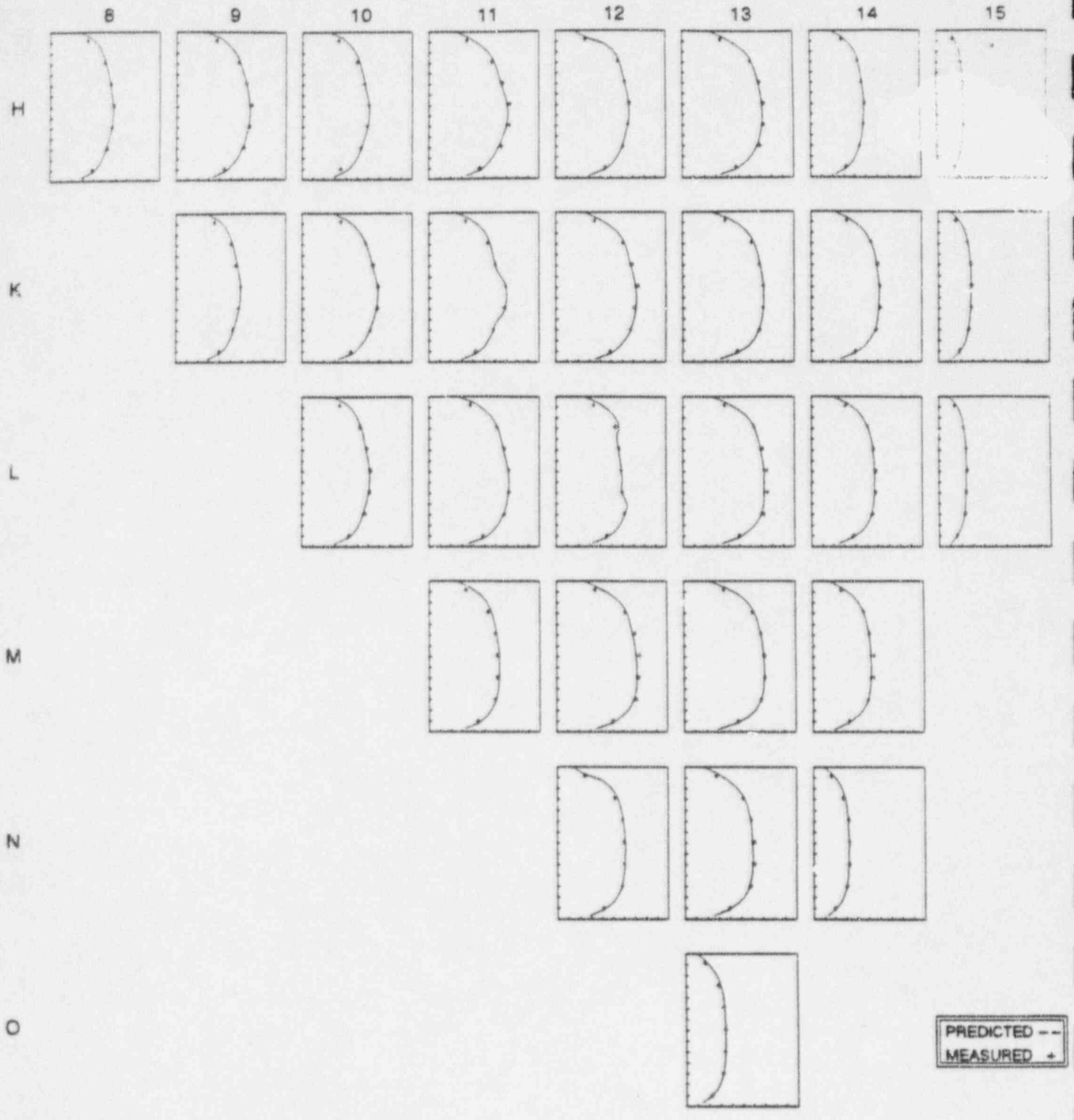

Figure 4.27

MOC 7 Total Power Distribution

Figure 4.28

EOC 7 Total Power Distribution

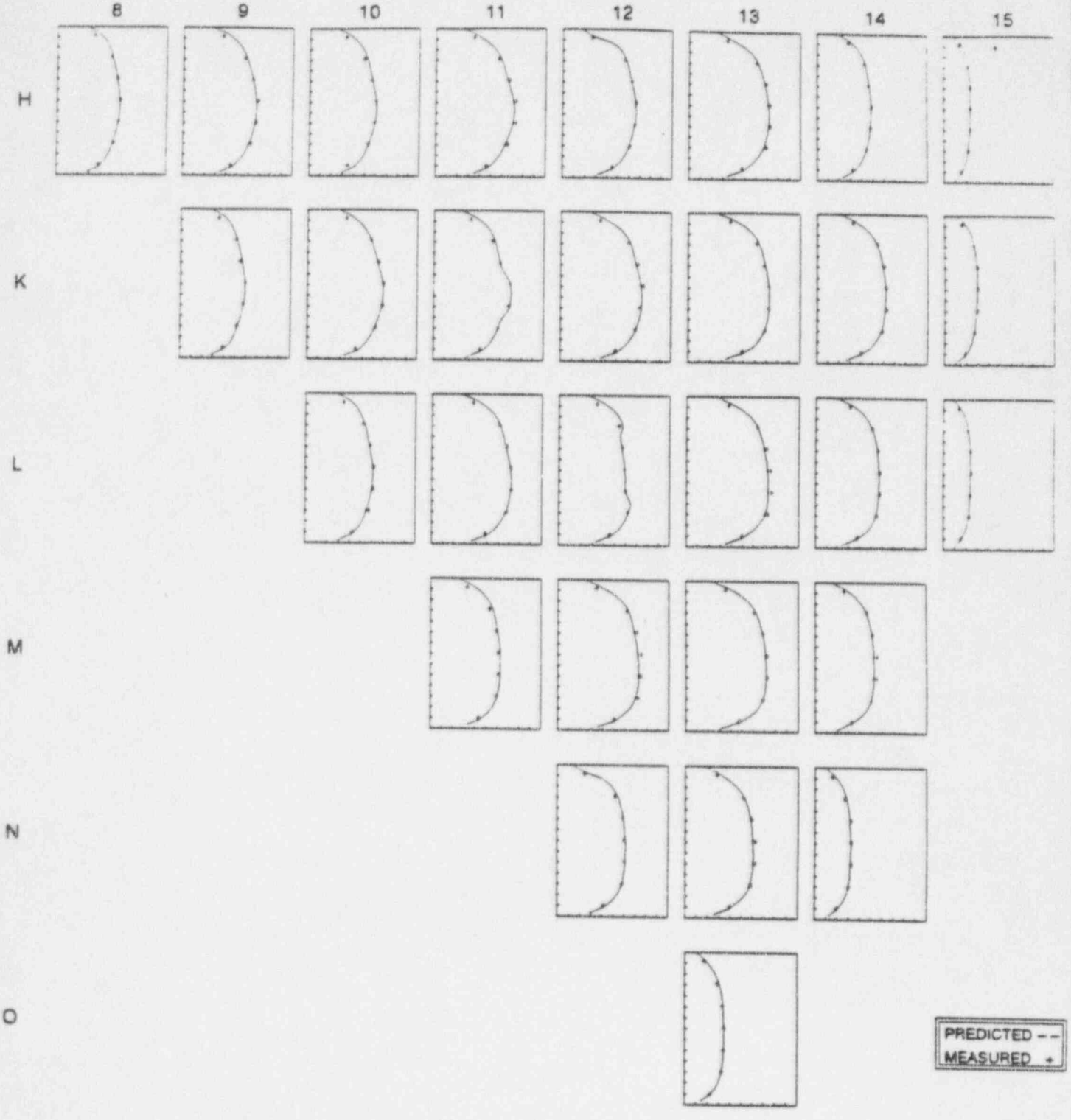

Figure 4.29

BOC 8 Total Power Distribution

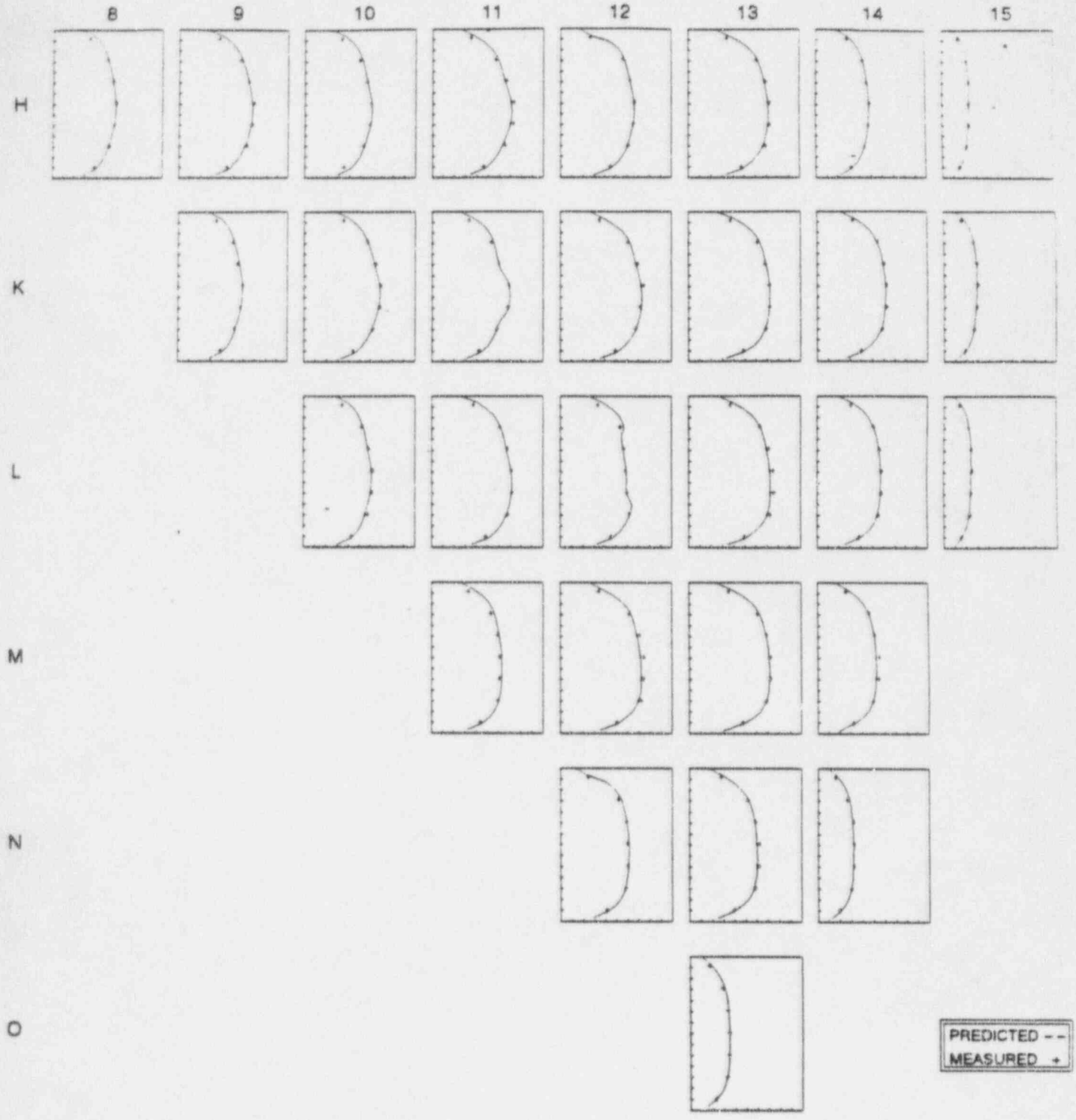

Figure 4.30

MOC 8 Total Power Distribution

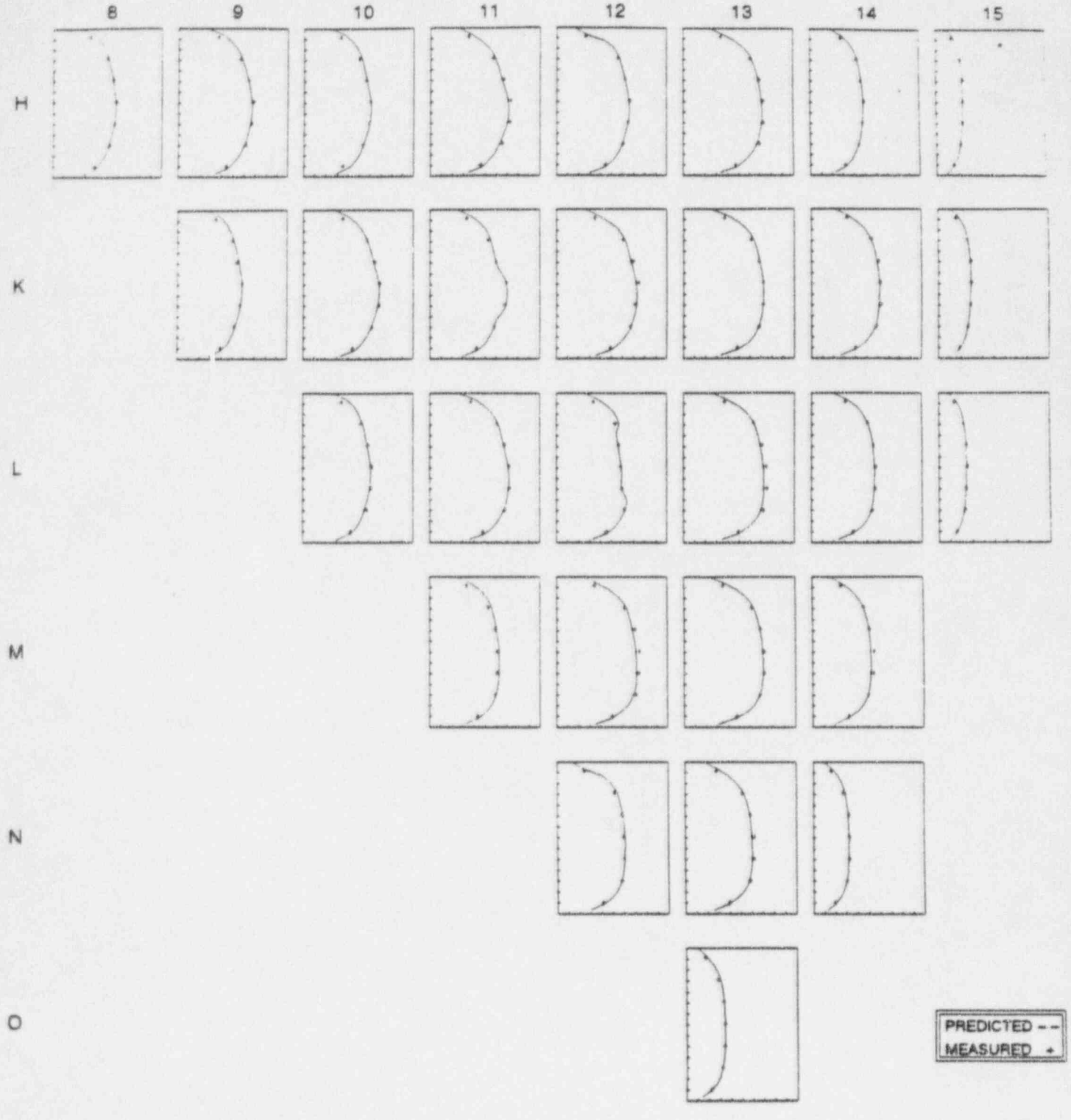

Figure 4.31

EOC 8 Total Power Distribution

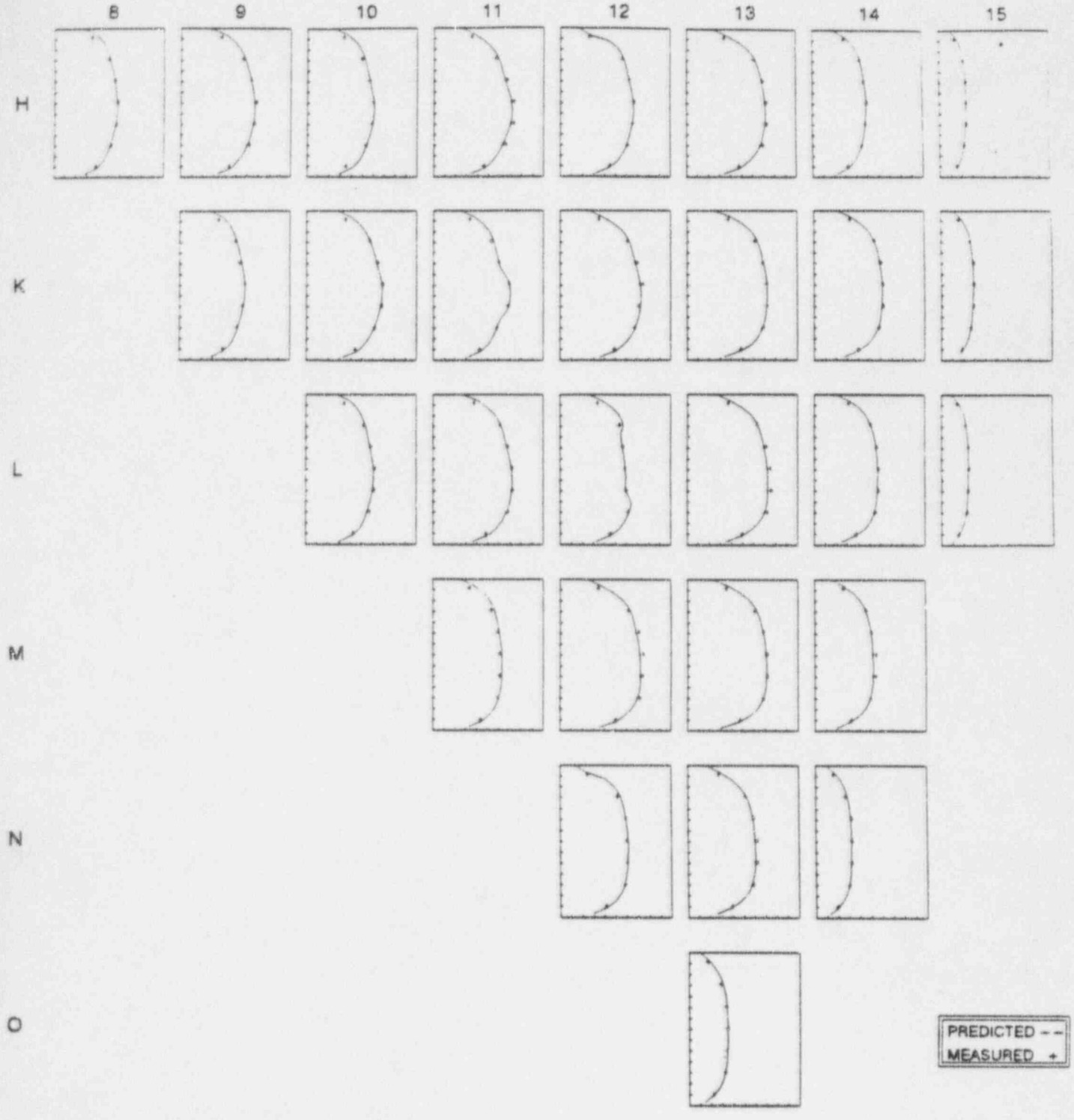

Figure 4.32

BOC 9 Total Power Distribution

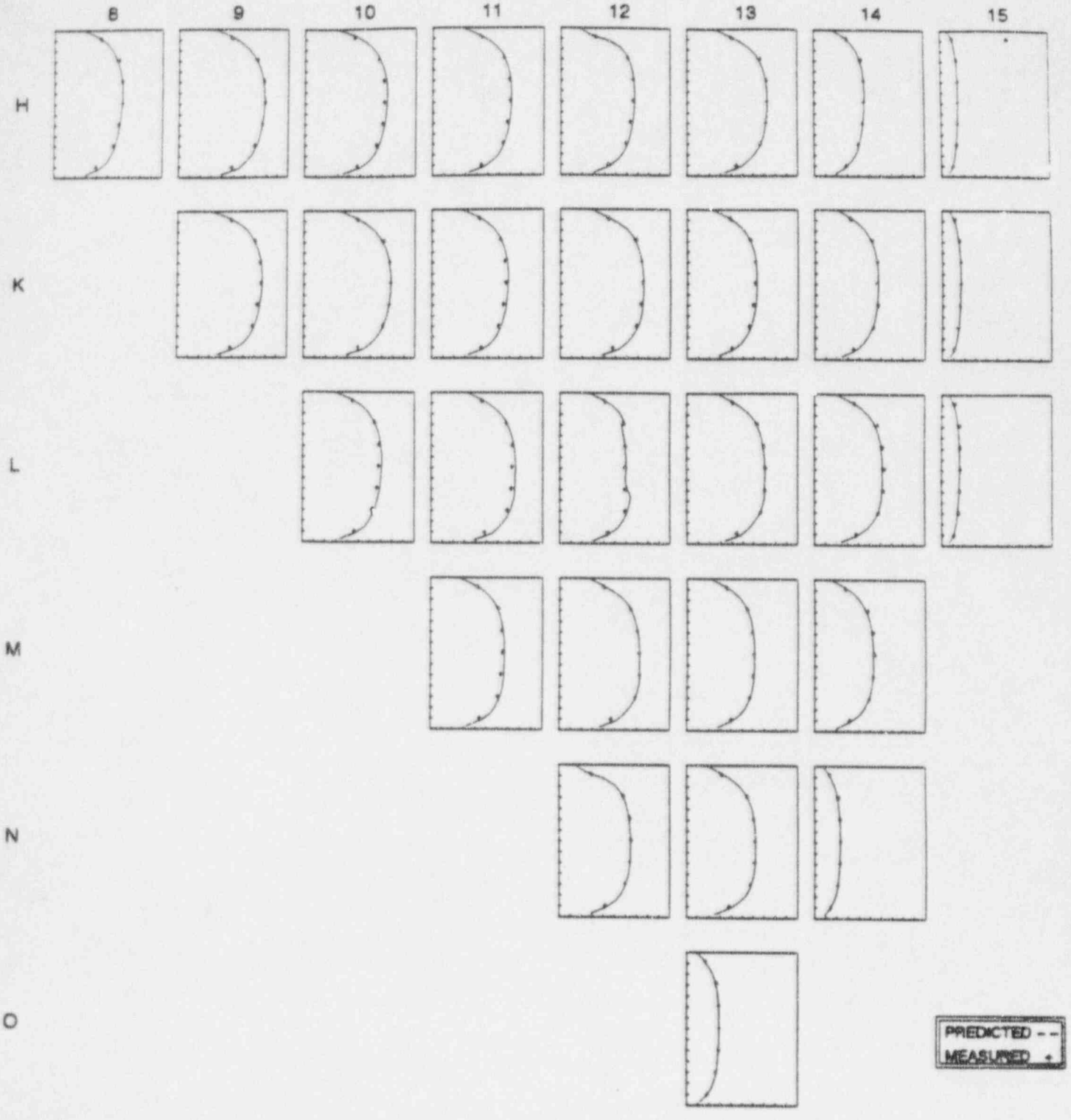

Figure 4.33

MOC 9 Total Power Distribution

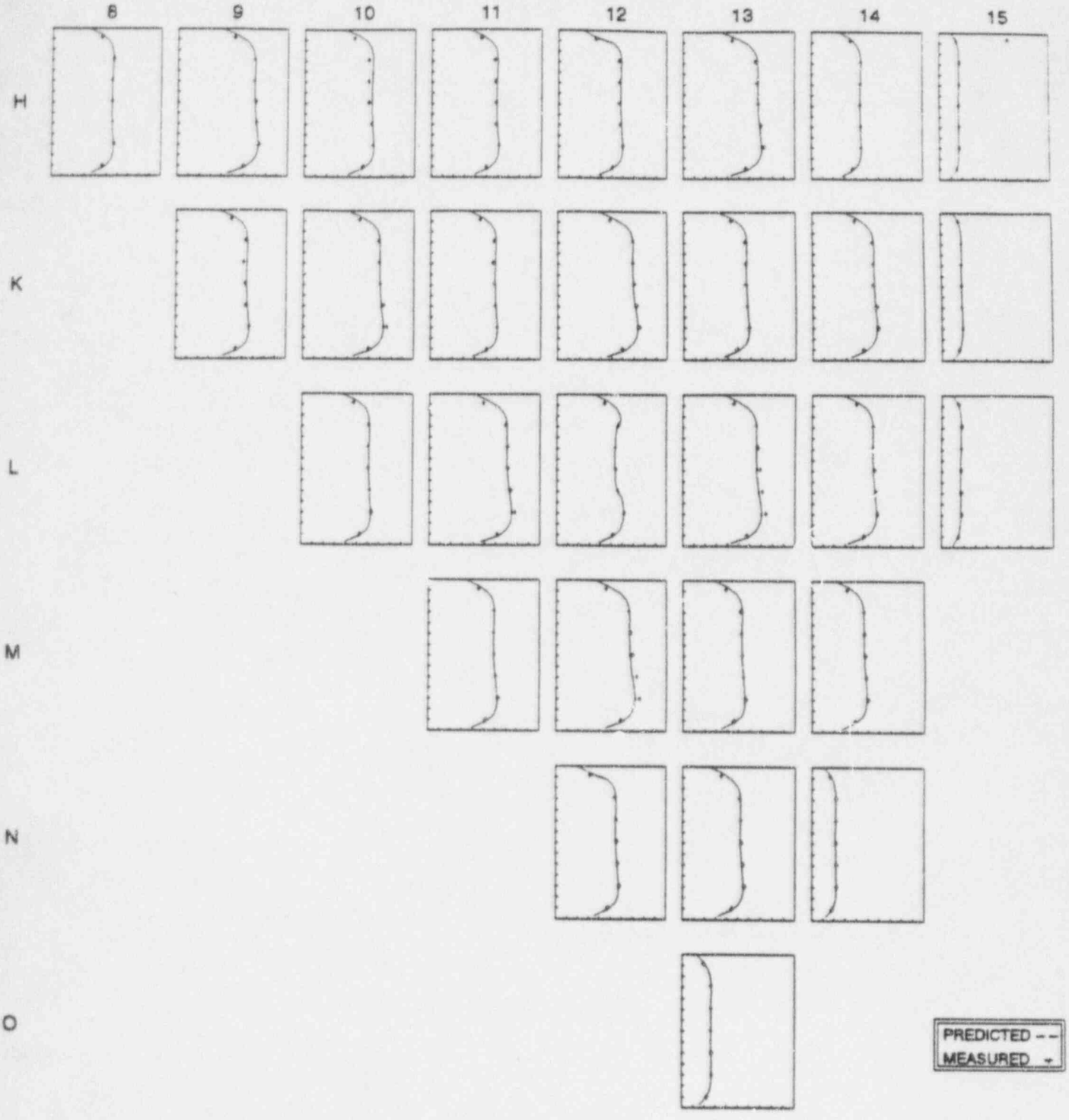

Figure 4.34

EOC 9 Total Power Distribution

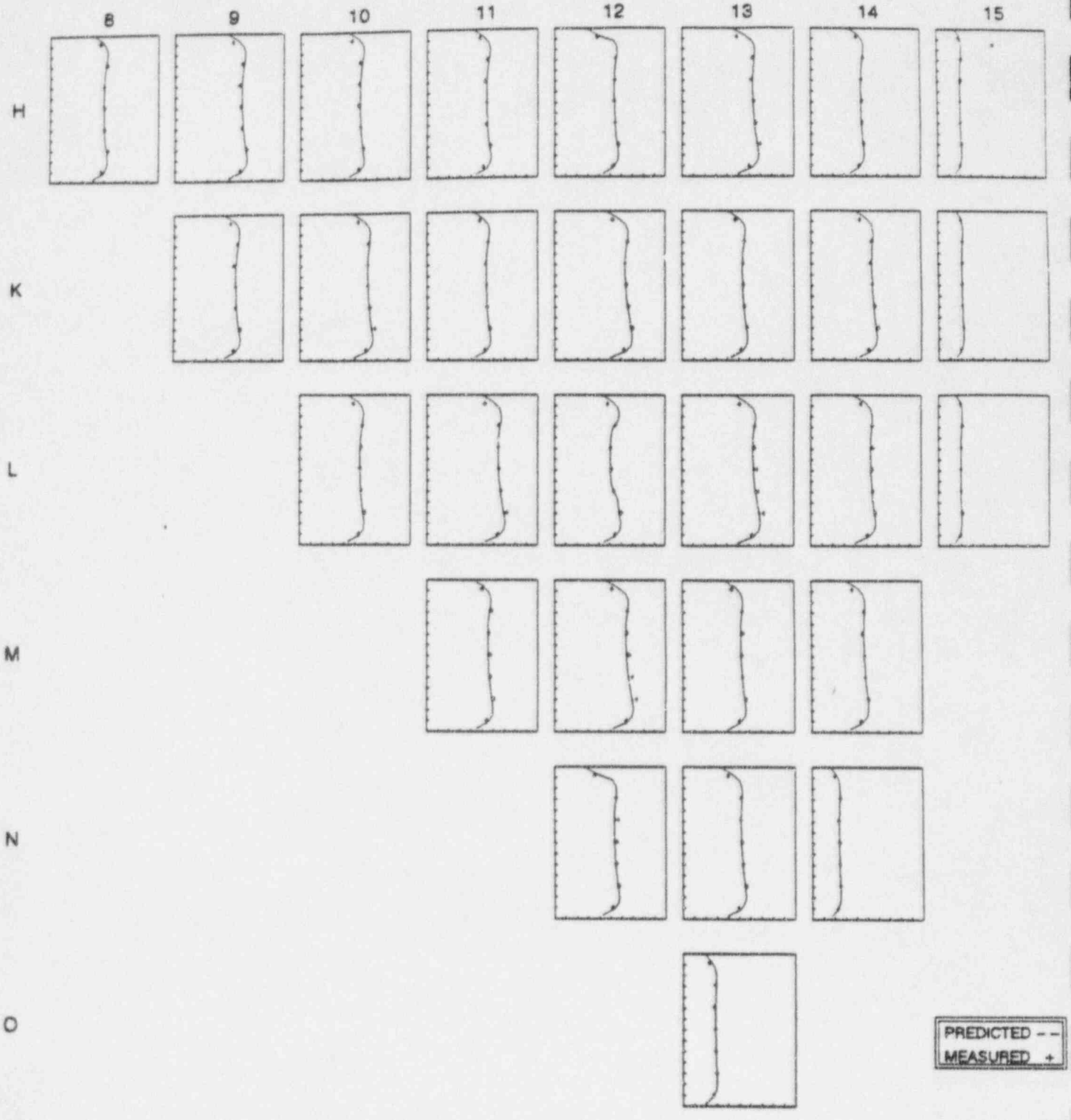

FIGURE 4.35

TMI CYCLE 9 100–50–100 POWER TRANSIENT

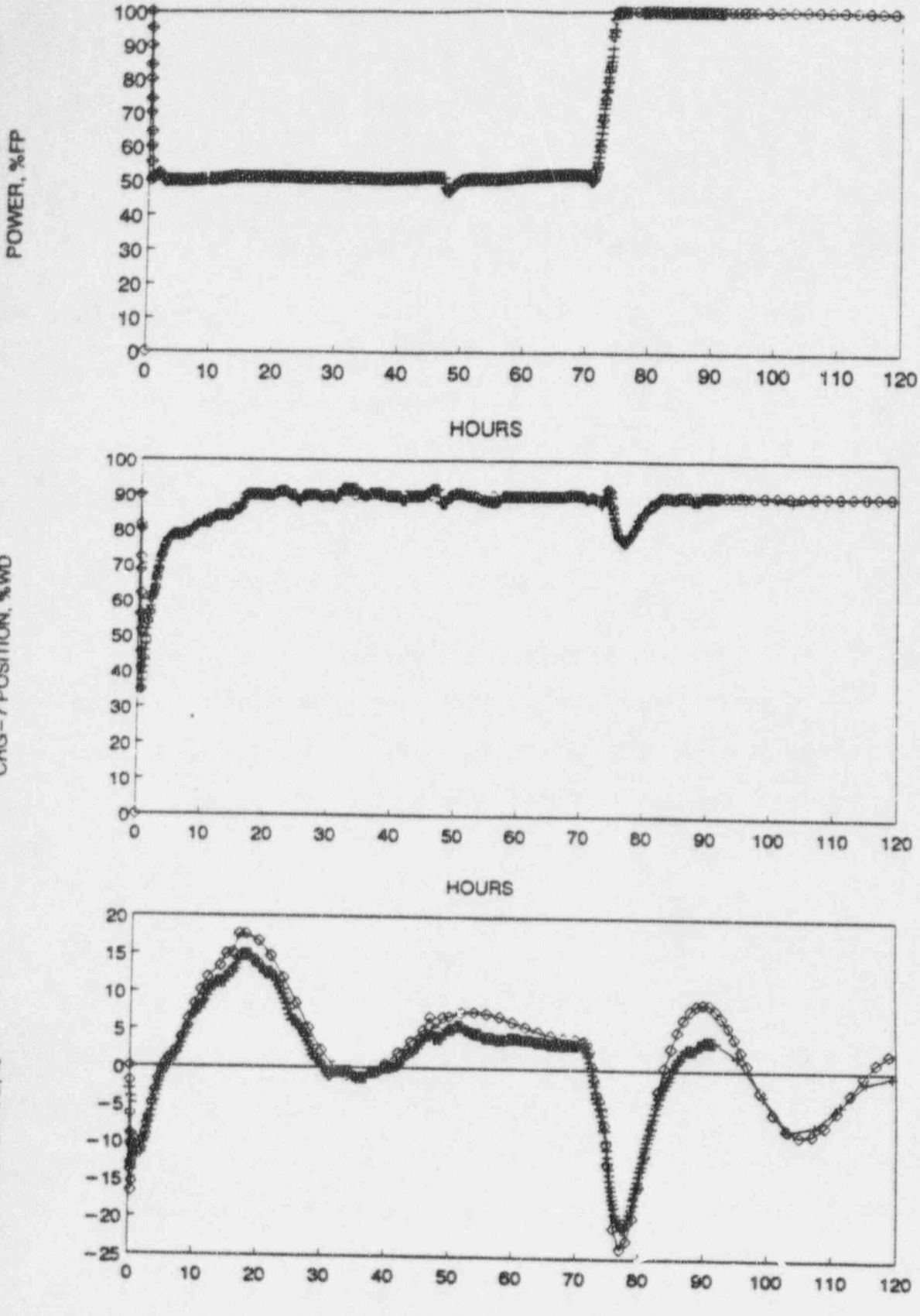

5.0 PIN POWER VALIDATION

SIMULATE-3 reconstructs the pin power from the calculated flux shapes and intranodal assembly powers. Since no measured pin power data is available at TMI-1, higher order computer codes, namely, CASMO-3 and PDQ (Refs. 1 and 29), are used for the pin power validation. In addition, the B&W cold critical experiments (Ref. 33) are also used to benchmark the pin power reconstruction.

5.1 Comparison with Higher Order Numeric Calculation

Two higher order computer codes, CASMO-3 and PDQ were used to benchmark SIMULATE-3 pin power reconstruction accuracy. CASMO-3, a transport theory code, is considered the higher order benchmark for the multiple assembly configuration. PDQ, a higher order diffusion code, is used to benchmark the pin power of a reactor core.

5.1.1 Multiple Assembly Configuration

A series of multiple assembly (2x2) configurations are setup to represent the possible combination of fuel enrichment, burnable poison rods, exposure, and control rod existence for typical TMI-1 core designs. The transport theory solution calculated by CASMO-3 is used as the higher order benchmark for SIMULATE-3.

The assembly fuel enrichment and burnable poison loading of the ten configurations studied are shown in Table 5.1. For each configuration, a 2x2 CASMO-3 run is submitted which directly calculates the spectral interaction between neighboring assemblies. This provides the "measured" value for the pin power comparison. Based on cross sections generated from single assembly CASMO-3 runs, SIMULATE-3 reconstructs the pin power of the assemblies using the surface discontinuity factors which account for the spectral interactions. Table 5.2 summarizes the comparison results.

The SIMULATE-3 calculated assembly powers and pin powers agree well with the CASMO-3 values, with an average RMS error of 0.00874. There is no observed trend except that the RMS error for rodded configurations is slightly higher.

The multi-assemblies pin power comparisons demonstrate that SIMULATE-3 pin power reconstruction is highly accurate.

5.1.2 TMI-1 Cycle 1 and Cycle 2

PDQ, a fine mesh diffusion code, is also used as the benchmark for the SIMULATE-3 reconstructed pin power. Both PDQ and SIMULATE-3 cross sections are based on the same single assembly CASMO-3 runs. The PDQ model has one mesh for each pin location. While the SIMULATE-3 model only has 4 meshes per fuel assembly.

The TMI-1 Cycle 1 core was depleted from 0 to 400 EFPD using PDQ and SIMULATE-3. The core was then shuffled for Cycle 2 and depleted to 250 EFPD using PDQ and SIMULATE-3. The assembly powers and peak pin powers from both calculations were compared at selected exposures of the cycles. Results are shown in Table 5.3. The RMS error is about 1% in assembly power and 2% for peak pin power. This again demonstrates the accuracy of the SIMULATE-3 pin power reconstruction technique. The quarter core assembly power and peak pin power comparisons at BOC, MOC, and EOC are shown in Figures 5.1 to 5.12.

5.2 Validation Versus B&W Critical Experiments

The B&W critical experiments (Ref. 33) measured pin power distribution for various PWR lattices consisting of different enrichments, large and small water holes, and poison materials. CASMO-3/SIMULATE-3 methodology was used to model these critical experiments. Cross section data were

generated based on single assembly CASMO-3 calculations. As shown in Figure 5.13, the critical core geometry was slightly modified at the core boundary in the SIMULATE-3 model. This should not affect the pin power of the center assembly.

SIMULATE-3 reconstructed pin powers were compared with the measured data. The pin by pin comparisons are shown in Figures 5.14 - 5.19. The close agreement in pin power distribution, 0.8% RMS for lattices without gadolinia and 1.3% RMS for lattices with gadolinia, demonstrates the accuracy of the SIMULATE-3 calculated pin power distribution. Table 5.4 summarizes the benchmark results.

Table 5.1 Assembly Loadings for Multi-Assembly Problems

Set	Variation	FA Type 1 wt % U^{235} BP Loading*	Initial Burnup (GWD/MTU)	FA Type 2 wt % U^{235} BP Loading*	Initial Burnup (GWD/MTU)
1	Enrichment	4.00	0	4.65	0
2	Control Rod	4.65	0	4.65 Control Rod In	0
3	Enrichment Control Rod	4.00	0	4.65 Control Rod In	0
4	Enrichment LBP	4.00	0	4.65 2.0 B_4C	0
5	LBP Gd Pin	4.65	0	4.65 2.0 B_4C 2.0 Gd	0
6	Enrichment Depletion	4.00	10	4.65	0
7	Enrichment Depletion Control Rod	4.00	15	4.65 Control Rod In	0
8	Enrichment Depletion APSR	4.00	0	4.65 APSR In	15
9	Depletion BP Pull	4.00	0	4.0 1.7 B_4C Pull	20 (with BP)
10	Enrichment Depletion BP Pull	4.65	0	4.0 1.7 B_4C Pull	20 (with BP)

* wt % B_4C

Table 5.2 Multi Assembly Pin Power Comparison *

Set	Mean	Std. Dev.	RMS	Peak Pin Rel. Diff	Worst Pin Rel. Diff
1	0.00001	0.00209	0.00209	0.00097	0.00420
2	0.00146	0.01228	0.01237	-0.01363	0.02667
3	0.00080	0.01058	0.01061	-0.01146	0.02804
4	0.00008	0.00470	0.00470	-0.00564	0.00877
5	0.00053	0.00925	0.00926	-0.00877	0.01323
6	0.00068	0.00860	0.00863	0.00924	0.01310
7	-0.00008	0.00665	0.00664	-0.00645	0.01962
8	0.00079	0.00925	0.00928	-0.01038	0.01684
9	0.00103	0.01094	0.01099	-0.01096	0.01715
10	0.00159	0.01269	0.01278	-0.01198	0.01957
Average	0.00069	0.00870	0.00874	-0.00691	0.01672

* Rel. Difference = (SIMULATE-3 - CASMO-3) /CASMO-3

Table 5.3 SIMULATE-3 and PDQ Power Comparisons*

	Assembly Power		Pin Power	
EFPD	RMS%	% DIFF AT PEAK ASSEMBLY	RMS %	% DIFF AT PEAK PIN
Cycle 1				
0	1.282	0.418	1.508	1.352
4	0.980	0.357	1.485	1.503
25	0.758	-0.607	1.574	0.556
50	0.631	0.379	1.567	1.640
100	0.693	1.116	1.653	2.404
150	0.778	1.515	1.683	2.790
200	0.703	1.297	1.661	2.604
250	0.652	1.096	1.652	2.389
300	0.579	0.816	1.604	2.123
350	0.802	1.039	1.604	2.270
Cycle 2				
0	1.3777	1.588	1.600	0.874
4	0.8436	1.725	1.519	1.365
25	0.7086	1.344	1.631	2.394
50	1.0576	1.355	1.605	2.501
100	0.7981	1.003	1.596	2.344
150	0.7120	0.699	1.606	2.065
200	0.8735	0.554	1.661	1.826
250	1.1061	0.563	1.749	1.733
300	1.2721	0.483	1.831	1.751
350	1.5128	0.579	1.978	1.806

* % Difference = (SIMULATE-3 - PDQ) * 100/PDQ

Table 5.4 B&W Critical Pin Power Results Summary

Core #	1	5	12	14	18	20
Fuel Assembly Design	2.46% 15x15 No Gd	2.46% 15x15 12 Gd	4.02% 15x15 No Gd	4.02% 15x15 12 Gd	4.02% 16x16 No Gd	4.02% 16x16 16 Gd
RMS Difference (S3 - Meas)	0.60%	1.40%	0.90%	1.10%	0.90%	1.30%
Error in Peak Pin (S3 - Meas)	0.27%	1.12%	0.35%	0.00%	0.81%	-1.40%

Figure 5.1

BOC 1 Radial Power Comparison Between SIMULATE-3 and PDQ

	8	9	10	11	12	13	14	15
H	1.385 1.420 -2.465	1.149 1.188 -3.291	1.057 1.073 -1.451	1.098 1.123 -2.213	1.101 1.105 -0.391	1.242 1.256 -1.078	1.542 1.536 0.418	1.043 1.029 1.332
K	1.149 1.188 -3.296	1.083 1.102 -1.670	1.078 1.105 -2.396	1.051 1.053 -0.184	1.122 1.137 -1.286	1.149 1.145 0.350	1.179 1.182 -0.199	0.942 0.930 1.325
L	1.057 1.073 -1.473	1.078 1.105 -2.412	1.037 1.034 0.324	1.080 1.070 0.983	1.031 1.019 1.189	1.095 1.100 -0.472	1.220 1.217 0.259	0.674 0.668 0.975
M	1.098 1.124 -2.259	1.051 1.054 -0.225	1.080 1.070 0.957	0.995 0.973 2.281	0.993 0.975 1.808	0.904 0.892 1.395	0.856 0.853 0.419	
N	1.101 1.106 -0.467	1.122 1.138 -1.356	1.031 1.020 1.133	0.993 0.976 1.776	0.839 0.823 2.008	0.749 0.749 0.059	0.488 0.484 0.855	
O	1.242 1.257 -1.178	1.149 1.146 0.254	1.095 1.101 -0.556	0.904 0.892 1.333	0.749 0.749 0.027	0.490 0.486 0.753		
P	1.542 1.538 0.300	1.179 1.183 -0.312	1.220 1.218 0.156	0.856 0.853 0.336	0.488 0.484 0.796	— SIMULATE-3 — PDQ — %DIFF		
R	1.043 1.031 1.206	0.942 0.931 1.202	0.674 0.668 0.860					

AVERAGE DIFFERENCE	-0.068
STANDARD DEVIATION	1.388

Figure 5.2

MOC 1 Radial Power Comparison Between SIMULATE-3 and PDQ

	8	9	10	11	12	13	14	15
H	1.378	1.281	1.159	1.227	1.123	1.184	1.199	0.785
	1.360	1.267	1.147	1.220	1.117	1.181	1.197	0.781
	1.297	1.088	1.087	0.610	0.586	0.229	0.212	0.535
K	1.281	1.176	1.234	1.137	1.196	1.079	1.036	0.738
	1.267	1.162	1.226	1.130	1.193	1.076	1.037	0.735
	1.088	1.181	0.651	0.607	0.233	0.298	-0.127	0.431
L	1.159	1.234	1.143	1.211	1.086	1.098	1.025	0.555
	1.147	1.226	1.136	1.214	1.085	1.102	1.030	0.556
	1.086	0.650	0.595	-0.220	0.058	-0.383	-0.493	-0.101
M	1.227	1.137	1.211	1.091	1.106	0.823	0.778	
	1.220	1.130	1.214	1.093	1.116	0.928	0.785	
	0.605	0.605	-0.221	-0.202	-0.929	-0.486	-0.837	
N	1.123	1.196	1.086	1.106	0.931	0.827	0.500	
	1.117	1.193	1.086	1.117	0.937	0.840	0.505	
	0.581	0.228	0.054	-0.931	-0.647	-1.491	-1.049	
O	1.184	1.079	1.098	0.923	0.827	0.544		
	1.182	1.076	1.102	0.928	0.840	0.552		
	0.221	0.292	-0.389	-0.490	-1.493	-1.520		
P	1.199	1.036	1.025	0.778	0.500	— SIMULATE-3		
	1.197	1.038	1.030	0.785	0.505	— PDQ		
	0.205	-0.136	-0.499	-0.843	-1.054	— %DIFF		
R	0.785	0.738	0.555					
	0.781	0.735	0.556					
	0.526	0.421	-0.111					

AVERAGE DIFFERENCE	0.031
STANDARD DEVIATION	0.721

Figure 5.3

EOC 1 Radial Power Comparison Between SIMULATE-3 and PDQ

	8	9	10	11	12	13	14	15
H	1.236	1.189	1.087	1.177	1.088	1.169	1.169	0.788
	1.223	1.177	1.078	1.167	1.082	1.166	1.171	0.790
	1.039	1.062	0.831	0.866	0.584	0.268	-0.153	-0.315
K	1.189	1.092	1.176	1.088	1.174	1.069	1.056	0.751
	1.177	1.082	1.165	1.081	1.167	1.067	1.060	0.755
	1.062	0.893	0.965	0.674	0.589	0.142	-0.334	-0.584
L	1.087	1.176	1.088	1.178	1.077	1.121	1.033	0.578
	1.078	1.165	1.081	1.171	1.073	1.122	1.042	0.584
	0.833	0.966	0.677	0.607	0.331	-0.122	-0.819	-1.015
M	1.177	1.088	1.178	1.081	1.138	0.967	0.815	
	1.167	1.081	1.171	1.078	1.139	0.972	0.825	
	0.869	0.676	0.609	0.364	-0.105	-0.512	-1.216	
N	1.088	1.174	1.077	1.138	0.991	0.922	0.558	
	1.082	1.167	1.073	1.139	0.995	0.934	0.567	
	0.591	0.595	0.334	-0.104	-0.384	-1.235	-1.571	
O	1.169	1.069	1.121	0.967	0.922	0.620		
	1.166	1.067	1.122	0.972	0.934	0.632		
	0.276	0.150	-0.117	-0.508	-1.234	-1.822		
P	1.169	1.056	1.033	0.815	0.558	--- SIMULATE-3		
	1.171	1.059	1.041	0.825	0.567	--- PDQ		
	-0.144	-0.328	-0.812	-1.211	-1.569	--- %DIFF		
R	0.788	0.751	0.578					
	0.790	0.755	0.584					
	-0.307	-0.577	-1.010					

AVERAGE DIFFERENCE	-0.025
STANDARD DEVIATION	0.796

Figure 5.4

BOC 2 Radial Power Comparison Between SIMULATE-3 and PDQ

	8	9	10	11	12	13	14	15
H	0.767	0.837	0.921	1.042	1.271	1.028	0.875	0.581
	0.767	0.839	0.919	1.039	1.268	1.029	0.882	0.584
	-0.052	-0.190	0.209	0.297	0.218	-0.080	-0.798	-0.482
K	0.840	0.990	1.025	1.113	1.395	1.036	0.800	0.559
	0.841	0.988	1.017	1.109	1.378	1.038	0.810	0.563
	-0.086	0.189	0.748	0.329	1.259	-0.218	-1.245	-0.764
L	0.934	1.034	1.020	1.126	1.348	1.068	0.961	0.455
	0.930	1.025	1.014	1.122	1.341	1.104	0.966	0.463
	0.448	0.834	0.575	0.363	0.490	-0.494	-0.518	-1.739
M	1.078	1.140	1.138	1.417	1.371	1.254	0.835	
	1.070	1.132	1.132	1.407	1.370	1.261	0.844	
	0.752	0.676	0.569	0.707	0.069	-0.545	-1.083	
N	1.359	1.444	1.372	1.380	1.109	1.043	0.556	
	1.350	1.420	1.360	1.377	1.117	1.055	0.566	
	0.676	1.725	0.856	0.195	-0.738	-1.171	-1.771	
O	1.071	1.070	1.120	1.267	1.049	0.619		
	1.066	1.066	1.120	1.271	1.059	0.631		
	0.520	0.364	-0.007	-0.304	-0.949	-1.874		
P	0.901	0.821	0.980	0.846	0.561	— SIMULATE-3		
	0.903	0.827	0.980	0.852	0.569	— PDQ		
	-0.199	-0.683	0.007	-0.699	-1.437	— %DIFF		
R	0.596	0.573	0.464					
	0.595	0.573	0.470					
	0.151	-0.051	-1.242					

AVERAGE DIFFERENCE	-0.119
STANDARD DEVIATION	0.793

Figure 5.5

MOC 2 Radial Power Comparison Between SIMULATE-3 and PDQ

	8	9	10	11	12	13	14	15
H	0.847	0.903	0.956	1.036	1.223	1.058	0.981	0.710
	0.844	0.901	0.952	1.030	1.216	1.055	0.983	0.711
	0.320	0.216	0.466	0.592	0.563	0.310	-0.231	-0.187
K	0.904	1.037	1.040	1.083	1.335	1.053	0.892	0.681
	0.901	1.031	1.032	1.077	1.325	1.051	0.898	0.684
	0.297	0.563	0.826	0.547	0.758	0.199	-0.667	-0.489
L	0.959	1.042	1.006	1.073	1.255	1.086	1.038	0.545
	0.954	1.033	1.000	1.067	1.248	1.087	1.044	0.552
	0.492	0.841	0.591	0.534	0.591	-0.055	-0.556	-1.219
M	1.048	1.090	1.075	1.286	1.257	1.203	0.878	
	1.041	1.084	1.069	1.278	1.254	1.206	0.887	
	0.629	0.590	0.547	0.624	0.215	-0.279	-0.965	
N	1.265	1.347	1.258	1.257	1.051	1.024	0.594	
	1.259	1.338	1.251	1.255	1.056	1.033	0.602	
	0.454	0.699	0.593	0.178	-0.425	-0.869	-1.384	
O	1.069	1.059	1.067	1.202	1.024	0.646		
	1.066	1.058	1.089	1.207	1.033	0.656		
	0.268	0.131	-0.136	-0.375	-0.862	-1.577		
P	0.983	0.894	1.038	0.878	0.593	— SIMULATE-3		
	0.987	0.900	1.045	0.887	0.602	— PDQ		
	-0.355	-0.678	-0.626	-0.960	-1.531	— %DIFF		
R	0.710	0.682	0.545					
	0.712	0.685	0.552					
	-0.322	-0.447	-1.268					

AVERAGE DIFFERENCE	-0.054
STANDARD DEVIATION	0.679

Figure 5.6

EOC 2 Radial Power Comparison Between SIMULATE-3 and PDQ

	8	9	10	11	12	13	14	15
H	0.936	0.978	1.001	1.034	1.166	1.060	1.038	0.798
	0.918	0.959	0.982	1.018	1.155	1.054	1.046	0.812
	2.012	1.944	1.968	1.613	0.972	0.567	-0.748	-1.774
K	0.977	1.091	1.067	1.065	1.254	1.047	0.946	0.767
	0.959	1.071	1.046	1.050	1.247	1.043	0.954	0.783
	1.877	1.889	1.976	1.461	0.549	0.394	-0.790	-1.993
L	1.000	1.067	1.016	1.046	1.181	1.062	1.059	0.614
	0.982	1.046	0.998	1.031	1.171	1.061	1.075	0.629
	1.879	2.004	1.783	1.423	0.843	0.090	-1.523	-2.397
M	1.038	1.066	1.045	1.203	1.179	1.152	0.891	
	1.022	1.051	1.031	1.193	1.175	1.161	0.910	
	1.602	1.467	1.366	0.808	0.327	-0.788	-2.063	
N	1.192	1.257	1.179	1.178	1.019	1.011	0.627	
	1.182	1.250	1.170	1.174	1.023	1.027	0.644	
	0.888	0.579	0.768	0.317	-0.342	-1.561	-2.576	
O	1.062	1.047	1.060	1.150	1.011	0.678		
	1.056	1.043	1.059	1.160	1.026	0.694		
	0.526	0.385	0.057	-0.828	-1.499	-2.342		
P	1.036	0.943	1.056	0.890	0.626	— SIMULATE-3		
	1.044	0.952	1.073	0.908	0.643	— PDQ		
	-0.746	-0.901	-1.588	-2.006	-2.625	— %DIFF		
R	0.796	0.765	0.612					
	0.810	0.781	0.628					
	-1.757	-1.983	-2.480					

AVERAGE DIFFERENCE	-0.019
STANDARD DEVIATION	1.528

Figure 5.7

BOC 1 Peak Pin Power Comparison Between SIMULATE-3 and PDQ

	8	9	10	11	12	13	14	15
H	1.475 1.497 -1.443	1.352 1.370 -1.321	1.130 1.138 -0.738	1.274 1.272 0.141	1.189 1.181 0.643	1.448 1.430 1.280	1.668 1.645 1.411	1.423 1.406 1.209
K	1.352 1.370 -1.321	1.181 1.194 -1.056	1.270 1.283 -1.021	1.125 1.119 0.518	1.343 1.336 0.524	1.264 1.249 1.225	1.444 1.425 1.340	1.371 1.353 1.330
L	1.130 1.139 -0.755	1.270 1.283 -1.036	1.103 1.098 0.483	1.246 1.230 1.326	1.117 1.099 1.656	1.316 1.298 1.348	1.423 1.401 1.549	1.168 1.152 1.389
M	1.274 1.273 0.086	1.125 1.120 0.473	1.246 1.230 1.276	1.076 1.045 2.990	1.192 1.160 2.723	1.016 0.993 2.317	1.229 1.216 1.044	
N	1.189 1.182 0.558	1.343 1.337 0.434	1.117 1.099 1.592	1.192 1.161 2.697	0.946 0.916 3.239	1.077 1.054 2.192	0.878 0.869 1.092	
O	1.448 1.431 1.174	1.264 1.250 1.120	1.316 1.300 1.246	1.016 0.994 2.241	1.077 1.054 2.153	0.820 0.813 0.849		
P	1.668 1.647 1.293	1.444 1.427 1.227	1.423 1.403 1.447	1.229 1.217 0.961	0.878 0.869 1.030	— SIMULATE-3 -- PDQ —%DIFF		
R	1.423 1.408 1.080	1.371 1.355 1.203	1.168 1.153 1.275					

AVERAGE DIFFERENCE	0.956
STANDARD DEVIATION	1.103

Figure 5.8

MOC 1 Peak Pin Power Comparison Between SIMULATE-3 and PDQ

	8	9	10	11	12	13	14	15
H	1.454	1.367	1.228	1.311	1.191	1.268	1.323	1.059
	1.417	1.333	1.200	1.280	1.169	1.244	1.302	1.048
	2.604	2.528	2.308	2.398	1.838	1.921	1.629	1.059
K	1.367	1.256	1.333	1.206	1.293	1.158	1.211	1.045
	1.333	1.226	1.298	1.183	1.265	1.140	1.190	1.031
	2.528	2.439	2.728	1.970	2.197	1.579	1.731	1.348
L	1.228	1.333	1.211	1.304	1.167	1.238	1.210	0.941
	1.200	1.298	1.188	1.278	1.152	1.216	1.197	0.930
	2.308	2.728	1.970	2.026	1.320	1.818	1.089	1.236
M	1.311	1.206	1.304	1.173	1.249	1.040	1.090	
	1.280	1.183	1.278	1.160	1.230	1.031	1.086	
	2.390	1.970	2.026	1.129	1.503	0.844	0.378	
N	1.191	1.293	1.167	1.249	1.046	1.127	0.869	
	1.169	1.265	1.152	1.230	1.039	1.112	0.866	
	1.838	2.189	1.320	1.503	0.645	1.376	0.314	
O	1.268	1.158	1.238	1.040	1.127	0.898		
	1.244	1.140	1.216	1.031	1.112	0.898		
	1.913	1.570	1.818	0.834	1.367	-0.002		
P	1.323	1.211	1.210	1.090	0.869	— SIMULATE-3		
	1.302	1.190	1.197	1.086	0.866	— PDQ		
	1.621	1.722	1.061	0.368	0.309	—%DIFF		
R	1.059	1.045	0.941					
	1.048	1.031	0.930					
	1.050	1.338	1.227					

AVERAGE DIFFERENCE	1.594
STANDARD DEVIATION	0.675

Figure 5.9

EOC 1 Peak Pin Power Comparison Between SIMULATE-3 and PDQ

	8	9	10	11	12	13	14	15
H	1.293 1.264 2.270	1.225 1.202 1.922	1.136 1.115 1.911	1.216 1.192 1.996	1.138 1.119 1.689	1.213 1.192 1.745	1.278 1.260 1.461	1.045 1.037 0.742
K	1.225 1.202 1.922	1.146 1.124 1.957	1.217 1.191 2.174	1.138 1.119 1.725	1.217 1.193 1.995	1.129 1.114 1.365	1.178 1.163 1.255	1.041 1.027 1.383
L	1.136 1.115 1.911	1.217 1.191 2.174	1.138 1.119 1.689	1.218 1.195 1.916	1.135 1.117 1.602	1.204 1.183 1.818	1.202 1.186 1.383	0.957 0.946 1.167
M	1.216 1.192 1.996	1.138 1.119 1.725	1.218 1.195 1.916	1.137 1.120 1.536	1.213 1.190 1.933	1.069 1.058 1.030	1.105 1.098 0.674	
N	1.138 1.119 1.698	1.217 1.193 1.995	1.135 1.117 1.602	1.213 1.190 1.941	1.085 1.073 1.071	1.174 1.151 2.025	0.940 0.929 1.132	
O	1.213 1.192 1.753	1.129 1.114 1.374	1.204 1.182 1.827	1.069 1.058 1.030	1.174 1.151 2.025	0.996 0.985 1.137		
P	1.278 1.260 1.469	1.178 1.163 1.264	1.202 1.186 1.383	1.105 1.098 0.674	0.940 0.929 1.125	— SIMULATE-3 — PDQ —%DIFF		
R	1.045 1.037 0.752	1.041 1.027 1.393	0.957 0.946 1.175					

AVERAGE DIFFERENCE	1.574
STANDARD DEVIATION	0.418

Figure 5.10

BOC 2 Peak Pin Power Comparison Between SIMULATE-3 and PDQ

	8	9	10	11	12	13	14	15
H	0.793	0.918	1.007	1.164	1.360	1.179	0.951	0.786
	0.782	0.906	0.992	1.144	1.346	1.149	0.937	0.780
	1.456	1.308	1.556	1.757	1.025	2.638	1.545	0.723
K	0.923	1.120	1.122	1.269	1.529	1.202	0.923	0.762
	0.910	1.109	1.128	1.268	1.493	1.187	0.922	0.757
	1.452	1.001	-0.54[illegible]	0.079	2.425	1.255	0.097	0.630
L	1.025	1.134	1.125	1.263	1.451	1.243	1.157	0.764
	1.007	1.138	1.105	1.242	1.435	1.228	1.147	0.760
	1.828	-0.307	1.856	1.707	1.122	1.180	0.845	0.472
M	1.211	1.305	1.275	1.582	1.466	1.366	1.140	
	1.185	1.298	1.252	1.561	1.456	1.345	1.132	
	2.220	0.501	1.84[illegible]	1.365	0.708	1.531	0.680	
N	1.459	1.573	1.473	1.481	1.263	1.254	0.990	
	1.437	1.529	1.452	1.467	1.251	1.217	0.985	
	1.510	2.884	1.467	0.982	0.592	3.057	0.526	
O	1.237	1.239	1.264	1.382	1.261	0.984		
	1.199	1.220	1.245	1.354	1.222	0.975		
	3.204	1.599	1.559	2.075	3.191	0.921		
P	0.982	0.946	1.178	1.156	1.000	— SIMULATE-3		
	0.961	0.939	1.162	1.143	0.981	— PDQ		
	2.205	0.698	1.342	1.111	0.900	—%DIFF		
R	0.808	0.781	0.781					
	0.796	0.771	0.773					
	1.515	1.237	1.068					

AVERAGE DIFFERENCE	1.345
STANDARD DEVIATION	0.814

Figure 5.11

MOC 2 Peak Pin Power Comparison Between SIMULATE-3 and PDQ

	8	9	10	11	12	13	14	15
H	0.873	0.976	1.028	1.135	1.306	1.150	1.041	0.943
	0.859	0.958	1.007	1.111	1.285	1.118	1.021	0.930
	1.599	1.843	2.045	2.197	1.642	2.853	1.969	1.434
K	0.977	1.146	1.112	1.202	1.434	1.172	0.986	0.915
	0.959	1.129	1.107	1.182	1.405	1.151	0.985	0.903
	1.893	1.506	0.497	1.726	2.071	1.869	1.140	1.299
L	1.032	1.115	1.085	1.175	1.338	1.191	1.206	0.891
	1.012	1.109	1.061	1.151	1.322	1.170	1.193	0.885
	2.027	0.559	2.223	2.067	1.210	1.777	1.124	0.660
M	1.151	1.209	1.177	1.408	1.342	1.286	1.168	
	1.126	1.188	1.153	1.389	1.329	1.260	1.154	
	2.211	1.725	2.099	1.331	0.948	2.063	1.178	
N	1.353	1.443	1.340	1.342	1.168	1.180	1.017	
	1.333	1.414	1.324	1.330	1.150	1.155	1.007	
	1.485	2.065	1.201	0.902	1.565	2.147	0.953	
O	1.167	1.179	1.192	1.286	1.180	1.003		
	1.135	1.157	1.172	1.260	1.155	0.994		
	2.801	1.866	1.733	2.055	2.156	0.944		
P	1.045	0.998	1.206	1.168	1.016	— SIMULATE-3		
	1.025	0.987	1.193	1.154	1.007	— PDQ		
	1.921	1.098	1.073	1.187	0.874	—%DIFF		
R	0.944	0.915	0.891					
	0.931	0.904	0.886					
	1.390	1.171	0.580					

AVERAGE DIFFERENCE	1.576
STANDARD DEVIATION	0.553

Figure 5.12

EOC 2 Peak Pin Power Comparison Between SIMULATE-3 and PDQ

	8	9	10	11	12	13	14	15
H	0.963	1.042	1.056	1.109	1.234	1.112	1.084	1.034
	0.931	1.004	1.020	1.072	1.207	1.084	1.081	1.029
	3.481	3.826	3.580	3.471	2.203	2.583	0.268	0.525
K	1.041	1.176	1.120	1.148	1.322	1.133	1.032	1.006
	1.003	1.145	1.092	1.118	1.300	1.105	1.017	1.003
	3.778	2.707	2.555	2.647	1.731	2.571	1.455	0.279
L	1.056	1.120	1.073	1.120	1.246	1.139	1.196	0.969
	1.020	.092	1.036	1.087	1.230	1.114	1.190	0.967
	3.570	.583	3.531	3.083	1.309	2.226	0.496	0.175
M	1.114	1.148	1.119	1.291	1.246	1.212	1.146	
	1.078	1.119	1.086	1.272	1.234	1.200	1.141	
	3.378	2.601	3.058	1.486	1.013	0.966	0.456	
N	1.261	1.325	1.245	1.245	1.109	1.137	1.025	
	1.237	1.302	1.228	1.232	1.086	1.119	1.018	
	1.907	1.806	1.360	1.039	2.108	1.581	0.698	
O	1.116	1.132	1.137	1.210	1.136	1.021		
	1.089	1.104	1.113	1.198	1.119	1.014		
	2.451	2.499	2.202	0.960	1.565	0.641		
P	1.082	1.030	1.193	1.144	1.023	— SIMULATE-3		
	1.079	1.015	1.188	1.139	1.017	— PDQ		
	0.325	1.458	0.463	0.457	0.630	—%DIFF		
R	1.031	1.003	0.966					
	1.026	1.001	0.965					
	0.497	0.240	0.111					

AVERAGE DIFFERENCE	1.781
STANDARD DEVIATION	1.149

Figure 5.13
B & W CRITICAL EXPERIMENT GEOMETRY

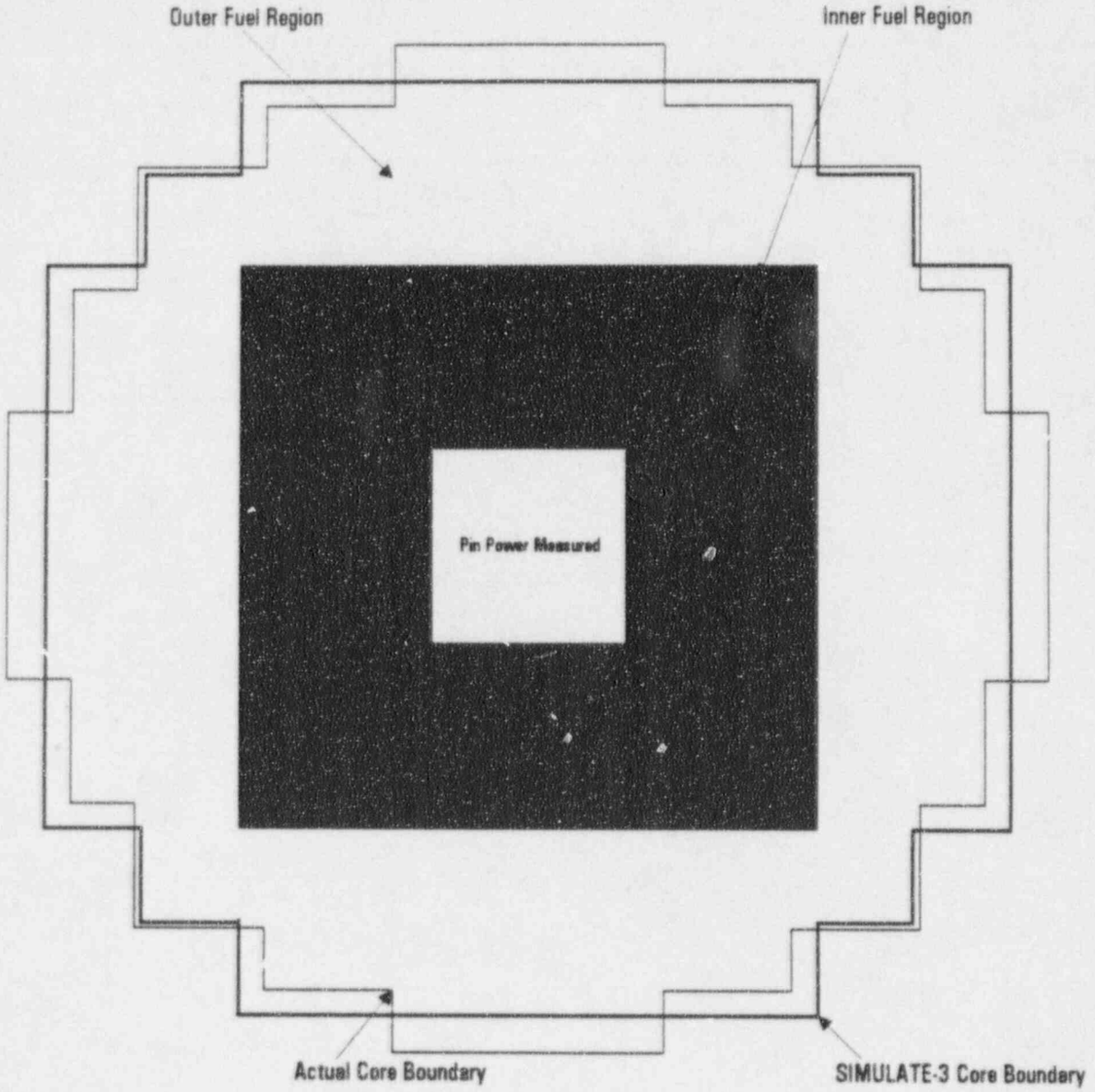

Figure 5.14

CORE 1
Normalized Midplane Power Distribution

	1.025	0.999	0.988	0.985	0.98[illegible]	0.963	0.942
RH DET	1.018	1.011	0.987	0.981	0.997	0.966	0.945
	0.007	-0.012	0.001	0.004	-0.015	-0.003	-0.003
	1.023	1.067	1.014	1.010	1.051	[illegible].984	0.946
	1.019	1.067	1.012	1.009	1.058	[illegible].999	0.945
	0.004	0.000	0.002	0.001	-0.007	-0.015	0.001
			1.065	1.086		1.041	0.952
		WATER	1.081	1.090	WATER	1.032	0.953
			0.004	-0.004		0.008	-0.001
			1.060	1.[illegible]67	1.088	0.991	0.945
			1.054	1.[illegible]84	1.086	0.989	0.945
			0.006	[illegible].883	0.002	0.002	0.000
					1.058	0.963	0.935
				WATER	1.059	0.965	0.934
					0.000	-0.002	0.001
					0.983	0.943	0.925
					0.988	0.938	0.923
					-0.005	0.005	0.002
						0.927	0.916
						0.925	0.914
						0.002	0.002
							0.907 — S3
							0.903 — MEAS
							0.004 — DIFF

AVERAGE DIFFERENCE 0.000
STANDARD DEVIATION 0.006

Figure 5.15

CORE 5
Normalized Midplane Power Distribution

RH DET	1.020	0.898	0.176	0.917	1.050	1.081	1.092
	1.005	0.913	0.178	0.932	1.036	1.063	1.072
	0.015	-0.015	0.006	-0.015	0.014	0.018	0.020
	1.013	1.023	0.905	1.003	1.131	1.106	1.098
	0.999	1.017	0.931	1.007	1.125	1.094	1.089
	0.014	0.006	-0.026	-0.004	0.006	0.012	0.009
			0.965	1.079		1.171	1.104
		WATER	0.988	1.087	WATER	1.158	1.100
			-0.023	-0.008		0.013	0.004
			0.180	1.028	1.149	1.101	1.092
			0.181	1.050	1.131	1.088	1.086
			-0.001	-0.022	0.018	0.013	0.006
					1.018	1.031	1.071
				WATER	1.048	1.035	1.070
					-0.030	-0.004	0.001
					0.188	0.942	1.058
					0.187	0.963	1.054
					0.001	-0.021	0.004
						1.019	1.067
						1.018	1.060
						0.001	0.007
							1.078 --- S3
							1.070 --- MEAS
							0.008 --- DIFF

GD PIN

AVERAGE DIFFERENCE	0.001
STANDARD DEVIATION	0.014

Figure 5.16

CORE 12
Normalized Midplane Power Distribution

RH DET	1.081	1.029	1.010	0.998	0.986	0.954	0.919
	1.075	1.041	1.006	1.019	1.000	0.960	0.923
	0.006	-0.012	0.004	-0.021	-0.014	-0.006	-0.004
	1.067	1.125	1.040	1.028	1.081	0.978	0.922
	1.067	1.125	1.044	1.034	1.075	0.987	0.927
	0.000	0.000	-0.004	-0.006	0.006	-0.009	-0.005
			1.131	1.122		1.053	0.924
		WATER	1.114	1.118	WATER	1.034	0.942
			0.017	0.004		0.019	-0.018
			1.080	1.142	1.112	0.976	0.912
			1.083	1.137	1.102	0.979	0.908
			-0.003	0.005	0.010	-0.003	0.004
					1.069	0.937	0.896
				WATER	1.071	0.939	0.895
					-0.002	-0.002	0.001
					0.963	0.909	0.878
					0.958	0.900	0.883
					0.005	0.009	-0.005
						0.883	0.859
						0.884	0.856
						-0.001	0.003
							0.837 --- S3
							0.845 --- MEAS
							-0.008 --- DIFF

AVERAGE DIFFERENCE	-0.001
STANDARD DEVIATION	0.009

Figure 5.17

CORE 14
Normalized Midplane Power Distribution

RH DET	1.095 1.091 0.004	0.972 0.992 -0.020	0.157 0.162 -0.005	0.966 0.976 -0.010	1.050 1.057 -0.007	1.049 1.038 0.011	1.032 1.028 0.004
	1.078 1.080 -0.002	1.117 1.118 -0.001	0.980 1.000 -0.020	1.045 1.054 -0.009	1.158 1.158 0.000	1.078 1.091 -0.013	1.037 1.028 0.009
		WATER	1.067 1.072 -0.005	1.145 1.138 0.007	WATER	1.163 1.140 0.023	1.039 1.038 0.001
			0.159 0.164 -0.005	1.110 1.114 -0.004	1.183 1.151 0.032	1.071 1.059 0.012	1.026 1.013 0.013
				WATER	1.067 1.080 -0.013	1.005 1.011 -0.006	1.004 1.003 0.001
					0.156 0.162 -0.004	0.925 0.942 -0.017	0.984 0.976 0.008
						0.965 0.965 0.000	0.974 0.978 -0.004
							0.962 — S3 0.959 — MEAS 0.003 — DIFF

GD PIN

AVERAGE DIFFERENCE -0.001
STANDARD DEVIATION 0.011

Figure 5.18

CORE 18
Normalized Midplane Power Distribution

RH DET	1.216	1.034	1.001	0.986	0.968	0.946	0.921
	1.205	1.033	0.997	0.977	0.959	0.941	0.909
	0.011	0.001	0.004	0.009	0.009	0.005	0.012
	1.061	1.032	1.027	1.013	0.981	0.949	0.920
	1.076	1.021	1.012	1.010	0.982	0.946	0.912
	0.005	0.011	0.015	0.003	-0.001	0.003	0.008
		1.080	**1.218**	1.204	1.039	0.957	0.917
		1.065	**1.228**	1.203	1.043	0.957	0.928
		0.015	**-0.010**	0.001	-0.004	0.000	-0.011
					1.175	0.964	0.912
					1.183	0.974	0.924
			LARGE WATER		-0.008	-0.010	-0.012
			HOLE		1.160	0.952	0.900
					1.170	0.970	0.909
					-0.010	-0.018	-0.009
					1.001	0.921	0.882
					0.995	0.924	0.886
					0.006	-0.003	-0.004
						0.889	0.861
						0.893	0.866
						-0.004	-0.005
							0.837 --- S3
							0.833 --- MEAS
							0.004 --- DIFF

AVERAGE DIFFERENCE	0.000
STANDARD DEVIATION	0.009

$$\sigma_D = \sqrt{\frac{\sum_{i=1}^{N} (D_i - \bar{D})^2}{N-1}}$$

where N is the total number of values.

The difference distribution is tested for normality using either the W test ($N \leq 50$) or the D' test ($N > 50$) of Ref. 34. If the difference distribution is normal, the one-sided 95/95 tolerance limit is used to determine the reliability factor. The one-sided upper tolerance limit, D_{upper} is defined by:

$$D_{upper} = \bar{D} + K_{95/95} \times \sigma_D$$

where the first term is the modeling bias and the second term is the 95/95 uncertainty factor which is the sampling standard deviation multiplied by the K value for a 95/95 upper tolerance limit. The value for K can be obtained from Table A-7 in Ref. 35 which accounts for the fact that sample uncertainty is used. If the difference distribution is not a normal distribution, the non-parametric tolerance method from Ref. 36 is used to obtain the one-sided 95/95 upper tolerance limit for sample size greater than 50. The D_{upper} value is then applied to the calculated parameters so that modeling bias and uncertainty are included, thus assuring conservative safety analysis results.

In summary, the reliability factor is applied to the calculated physics parameters to obtain the values to be used in reload analysis. For physics parameters which are based on the absolute difference between the calculated and measured values, one has

$$Parameter_{safety} = Parameter_{calc} + Reliability\ Factor$$

which can be rewritten as

$$Parameter_{safety} = Parameter_{calc} + Bias + UF_{95/95},$$

or

$$Parameter_{safety} = Parameter_{calc} + Bias - UF_{95/95},$$

where

$$Bias = -\overline{D},$$

and $UF_{95/95}$ is the 95/95 one sided uncertainty factor which is always applied in the direction so that the reload analysis results will be more conservative.

The same method can be applied when relative difference, i.e.,

$$D_i = \sum_{i=1}^{N} \frac{C_i - M_i}{M_i}$$

is used. For physics parameters which are based on the relative difference between the calculated and measured values, one has

$$Parameter_{safety} = Parameter_{calc} \times (1 + Reliability\ Factor)$$

The above equation can be rewritten in terms of bias and $UF_{95/95}$, i.e.,

$$Parameter_{safety} = Parameter_{calc} \times (1 + Bias + UF_{95/95})$$

or

$$Parameter_{Safety} = Parameter_{calc} \times (1 + Bias - UF_{95/95})$$

Again, the 95/95 uncertainty factor, $UF_{95/95}$, is applied in the direction so that the reload analysis results will be conservative.

6.2 HZP BOC ARO Critical Boron

The reliability factor for HZP ARO critical boron is determined based on the TMI-1 Cycles 1 to 10 start-up physics test results shown in Table 4.4. The differences between calculated and measured critical boron concentration range from -31 ppm to 15 ppm with a sample mean and standard deviation of -13 ppm and 14 ppm respectively. The difference distribution is found to be a normal distribution using the W test of Ref. 34. For a sample size of 10, the K factor for 95/95 upper tolerance limit is 2.911 and the reliability factor is 54 ppm.

6.3 HZP BOC Control Rod Worth

The control rod worth for the individual control rod Groups 5, 6 and 7 are measured using the boron dilution technique during the hot zero power start-up test. The reliability factor for control rod worth is determined based on the TMI-1 Cycles 1 to 10 start-up physics test results shown in Table 4.5. The % differences between calculated and measured control rod worth range from -9.25% to 9.90% with a sample mean and standard deviation of -2.78% and 4.21%, respectively. The difference distribution failed the W normality test of Reference 34 for 95% confidence. Based on the difference distribution range, the reliability factor for individual control rod worth is chosen to be -15%. This is a conservative estimate considering the mean and standard distribution of the difference distribution (See Table 4.5).

The reliability factor for the regulating control rod Groups 5, 6 and 7 combined, can be determined

based on the TMI-1 Cycles 1 to 10 start-up physics test results shown in Table 4.6. The percent differences between calculated and measured control rod worth range from -6.58% to 1.24% with a sample mean and standard deviation of -2.93% and 3.15%, respectively. The difference distribution failed the W normality test of Reference 34 for 95% confidence. Because of the difference range, the reliability factor for the combined regulating control rod worth is chosen to be -10%. This is a conservative estimate considering the mean and standard deviation of the difference distribution.

6.4 HZP BOC Isothermal Temperature Coefficient

The reliability factor for the isothermal temperature coefficient is determined based on the TMI-1 Cycles 1 to 10 start-up physics test results shown in Table 4.7. The difference between calculated and measured isothermal temperature coefficient ranges from 0.4 PCM/°F to 1.61 PCM/°F with a sample mean and standard deviation of 0.88 and 0.34 PCM/°F respectively. The difference distribution is found to be a normal distribution using the W test. For a sample size of 17, the K factor for 95/95 upper tolerance limit is 2.486. With a bias of -0.88 PCM/°F, the reliability factor is -0.036 PCM/°F for overheating accidents and -1.722 PCM/°F for overcooling accidents.

6.5 HFP Critical Boron

The reliability factor for the hot full power critical boron is determined based on the Cycles 8 and 9 comparisons shown in Table 4.1. The difference distribution ranges from -36 ppm to 8 ppm with a mean of -9 ppm and a standard deviation of 9 ppm. The difference distribution is normal based on the D' test (Ref. 34) results with a 95% significance level. For a sample size of 52, the K factor for 95/95 upper tolerance limit is 2.049 and the reliability factor is 28 ppm.

6.6 Peak Power

The nuclear reliability factors for predictions of the peak radial and total (maximum axial segment)

Figure 5.19

CORE 20
Normalized Midplane Power Distribution

RH DET	1.300	1.092	1.065	1.060	1.048	1.033	1.026
	1.277	1.082	1.059	1.043	1.043	1.017	1.010
	0.023	0.010	0.006	0.017	0.005	0.016	0.016
	1.120	1.003	1.064	1.080	1.036	0.957	0.997
	1.110	1.011	1.052	1.075	1.034	0.973	0.979
	0.010	-0.008	0.005	0.005	0.002	-0.016	0.018
		0.164	1.214	1.290	1.046	0.161	0.935
		0.168	1.238	1.268	1.073	0.164	0.954
		-0.004	-0.024	0.022	-0.027	-0.003	-0.019
					1.266	0.982	0.992
					1.284	0.972	0.999
			LARGE WATER		-0.018	0.010	-0.007
			HOLE		1.279	1.043	1.005
					1.280	1.045	0.999
					-0.001	-0.002	0.006
					1.083	0.947	0.968
					1.077	0.962	0.978
					0.006	-0.015	-0.010
						0.154	0.892
						0.152	0.900
						-0.004	-0.008
							0.925 --- S3
							0.931 --- MEAS
							-0.006 --- DIFF

GD PIN

AVERAGE DIFFERENCE	0.000
STANDARD DEVIATION	0.013

6.0 RELIABILITY FACTORS

TMI-1 reload analysis requires physics parameters input from physics calculations. Reliability factors are used to ensure that the calculated parameters such as the temperature coefficient, hot pin power, etc., to be used for determination of operating limits and setpoints, include the model uncertainties and the sampling uncertainties. The reliability factors determined in this report are based on TMI-1 Cycles 1 through 10 operation data. These values are typical of the values used in reload analysis, but they will be evaluated, and revised if needed, as more operation data is available.

6.1 Method Description

The reliability factor can be determined by first determining the difference between calculated and measured values, i.e.,

$$D_i = C_i - M_i$$

where

D_i = ith difference,

C_i = ith calculated value,

M_i = ith measured value.

This difference distribution is then tested for normality using the method described in ANSI N15.15 (Ref. 34). The sample mean and standard deviation of the difference distribution are calculated as:

$$\bar{D} = \frac{\sum_{i=1}^{N} D_i}{N} = \frac{\sum_{i=1}^{N} (C_i - M_i)}{N}$$

and

powers are determined by statistically combining the corresponding global reliability factor with the local reliability factor. The former is based on the assembly nodal power distribution, and the latter is based on the radial-local factor. This section describes the calculation of individual component's reliability factor and those of the combined peaking factors.

6.6.1 Radial-Local Factor

The radial-local factor is defined as the ratio of the pin power to the assembly radial power. The SIMULATE-3 reconstructed pin powers have been benchmarked against B&W critical experiments and multi-assembly analyses in Section 5. The statistical results of the radial-local factor comparisons are shown in Table 6.1 and the frequency plots are shown in Figures 6.1 - 6.2. Although the relative difference distributions appear to be normal, the D' test indicates that the combined relative difference distribution is not a normal distribution for a 95% significance level. The 95/95 nuclear reliability factor is determined to be 1.007 using the non-parametric upper tolerance limit which is very close to the 1.008 value calculated assuming normal distribution. For conservatism, the radial-local nuclear reliability factor is 1.008.

6.6.2 Assembly Radial Power

The reliability factor for the assembly radial power has been determined by comparisons against the TMI-1 Cycles [illegible] plant data at selected state points (Section 4). All of the eighth core locations are used in determining the uncertainty. The statistical results of the assembly radial power comparisons are shown in Table 6.2 and the frequency plot is shown in Figure 6.3. The sample mean and standard deviation of the relative difference distribution is -0.00191 and 0.01814, respectively. The combined relative difference distribution is slightly skewed as shown in the frequency plot and it is not a normal distribution based on the D' test criteria for a 95% significance level. Using the non-parametric method, the 95/95

nuclear reliability factor is determined to be 1.033 which happens to be the same value if calculated assuming normal distribution.

6.6.3 Assembly Total Power

The nuclear reliability factor for the assembly total power (maximum axial segment power) has been determined by comparisons against TMI-1 Cycles 6-9 plant data at selected state points (Section 4). For the peak power statistics, the three highest measured segments are used. The statistical results are shown in Table 6.3 and the frequency plot is shown in Figure 6.4. The sample mean and standard deviation of all data is -0.015 and 0.02266, respectively. The frequency plot shows that the distribution is skewed and the D' test indicates that the distribution is not a normal distribution for a 95% significance level. The 95/95 nuclear reliability factor is 1.051 using the non-parametric method which is slightly less than the 1.053 value determined assuming normal distribution. For conservatism, the assembly total power nuclear reliability factor is 1.053.

6.6.4 Radial Pin Power

The nuclear reliability factor for the radial pin power is obtained by using a Monte Carlo method to combine the uncertainties of assembly radial power factors and radial-local factors. The Monte Carlo simulation randomly sampled the data from the assembly values and the radial-local components. The predicted values were multiplied to simulate calculated radial pin power factors. The corresponding measured values from Cycles 6-9 were also multiplied to give the "measured" factors. The relative difference distribution is then obtained and Satterthwaite's approximation (Ref. 37) was used to determine the equivalent degrees of freedom. The difference distribution is not a normal distribution based on the D' test for a 95% significance level. The 95/95 nuclear reliability factor determined from the non-parametric method is 1.033 which is slightly less than the 1.035 value obtained

assuming normal distribution. For conservatism, the radial peak pin power nuclear reliability factor is 1.035.

6.6.5 Total Pin Power

The nuclear reliability factor for the total pin power is obtained by using the Monte Carlo method described in Section 6.6.4 to combine the uncertainties of assembly total power factors and radial-local factors. The difference distribution obtained is not a normal distribution based on the D' test for a 95% significance level. The 95/95 nuclear reliability factor determined from non-parametric method is 1.054 which is slightly less than the 1.055 value obtained assuming normal distribution. The total peak pin power nuclear reliability factor is 1.055.

Table 6.1 Radial-Local Factor Statistical Results*

	# of Points	Mean Difference	Standard Deviation	Normality
B&W Critical Experiment	192	-0.00073	0.01143	Yes
Multi-Assembly Problems	15930	0.00003	0.00449	No
Combined	16122	0.00003	0.00464	No

* Difference = SIMULATE-3 - Measurement

Table 6.2 Assembly Radial Power Statistical Results*

Cycle	Number of Points	Mean % Difference	Standard Deviation	Normality
6	522	-0.00053	0.01031	No
7	667	+0.00001	0.01048	No
8	406	-0.00140	0.02739	No
9	667	-0.00400	0.02077	No
All	2262	-0.00191	0.01814	No

* % Difference = (SIMULATE-3 - Measurement) * 100/Measurement

Table 6.3 Assembly Total Peak Power Statistical Results*

Cycle	Number of Points	Mean % Difference	Standard Deviation	Normality
6	1566	-0.01840	0.0146	No
7	2001	-0.01553	0.01843	No
8	1218	-0.0146	0.03367	No
9	2001	-0.01202	0.02294	No
All	6786	-0.015	0.02266	No

* % Difference = (SIMULATE-3 - Measurement) * 100/Measurement

Figure 6.1
Frequency Distribution of B&W Criticals Comparisons

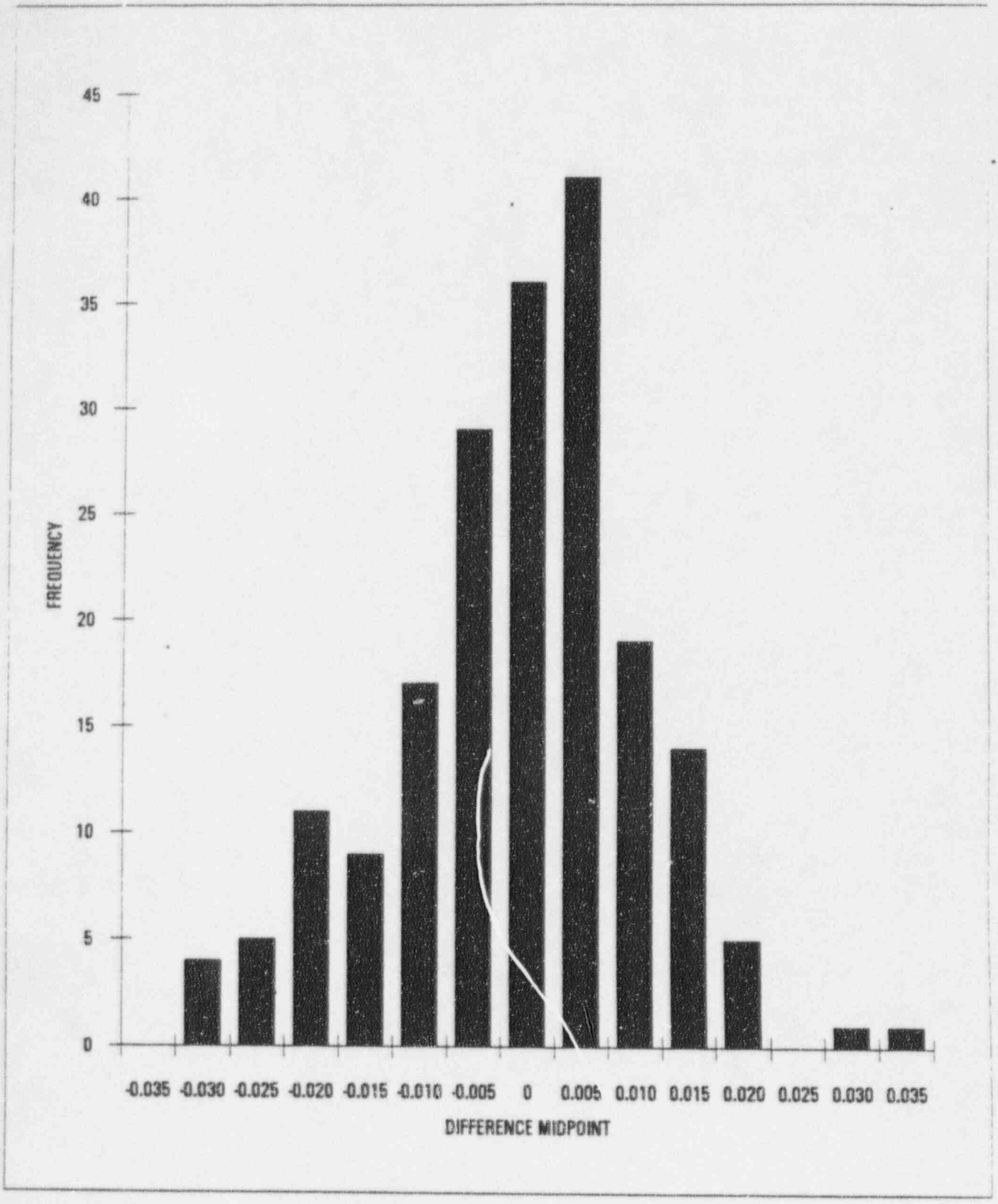

Figure 6. 2
Frequency Distribution of Multi-Assembly Comparisons

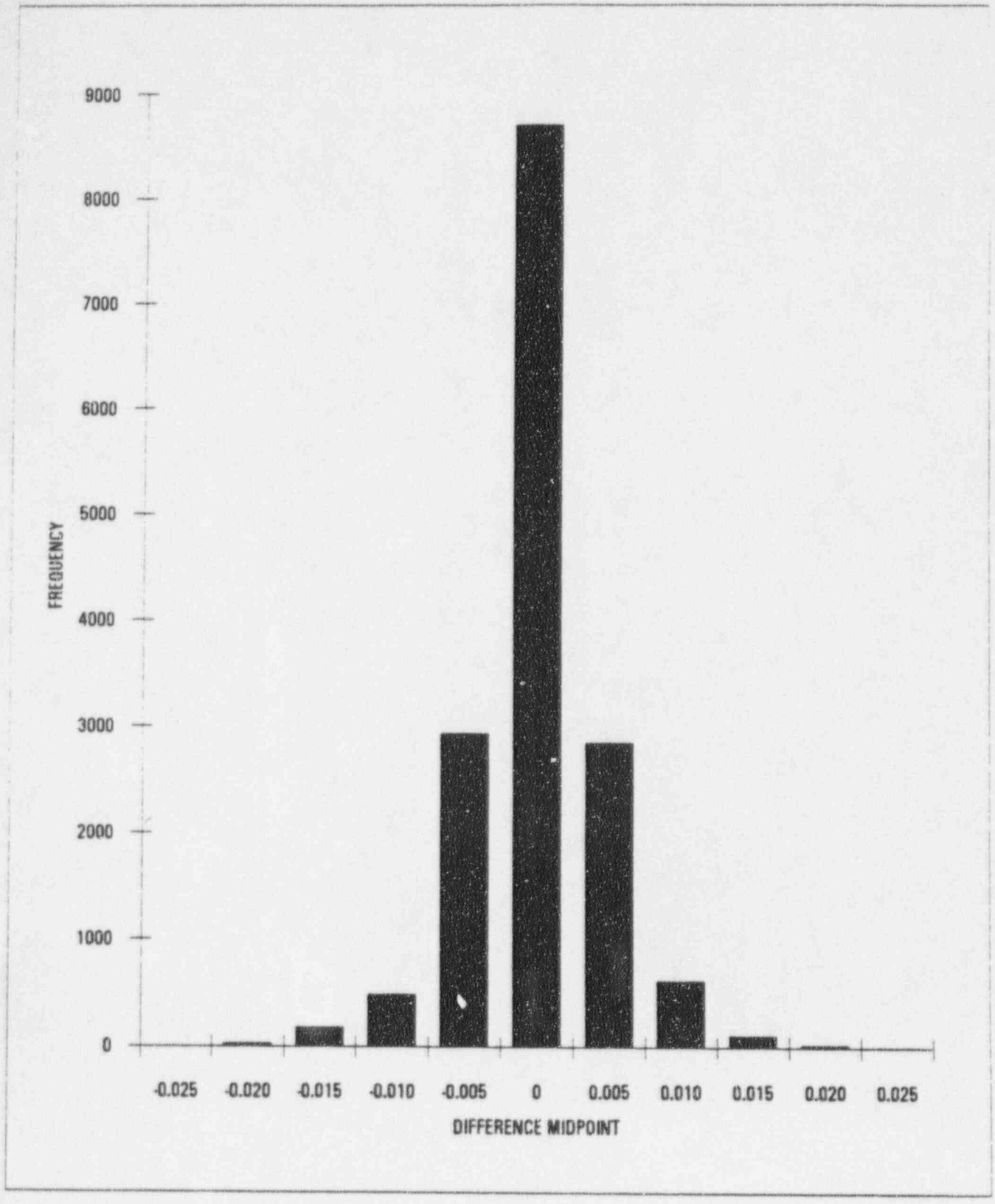

Figure 6.3
Frequency Distribution of Assembly Radial Power Comparisons

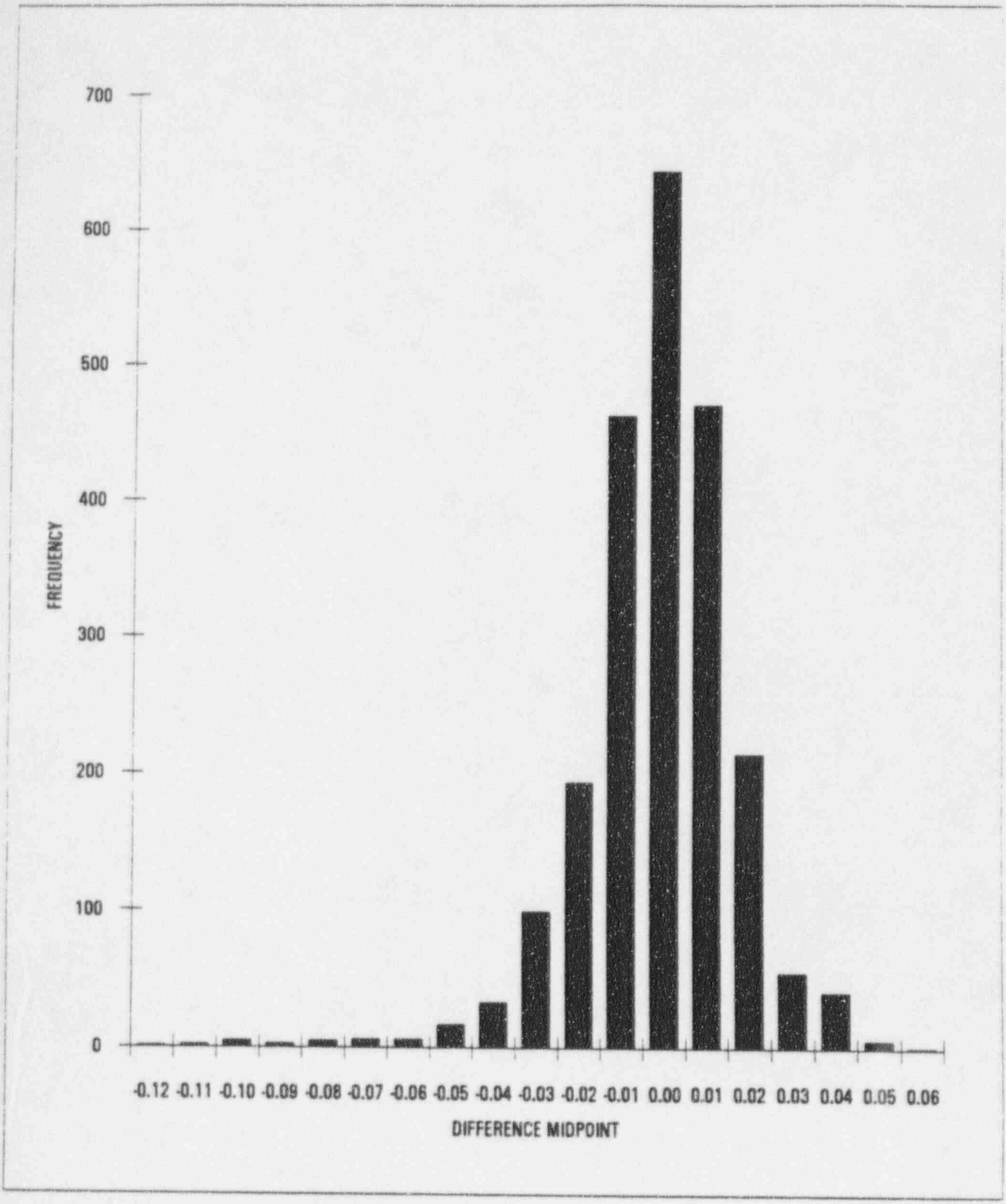

Figure 6.4
Frequency Distribution of Assembly Total Power Comparisons

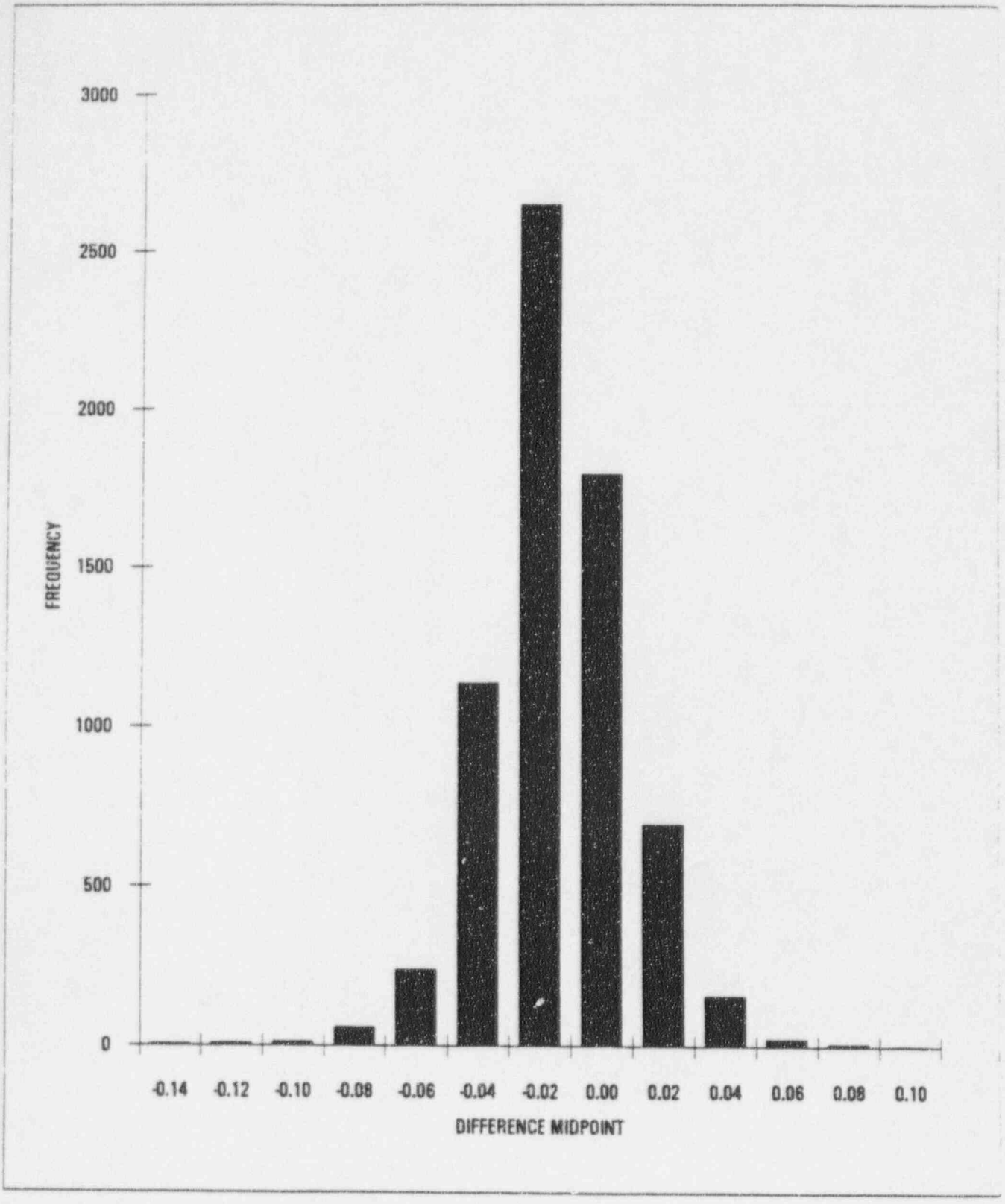

7.0 CONCLUSION

This report justifies GPUN's use of CASMO-3 and SIMULATE-3 for reload design of TMI-1, a B&W 177 fuel assembly plant. CASMO-3 and SIMULATE-3 are widely used computer codes in the industry and have been extensively benchmarked by the developer, Studsvik. This report emphasizes the application of CASMO-3 and SIMULATE-3 in modeling TMI-1 cores and compares the results to actual plant operations data; thus, demonstrating GPUN's capability to use these models in performing in-house physics analysis.

The in-house benchmark includes a comparison of calculated and measured data from various beginning-of-cycle hot zero power startup tests, as well as steady-state and plant power maneuvering operations. All the comparisons show very good agreement between calculated and measured data. The benchmark results and corresponding reliability factors are summarized in Table 7.1. These reliability factors are based on TMI-1 Cycles 1 through 10 operation data and they will be reevaluated each cycle to ensure that 95/95 tolerance/confidence is satisfied.

It is concluded that CASMO-3 and SIMULATE-3 accurately model the TMI-1 core and that GPUN has the capability to use these models in performing reload physics analysis in support of licensing TMI-1 cores.

Table 7.1 Summary of TMI-1 Applications

	Number of Cycles	Degrees of Freedom	Mean*	Standard Deviation	95/95 Reliability Factor
HZP BOC ARO Critical Boron	10	9	-13 ppm	14 ppm	54 ppm
HZP BOC Individual CR Group Worth	10	29	-2.78%	4.21%	-15%
HZP BOC Regulating CR Group Worth	10	9	-2.93%	3.15%	-10%
HZP BOC Isothermal Temp. Coefficient	10	16	0.88 PCM/°F	0.34 PCM/°F	-0.036 PCM/°F* or -1.722 PCM/°F
HFP Critical Boron	2	51	-9 ppm	9 ppm	28 ppm
Radial-Local Factor		16121	0.00003	0.00464	1.008
Assembly Radial Power	4	2261	-0.19%	1.81%	1.033
Assembly Total Power	4	6785	-1.50%	2.27%	1.053
Radial Pin Peak	4	2746	-0.22%	1.94%	1.035
Total Pin Peak	4	2468	-1.56%	2.30%	1.055

* Difference = SIMULATE-3 - Measurement
% Difference = (SIMULATE-3 - Measurement) * 100/Measurement

* -0.036 PCM/°F for overheating accidents and -1.722 PCM/°F for overcooling accidents.

8.0 REFERENCES

1. M. Edenius and B. H. Forssen, "CASMO-3, A Fuel Assembly Burnup Program V4.7," Studsvik/NFA-89/03, Rev. 3, June 1993, Studsvik Energitenik.

2. J. A. Umbarger, "TABLES-3, Library Preparation Code for SIMULATE-3," Studsvik/SOA-92/03, Rev. 0, April 1992.

3. K. S. Smith, J. A. Umbarger and A. S. DiGiovine, "SIMULATE-3, Advanced Three-Dimensional Two-Group Reactor Analysis Code V4.02," Studsvik/SOA-92/01, Rev. 0, April 1992.

4. P. Jernberg, "CASMO-3 Benchmark Against Critical Experiments," Studsvik/NFA-86/11, August 1986.

5. L. E. Strawberry and R. F. Barry, "Criticality Calculations for Uniform Water-Moderated Lattices," Nuclear Science and Engineering, 23, 58-73 (1965).

6. E. Blomsjo, M. Edenium, and R. Persson, "Critical Experiments up to 245°C with H_2O-Moderated UO_2-Rod Lattices in KRITZ," AE-RF-71-267, Studsvik, AB Atomenergi, Sweden.

7. J. R. Brown et. al., "Kinetics and Buckling Measurements on Lattices of Slightly Enriched Uranium of UO_2 Rods in Light Water," Bettis Plant WAPD-176, 1958.

8. R. D. Leamer et. al., "PuO_2-UO_2 Fueled Critical Experiments," WCAP-3726-1, Westinghouse 1967.

9. "Listing of Thermal Benchmark Experiments", U.S. Atomic Energy Commission RRD: TP:043 (1974).

10. E. Johansson, "The Reactivity from CASMO/DIXY Calculations with the Libraries E3LI69C and E3L69GB for Various Experimental Cores," Studsvik/NR-85/73, 1985.

11. M. N. Baldwin; G. S. Hooveler; R. L. Eng; and F. G. Welfare, "Critical Experiments Supporting Close Proximity Water Storage of Power Reactor Fuel," BAW-1484-7, Babcock & Wilcox, 1979.

12. E. Johansson and M. Edenius, "Benchmark of CASMO/CPM 69-Group Library Based on ENDF/B-5--E", Proceedings: Thermal Reactor Benchmark Calculations, Techniques, Results and Applications P25-1, EPRI, NP-2855, 1983.

13. K. S. Smith, "Pin Power Reconstruction: Benchmarking Against the B&W Critical Experiments," Trans Am. Nuc. Soc., 56, 531, 1988.

14. K. S. Smith and D. M. VerPlanck, "KWU-PWR: SIMULATE-3P Solution to the KWU PWR Depletion Benchmark Problem," Studsvik/SDA-89/06, 1989.

15. K. S. Smith and K. R. Rempe, "Testing and Applications of the QPANDA Nodal Model," International Topical Meeting on Advances in Reactor Physics, Mathematics, and Computations," II, 861, Paris, April 1987.

16. A. S. DiGiovine et. al., "CASMO-3G Validation," YAEC-1363, Yankee Atomic Electric Company, April, 1988.

17. A. S. DiGiovine et. al., "SIMULATE-3 Validation and Verification," YAEC-1659, Yankee Atomic Electric Company, September 1988.

18. "Nuclear Design Methodology Using CASMO-3/SIMULATE-3P," DPC-NE-1004, Duke Power Company, January 1990.

19. "Core Operation Report - Three Mile Island Unit 1, Cycle 1 Operation, September 2, 1974 - February 21, 1976," BAW-1443, October 1976.

20. "Core Operation Report - Three Mile Island Unit 1, Cycle 2 Operation, May 24, 1976 - March 18, 1977," BAW-1459, April 1977.

21. "Core Operation Report - Three Mile Island Unit 1, Cycle 3 Operation, May 13, 1977 - March 17, 1978," BAW-1503, August 1978.

22. "Core Operation Report - Three Mile Island Unit 1, Cycle 4 Operation, April 28, 1978 - February 17, 1979," BAW-1579, September 1979.

23. "Core Operation Report Three Mile Island Unit 1, Cycle 5 Operation, October 3, 1985 - October 31, 1986," BAW-1987, April 1987.

24. "Core Operation Report Three Mile Island Unit 1, Cycle 6, March 23, 1987 - June 17, 1988," BAW-2056, September 1988.

25. "Core Operation Report Three Mile Island Unit 1, Cycle 7, August 14, 1988 - January 5, 1990," BAW-2110, July 1990.

26. BAW 2152, "Core Operation Report, Three Mile Island Unit 1 Cycle 8, March 3, 1990 - September 27, 1991," August 1992.

27. BAW-2216, "Core Operation Report TMI-1 Cycle 9, November 14, 1991 to September 10, 1993," B&W Fuel Company, January 1994.

28. "TMI-1 Cycle 10 Startup Report," GPU Nuclear Letter C311-94-2003, from T. G. Broughton, Vice President, TMI-1, to the NRC, dated January 13, 1994.

29. "ARMP-02: PDQ7-E/HARMONY User's Manual," EPRI NP-4574-CCM, II, 9, V2, April 1987.

30. M. Edenius and C. Gragg, "MICBURN-3, Microscopic Burnup in [illegible] Absorber Rods, V.1.5," Studsvik/NFA-89/11, November 1989.

31. "Nuclear Application Software Package," BAW-10123, February 1978.

32. "Metropolitan Edison NSS On-Line Computer Programs for the 855 System," NPGD-TM-308, Babcock & Wilcox, Dec. 1974.

33. "Urania Gadolinia: Nuclear Model Development and Critical Experiment Benchmark," DOE/ET/34212-41, BAW-1810, April 1984.

34. "Assessment of the Assumption of Normality Employing Individual Observed Values," ANSI N15.15-1974.

35. Mary Gibbons Natrella, "Experimental Statistics," John Wiley & Sons (1966).

36. P. N. Somerville, "Tables for Obtaining Non-Parametric Tolerance Limits," Annals of Mathematical Statistics, Vol. 29, No. 2 pp. 599-601 (1958).

37. C. A. Bennett and F. L. Frankin, "Statistical Analysis in Chemistry and the Chemical Industry," John Wiley & Sons, New York, NY, (1961).